UNIVERSIDADE FEDERAL DE SANTA CATARINA
SYSTEMS AND AUTOMATION ENGINEERING GRADUATE
PROGRAM (PPGEAS)

Marcelo Menezes Morato

FAULT ANALYSIS, OBSERVATION AND CONTROL OF BRAZILIAN
SUGARCANE MICROGRIDS:
ROBUST LINEAR PARAMETER VARYING METHODS

Florianópolis

2019

Marcelo Menezes Morato

FAULT ANALYSIS, OBSERVATION AND CONTROL OF BRAZILIAN SUGARCANE MICROGRIDS: ROBUST LINEAR PARAMETER VARYING METHODS

Dissertation presented to the Systems and Automation Engineering Graduate Program (PPGEAS) in partial fulfillment of the requirements for the degree of Master of Science in Systems and Automation Engineering.

Supervisor: Julio Elias Normey-Rico, P.h.D.
Co-supervisor: Paulo Renato da Costa Mendes, P.h.D.

Florianópolis

2019

Marcelo Menezes Morato

FAULT ANALYSIS, OBSERVATION AND CONTROL OF BRAZILIAN SUGARCANE MICROGRIDS: ROBUST LINEAR PARAMETER VARYING METHODS

This Dissertation is recommended in partial fulfillment of the requirements for the degree of "Master of Science in Systems and Automation Engineering", which has been approved in its present form by the Systems and Automation Engineering Graduate Program (PPGEAS).

Florianópolis, June 3rd 2019.

Werner Kraus Junior, P.h.D.
Graduate Program Coordinator
Universidade Federal de Santa Catarina

Dissertation Committee:
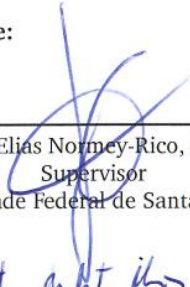
Julio Elias Normey-Rico, P.h.D.
Supervisor
Universidade Federal de Santa Catarina

Paulo Renato da Costa Mendes, P.h.D.
Co-supervisor
Universidade Federal de Santa Catarina

Daniel Martins Lima
Universidade Federal de Santa Catarina

Eugênio de Bona Castelan Neto
Universidade Federal de Santa Catarina

Marcelo de Lellis Costa de Oliveira
Universidade Federal de Santa Catarina

ACKNOWLEDGEMENTS

Eu gostaria de agradecer aqui todos que me apoiaram e me motivaram ao longo destes últimos anos de graduação e de mestrado.

Logo, começo por agradecer profundamente minha namorada e melhor amiga Lara, que me deu o amor, o suporte e o companheirismo em todas as horas.

Em especial, agradeço aos meus pais Débora e José Rubens, pelo carinho e incentivo à curiosidade científica (e ambiental), desde que sou pequeno. Também, agradeço aos meus amados avós Dette e Antônio, padrinhos Estera e Emilio e a todos os primos de Floripa: Gui, Tanira, Thais, Guto, Mallu, Thiago, Samya e Alyssa. Lembro também de agradecer toda a família da Lara, que comigo é sempre muito carinhosa, em especial a: Denise, Alexandre e a Flávia. Ao Sunshine agradeço, além da amizade, pela parceria e colaboração no projeto do Mexilhão!

Não poderia deixar de lembrar dos meus orientadores Julio e Paulo. Desde 2015, quando entrei como PIBIC no GPER, ambos têm me acolhido e ajudado de uma forma fantástica, me guiando com muita confiança e competência. Agradeço, sinceramente, por todo este trajeto juntos que, sem dúvida, continuará rendendo muitos trabalhos amistosos.

Aos meus amigos e amigas, faço um agradecimento pelos momentos de descontração e por conselhos que (in)diretamente me ajudaram neste trajeto.

Os colegas de laboratório, de profissão e de departamento também sempre me apoiaram e prestigiaram. A eles, faço um agradecimento sincero e um voto pela continuidade na pesquisa de Controle de processos. Em especial, menciono minha alegria por ter colaborado com Alice, Aline, Bruno, Emanuel, José e Henrique. Lembro aqui também dos servidores administrativos do DAS e PPGEAS, em especial da Lívia. Continuo por agradecer todos os colaboradores de pesquisa deste último ano, principalmente ao prof. Carlos Bordons e ao prof. Olivier Sename, que comigo continuaram trabalhando apesar das distâncias.

Em termos de financiamento, devo reconhecer que fazer ciência é um trabalho duro. Para perplexidade de alguns que não o sabem, este trabalho é de dedicação exclusiva e, por tanto, faz-se necessário o financiamento dos pós-graduandos através de bolsas de mestrado / doutorado. Reconheço que sem o financiamento do *CNPq*, este trabalho talvez não teria sido possível.

Lastimavelmente, hoje, está em curso um ataque claro contra a Universidade Pública, às ciências (e ao meio ambiente). Sinceramente,

espero que os tempos de terraplanismo sejam deixados para trás e que, novamente, as instituições de ensino, pesquisa e extensão sejam devidamente valorizadas.

E, por fim, reconheço que fez-se necessário o acesso a diversos artigos científicos e referências técnicas para a devida fundamentação deste trabalho. Estes foram integralmente acessados usando plataformas digitais de livre acesso, tal como o sci-hub. O Autor reitera **nunca** reconhecer a literatura científica como propriedade privada, e sim como material de livre difusão.

Eu vi um menino correndo
Eu vi o tempo
brincando ao redor do caminho daquele menino
Eu pus os meus pés no riacho
E acho que nunca os tirei
O sol ainda brilha na estrada e eu nunca pas-
sei
...
A vida é amiga da arte
É a parte que o sol me ensinou
O sol que atravessa essa estrada que nunca
passou
...
Aquele que conhece o jogo,
o jogo das coisas que são.
É o sol, é o tempo, é a estrada, é o pé e é o
chão

RESUMO

Indubitavelmente, os processos tecnológicos modernos são suscetíveis a falhas. Isso se deve, principalmente, a fatores de instrumentação. Sistemas (híbridos, renováveis) de energia também fazem parte destes processos vulneráveis a panes. Possíveis falhas nestas unidades podem levá-las a não cumprir restrições operacionais, fato que resulta em privação econômica e na falta de energia disponível para a rede externa. Empresas do setor de energia vêm investindo fortemente em tecnologias para usar as fontes renováveis (do vento, solar, da biomassa, entre outras) de forma mais eficiente, mas os efeitos causados por ter a geração de energia perturbada pela presença de falhas pode vir a ser até pior do que a ausência de renováveis, pois pode levar uma parada total na geração.

Portanto, esta dissertação de Mestrado tem como objetivo estudar o complexo paradoxo causado quando ocorrem falhas em sistemas de geração de energia (incluindo sistemas com fontes renováveis). Este trabalho se desdobra em dois grandes eixos: *i*) Desenvolvimento e aplicação de técnicas de Estimativa, Detecção e Diagnóstico de Falhas; e *ii*) Desenvolvimento e implementação de estratégias de Controle Tolerante a Falhas. A grande parte das técnicas utilizadas na construção aqui apresentada é derivada de estratégias lineares paramétrico-variantes com garantias de robustez, além de abordagens de Controle Preditivo baseado em Modelo.

Os métodos propostos nos eixos *i* e *ii* são cuidadosamente analisados através de diversos ensaios em simulação em processos de geração de energia na indústria da cana-de-açúcar e demonstram-se satisfatórios.

Palavras-chave: Sistemas de Energia Renovável. Gestão de Falhas. Sistemas Lineares a Parâmetros Variantes. Controle Preditivo baseado em Modelo. Controle Tolerante a Falhas.

RESUMEN

Los procesos tecnológicos modernos son, sin duda, suceptibles a fallas. Esto se debe principalmente a factores de instrumentación. Los sistemas renovables de energía también son vulnerables a fallas. Posibles fallas en estas plantas pueden llevarlas a no cumplir restricciones, lo que resulta en la déficit económico y en la falta de energía disponible para la red externa. Las empresas de energía vienen invirtiendo fuertemente en tecnologías para usar las fuentes renovables (del viento, solar, de la biomassa) de forma más eficiente, pero tener la generación de energía perturbada por fallas puede llegar a ser peor que la ausencia de renovables.

Esta Disertación de Maestría tiene como objetivo estudiar el efecto causado por fallas en sistemas híbridos de generación de energía. Este trabajo se desdobla en dos grandes ejes: *i*) Desarrollo y aplicación de técnicas Estimación, Detección y Diagnóstico de fallas en Sistemas de Energía Renovable; y *ii*) Desarrollo e implementación de estrategias de control tolerante a fallas, para estas mismas plantas de energía. La gran parte de las técnicas utilizadas en la construcción aquí presentada son derivadas de estrategias lineales paramétrico-variantes con garantías de robustez. Los métodos propuestos en los ejes *i* y *ii* son cuidadosamente analizados a través de diversos ensayos en simulación y se demuestran satisfactorios.

Palabras-Clave: Sistema de Energía Renovable. Gestión de Fallas. Sistemas Lienales a Parámetros Variantes. Control Preditivo basado en Modelo. Control Rolerant a Fallas.

RESUMÉ

Les procédés technologiques modernes sont sujets aux fautes. Ceci est principalement dû à des facteurs instrumentaux. Les systèmes énergétiques (hybrides, renouvelables) entrent également dans la liste des plantes vulnérables aux pannes. Des fautes potentielles dans ces centrales peuvent les amener à ne pas respecter les restrictions d'exploitation, ce qui se traduira par des déficits économiques et par le manque d'énergie disponible pour le réseau externe. Les entreprises énergétiques ont beaucoup investi dans les technologies qui permettent les opérateurs d'utiliser plus efficacement les sources d'énergie renouvelables (éolien, solaire, biomasse), mais étant donné que la production d'électricité peut être perturbée par la présence de fautes, ne pas gérer les des ces défaillances en ces systèmes c'est encore pire que l'absence totale de ces énergies renouvelables.

Donc, ce Mémoire de Maîtrise vise à étudier l'effet des fautes dans les systèmes renouvelables de production d'énergie. Ce travail est divisé en deux axes principaux: *i*) Le développement et l'application des techniques d'estimation, de détection et de diagnostic des fautes dans les systèmes à énergies renouvelables; et *ii*) L'élaboration et mise-en-œuvre de stratégies pour la commande tolérant aux fautes pour ces mêmes centrales. La plupart des techniques utilisées dans le développement présentée ici sont dérivées des stratégies linéaires à paramètre variant, avec des garanties de robustesse. Les méthodes proposées sur les axes *i* et *ii* sont soigneusement analysées au moyen des plusieurs essaies en simulation.

Mots-clés: Systèmes d'énergie renouvelable. Gestion des fautes. Systèmes Linéaires à Paramètres Variants. Commande Prédictif basé sur Modèle. Commande Tolérant aux fautes.

ABSTRACT

Modern technological processes are, without doubts, prone to faults. This fact derives mainly from instrumentation issues. Hybrid, renewable energy systems also belong to those that are susceptible to faults. Possible faults in these plants may lead them to not comply with operational constraints, which results in direct economic deprivation and in a lack of energy available to the external network. Energy companies have been progressively investing in technologies that allow the adequate and more efficient use of renewable sources (wind, solar, biomass, among others), but it seems that to have the energy generation disrupted by the presence of faults can be even worse than to have an absence of renewables.

Therefore, this Master Dissertation has the goal to study the effect caused by faults in hybrid energy generation systems. This work's unfoldings are divided into two main branches: *i*) Development and application of Diagnosis, Estimation and Detection of Faults in Renewable Energy Systems; and *ii*) Development and implementation of Fault-Tolerant Control strategies for these same energy plants. The majority of the developed techniques derive from linear parameter varying systems with robustness guarantees.

The methods proposed in branches *i* and *ii* are carefully analysed through various simulation experiments related to energy generation in sugarcane industries and prove themselves satisfactory.

Keywords: Renewable Energy Systems. Fault Management. Linear Parameter Varying Systems. Model Predictive Control. Fault Tolerant Control.

LIST OF FIGURES

LIST OF TABLES

NOMENCLATURE AND SYMBOLOGY

Acronyms

LPV	Linear Parameter Varying
LTI	Linear Time-Invariant
MPC	Model Predictive Control
LFT	Linear Fractional Transformation
LMI	Linear Matrix Inequality
FE	Fault Estimation
FDD	Fault Detection and Diagnosis
FTC	Fault-tolerant Control
CHP	Combined Heat and Power
PV	Photovoltaic
SP	Set-Point
SOC	State-of-charge

Operators

$\dot{x}(t)$	Time-derivative $\frac{dx}{dt}(t)$
$\text{Tr}\{\cdot\}$	Matrix Trace
$\overline{\sigma}(\cdot)$	Maximal singular value
$\mu(\cdot)$	Structured singular value
$F_u(\cdot)$	Upper LFT
$F_\ell(\cdot)$	Lower LFT

Variables

ΔT	Sampling period
λ	Fault term
ρ	Scheduling parameter
$\mathcal{P}$	Polytope
Δ	Uncertainty
e	State estimation error
e_λ	Fault term estimation error
x	State vector
y	Measured outputs vector
z	Controlled outputs vector
X_{Bat}	Battery Bank normalized SOC
X_{Bag}	Bagasse stock normalized level
X_{Str}	Straw stock normalized level
X_{Bg}	Bio-gas tank normalized level
X_T	Hot water tank normalized level
w	Disturbance vector
ν	Measurement noise

q	Concatenated disturbances and other inputs
i	All concatenated inputs
Wnd_{in}	Wind speed present on the canebrakes
$Irrd_{in}$	Available solar irradiance
Bag_{in}	Bagasse income to the stocks
Str_{in}	Straw income to the stocks
Bg_{in}	Bio-gas income to the bio-gas tank
u	Manipulated variables (inputs) vector
SP_{TU}^A	Higher Eff. Turbine's SP
SP_{TU}^B	Lower Eff. Turbine's SP
Pot_{Net}	Power to the Ext. Net.
SP_C^B	Boiler's SP
Q_V^{Out}	High-Mid. Press. Red. Valve's SP
Q_{Esc}^M	Mid. Press. Steam Escape Flow
Q_{Esc}^B	Low Pressure Steam Escape Flow
SP_{CHP}	*CHP*'s SP
SP_{Ch}	Water Chiller's SP
SP_{TC}	Heat Exchanger's SP
Pot_{Bat}	SP of Energy Flow to the Battery Bank
Q_V^{MB}	Mid.-Low Press. Red. Valve's SP
Q_{Esc}^{Tank}	SP of Hot Water Escape Flow

Indexes

$\mathcal{M}_a$	Augmented
$\mathcal{M}_2$	Related to the H_2 norm
$\mathcal{M}_\infty$	Related to the H_∞ norm
$\mathcal{M}^j$	From the point-of-view of subsystem j
$\mathcal{M}^{\text{faulty}}$	Faulty signal
$\mathcal{M}^{ot}$	Other inputs
$\overline{\mathcal{M}}$	Nominal Matrix
$\Delta\mathcal{M}$	Uncertain Matrix

CONTENTS

Part I

Preamble

1 INTRODUCTION

Eco-friendly development and a sustainable future for the planet are, nowadays, universal values. In broad terms, the concept of sustainable development is an effort to couple the growing concerns about diverse environmental issues together with socio-economic affairs [1]. To construct such a sustainable world, the integration of renewable sources to every country's energetic matrix (grid) is indeed a good alternative to avoid greenhouse emissions and reduce environmental impact. Note that these *renewables* relate to a diverse set of distributed energy resources (*DERs*): hydro, wind and solar power, biomass (derived from sugarcane residuals [2], micro and macro *algae* [3], animal waste [4] *etc*), biogas [5], geothermal heat, biofuels (ethanol, biodiesel *etc*) and so forth [6]; more and more technological possibilities are progressively becoming feasible over the course of the last few years [7, 8].

Much is discussed about the use of renewable sources, but it is important to remark that, although these seem very appealing, they are intermittent, difficult to predict (specially solar irradiance curves), heavily dependent on the weather conditions and dealing with them is a defying factor for system safety and technical-economical network management.

The integration of renewable sources to power systems can indeed be a good alternative to avoid greenhouse emissions and environmental impact. Nonetheless, the open issue to be investigated is how these sources can be integrated without loosing efficiency and dispatchability of energy plants. This topic has been deeply discussed yet, to detach from discourse and attain a true practice, some tools are still missing in order to truly integrate renewable sources to the modern electric grid. These tools refer to energy planning frameworks, that enable one to properly *i)* control (manage) and *ii)* supervise (in terms of diagnosis) these plants, improve their efficiency and maintained operation, reducing maintenance and enhancing resilience.

The Control Systems community has given attention to this certain question of prime importance, presenting solutions for the first set of tools (*i*): advanced control works, specially based on Model Predictive Control (*MPC*), seem to be the correct and adequate choice to plan out the energy generation of renewable microgrids [9, 10, 11, 12, 13, 14, 15]. A deep discussion about how can process control enhance the safety and reliability of energy systems, altogether with sustainability (social, economic and environmental issues), is presented in [16]. Note that distributed power genera-

tion refers herein to the dismantlement of large generation units into smaller ones, located near the end user. A system based on distributed generation (operated by the same distributor / company) does not necessarily need to have local loads and storage facilities at each smaller plant; the distributed generation units can be coordinated to (exchange energy between themselves and) produce a combined energy contribution to the local network. The essential idea is that uniting and coordinating many smaller plants together can yield better production (and greater bargaining power).

To handle such systems, throughout this work, the concept of (what have progressively been called) microgrids is used [17]: a set of generators, loads and storage units that operate together, in isolated mode, or connected to the main grid, located near the end user, that can be integrated into a network or operate autonomously.

Definition 1. *Fault is understod, hereafter, as when a controlled system departs from an acceptable range of operation, and when this phenomenon can be quantified in a concentrated parameter that is associated with the process itself [18].*

Nonetheless, given that modern technological processes are very susceptible to faults, especially due to instrumentation issues, the second set of tools for supervision (*ii*) are still scarce, specially from a tertiary control point-of-view, i.e. in the energy-generation planning layer. Real instrumented systems present evermore an increase on complexity and become more vulnerable to faults, which is also very true for energy systems and power microgrids. Possible faults on these systems may lead these plants to not comply with their operational constraints, which results in economic deprivation and in a lack of the available power to the external network. Energy companies have been investing in technologies to make a better, proper use of these renewable energy sources (wind, solar, biomass and so forth) but to have their generation disrupted by the presence of a fault may be worse than the absence of renewables, as pointed out in [19].

To ensure sufficient measures of reliability and safety, Fault Detection (*FD*, as illustrated by Figure[1] 1.1) and Fault Estimation

---

[1]*All Figures and Tables in this document were developed by the Author. When this is not true, references are given.*

(*FE*) methodologies have been sought. Fault-Tolerant Control[2] (*FTC*) loops for energy generation planning are also in fashion and the literature lacks works in this direction. The differences between Fault Detection (*FD*) and *FE* frameworks are subtle: while the first schemes qualify if a system is in a faulty state, the later can also quantify how much does this level of faults affects the system's operation.
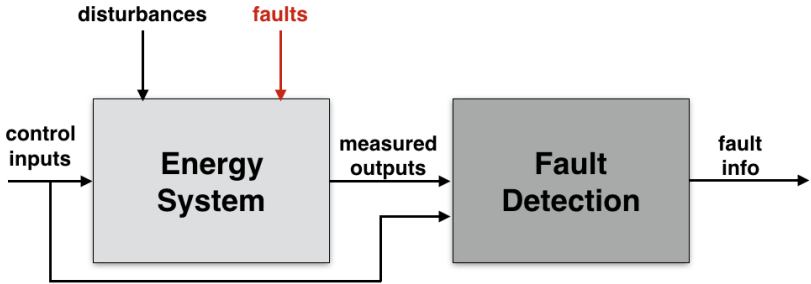
Figure 1.1: Fault Detection System.

The Problem: Tools to deal with faults in modern (renewable, hybrid) microgrids, from the tertiary / supervisory viewpoint), are lacking. Today, such tools are not available and the compensation of faults in microgrids is simply not performed. Therefore, the Problem tackled by this Master Dissertation is the development of such (*FD, FDD* and *FTC*) tools.

Hypothesis: The essential investigation supposition to tackle the above-mentioned Problem is that these tools can be essentially derived from Linear Parameter Varying observers and *MPC*-based schemes. It will become evident that this speculation is reasonable altogether with the literature review that is presented in the sequel. It must be remarked that all works cited next surround an indisputably "**hot topic**", dealing with open issues with respect to modern microgrid applications.

---

[2]*Active* FTC *systems are today crucial for any real application, in order to always maintain a controlled system operational whenever malfunctions and/or failures occur. The main issue of* FTC*, today, is an efficient integration of reconfiguration techniques to a Fault Detection and Diagnosis (*FDD*) scheme.*

Main Idea: The essential proposition of this Master Dissertation is synthesized in Figure 1.2. In this Figure, the upper block entitled "Faulty Microgrid" represents an energy-generation system of multiple sources (and multiple storage, conversion, transmission subsystem), which is assumably under faulty conditions. This means that the subsystems may not be behaving as expected, which means a reconfiguration mechanism must be deployed by the controller s.t. the global process, under closed-loop, continues to produce as much energy as it is expected of it (re-coordinating the amount of energy that each subsystem must produce). To achieve such reconfiguration, two modular blocks work together: *a)* Fault Estimation system and *b)* a Model Predictive Controller. The first consists in *LPV* asymptotic observers which compute a set of signals that corresponds to the level of faults in each subsystem of the microgrid. It can be guaranteed that they are able to compute these signals once the asymptotical estimation errors are minimized (under some mathematical formalism) and converge to zero. The latter has access to an *LPV* model of the (faulty) plant, which makes predictions to how it will behave for the next N_p discrete-time steps. This model-based predictions are made under the assumption that the faults will remain constant and having some kind of estimation of the future renewable disturbances. With these predictions, a cost function is minimized with respect to some performance goals: the *MPC* solves a constrained quadratic problem in order to find control actions to be applied to the microgrid such that the energy-related outputs obey the expected objectives (complying with load demands and not disrespecting operational constraints). Note that this global structure is developed in modular parts *a* (*FE* system) and *b* (*MPC*).

Once it becomes evident that there is a vague space for the development of such tools (after the literature review), the objectives and intents of this work are layed out, as well as the scientific research methodology.

Remark 1. *In this work, generalized methods for (renewable) microgrids are proposed. Nonetheless, the case of Brazilian sugarcane microgrids is taken as the main application example through the simulation essays. Therefore, Chapter 2, is dedicated to further explain the state-of-the-art of these systems.*
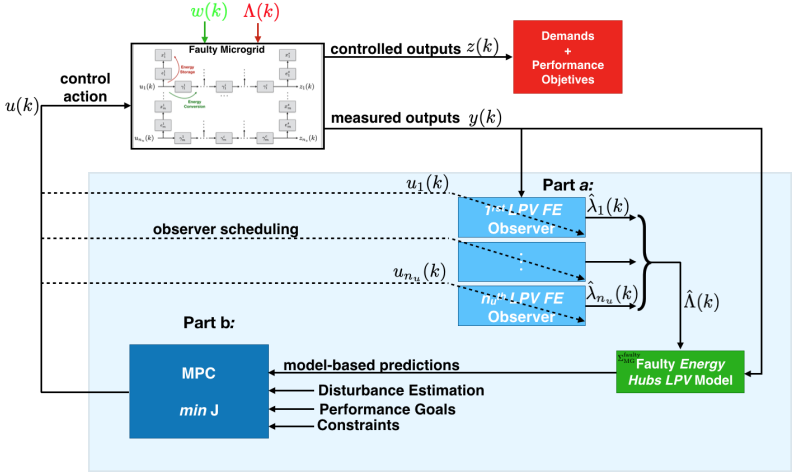
Figure 1.2: Proposed Fault-tolerant *EMS*.

1.1 LITERATURE SURVEY

The study of the effect of faults in microgrids is a serious issue for the future worldwide plans of energy generation. Renewable energy is less consistent, with many unpredictability-related issues, and, having accurate schemes that manage their incipient faults will surely be important for all developing countries.

1.1.1 Fault-Tolerant Control

Therefore, some important tools that must be available for the adequate energetic planning of renewable microgrids are effective *FTC* loops. These would, while dealing with long-term energy generation scheduling, make the energy production immune to incipient faults of the controlled plant. These tools would also reduce the frequency of manual operator intervention on the microgrid automatic supervisor, as to inform that faults have happened and a given system cannot be accounted for the generation on the next few hours or days.

Works that develop *FTC* policies for microgrids are **very rare, which has been discussed openly by the Control community** in

recent workshops and debates[3]. Some papers that sketch prelimi-
nary results must be mentioned:

**In terms of those that derive from *MPC*, as supported by
recent control-oriented microgrid literature:**

- An *FTC-MPC* strategy[4] is developed in [20, 21] to ensure the
  proper amount of energy in the storage devices is kept, so that
  consumer demand is always covered. In these works, the fault
  term is included in the optimization procedure, therefore find-
  ing a time-varying control policy that incorporates the variabil-
  ity of the energy plant's behaviour due to faults in the nominal
  process model.

- With a similar strategy, [22] develops an *MPC* scheme that
  diagnoses and mitigates the effects of faults in a microgrid.
  In that paper, a reconfiguration block acts to make changes
  on constraints as well as references of the *MPC* in order to
  optimize the microgrid operation, according to the level of
  faults that has been detected.

Other methods:

- In [23], a stabilizing *FTC* scheme is developed by implement-
  ing a local stabilizing agent (found via optimization) on each
  constant power load, that may yield instability in DC-power
  systems under certain operating conditions.

- Considering a doubly fed induction generator wind power mi-
  crogrid, [24] proposes a fault-tolerant control paradigm by

---

[3]*For instance, see the topic on the* IFAC *blog, which enlightens
the need for fault detection to enhance safety and supervision of en-
ergy conversion systems:* <http://blog.ifac-control.org/fault-detection/
fault-detection-supervision-and-safety-for-energy-conversion-systems-wind>
<-turbines-and-hydroelectric-plants/>.

[4]*Essentially, when an* MPC *loop works as an active* FTC *system, the recon-
figuration law of the controller, when faults on the supervised system occur, is
based on either model-reconfiguration itself or on variations upon the objec-
tive function of the* MPC.

means of an integral sliding mode controller. The sliding motion is able to rapidly compensate model fluctuations due to faults, yet the quantification of the level of fault is not precise (unknown from the controller's perspective).

- With interesting results, [25] designed a supervisory controller that acts as *FTC* for the management of a hybrid AC/DC microgrid, compensating the effects of faults by performing a re-distribution of load and demands.

All the above mentioned works assume the detection and quantification of faults (or some part of it) to be known by the controller loop, which does not reflect reality. Indeed, works in the *FTC* direction are scarse because there must first be available solid Fault Detection/Fault Estimation tools for microgrids, such that the control loop becomes able to account for the state of the energy plant (faulty or healthy) and, then, compute adequate reconfiguration mechanisms.

1.1.2 Fault Detection / Estimation

Fault detection is an important topic of process engineering. Such tools provide prevention of the failures of local components, reduction of maintenance costs and detection of degradation. They also offer concise information on the performance and on the operation of controlled systems, allowing condition-based monitoring and partially solving the problem of life shortening of equipments that arise with excessive maintenance [19].
In order to discuss and compare different methods, one recalls rapidly the five most important desirable characteristics of Fault Detection / Estimation systems, according to [26]:

- Fast detection and diagnosis: they must respond timely when detecting process malfunctions/failures, so that control laws to recondition the system can be computed in avid time;

- Isolability: they must distinguish between different kinds of faulty events;

- Multiple identifiability: they must detect multiple kinds / sources of faults at once, which can be rather tricky due to coupled, interacting nature of faults;

- Robustness: they must be robust to noise and model uncertainties;

- Novelty identificability: they must distinguish novel, unknown faults from normal operation or known kinds of malfunctions.

Note that the main purpose of *FD* is to bring up a set of symptoms which indicate the differences from the healthy scenario / condition and the faulty status. *FD* methods are, therefore, either based on signal threshold, signal models or process models.

There is a real need to open a discussion about the challenges of *FD/FE* and supervision for energy conversion systems. Unfortunately, one must bear in mind that their state-of-practice in the energy industry is still very limited (or practically null). Most management systems for microgrids are only *PLC*s with some alarms that indicate operating point escapes from the controlled subsystems, which means **there is a lot of progress to be done in this field**.

After all, literature does present some interesting (and powerful) *FE* techniques, such as the fast adaptive fault estimation (*FAFE*) method for nonlinear plants [27, 28], the robust observer seen in [29], Linear Parameter Varying[5] observers in [30] and Moving-Horizon Estimation (*MHE*) schemes [31]. Although being very robust tools, these do not consider the specificities of energy plants, and have not been properly tested or adapted for the case of modern microgrids, specially from the supervisory / tertiary control level.

As far as the author knows, *FD/FE* for modern microgrids at a higher control level, working in parallel to the energy generation planning layer, has been developed in rather few works. This is, schemes that deal with the design of systems that detect, diagnose and quantify the state of the whole controlled plant, if it is healthy or faulty.

Remark 2. *There are works that deal with fault detection applied to some of the subsystems that compose many modern microgrids, such*

---

[5]*The control of* LPV *systems has attracted a great deal of attention in the last decade, since they have shown to be an interesting extension of the Robust Control theory applied to nonlinear systems. The* LPV *approach is today known and well-suited to handle system non-linearities by modelling them as varying parameters (or to settle the controller performances as varying through gain-scheduling).*

as photovoltaic panels or wind turbines[6]. *This is not the focus of this work. One investigates, herein, works that design* FTC/FD *structures that are able to qualify and quantify whether one (or more) of the various subsystems that compose a given microgrid is faulty. There is an essential difference between these two approaches. As an illustrative example, take the plant that is detailed in [2], composed of different boilers, turbines and panels; an* FE *applied to this system should be able to gather the information if one of these local subsystems presents a fault in its energy output, from a supervisory level. It should not need to measure the local variables of each subsystem, but solely the global variables (energy production, loads, states and demands) of the complete microgrid and, thence, be able to isolate and quantify how much of failure does one of the local subsystems presents.*

One can divide the works that have been developed for the fault estimation / detection of modern microgrids in three distinct sets: those applied to *DC* microgrids, that stand for the vast majority; those that use statistical methods; and those that in fact gather stronger results (by this, author means schemes that, from a tertiary supervisory layer, can indeed detect, isolate, locate and quantify the faults of different subsystems of modern, renewable microgrids):

FE/FD **applied to** *DC* **power systems:**

- In [37], a fault location technique is developed for a low-voltage *DC* microgrid, that is able to directly diagnose where faults occur by the analysis of the frequencial spectrum of circulating currents, with no need for iterative loops.

- The issue of fault location has also been dealt with in [38], for a voltage sourced converter-high voltage direct current system. In this paper, the method analyses both the frequencial spectrum of circulating currents, as well as time and energy

---

[6]*Nonetheless, some works that deal with fault detection of individual energy subsystem (at a lower control level, with a much more limited scope) are mentioned: [32] presents a monitoring and fault diagnosis system for wind power systems; [33], presents the detection of fault on photovoltaic panels, with a power losses analysis approach; [34] detects and classifies faults on steam turbines using neuro-fuzzy methods; [35] presents the handling of faults for a wind system; the work [36] presents a* FD *system for wind turbines using available information of a supervisory (*SCADA*) system.*

conditions, capturing fault features by a Hilbert-Huang Transform.

- For a *VSC*-based system, a fault detection methodology is presented in [39], considering the analysis of transient behaviour of capacitive discharges.

- Paper [40] develops a fault detection and isolation scheme for a *DC* microgrid based on photovoltaic (*PV*) panels, derived from a discrete-frame differential current solution for the classification of faults.

The advantages of the above methods are that they are relatively fast, since they use current / voltage knowlege to locate (or isolate) faults in these *DC* microgrids. Nonetheless, they are disadvantageous (face to works that are mentioned in the sequence) since they do not use energy-generation-related outputs (i.e. power available to external network, power dispatched by *PV* panels *etc*), which means they cannot be directly incorporated to the tertiary supervisory schemes that solely measure such variables, needing additional measurements that are usually found in lower levels of the control structure (that are, sometimes, physically apart).

Remark 3. *It is evident that literature lacks works which deal with* FD/FE *applied to purely* AC *microgrids, which is certainly a topic to be further explored.* AC *plants present various kinds of faults (in transmission lines, for instance) that may cause instability issues and, in such case,* FTC *methods for these plants should be researched.*

Statistical *FD/FE* works:

- The first work that designed a fault estimator for power systems was presented in 1997: an adaptive, statistical method that is able to isolate and identify the location of faults [41], using simple statistical gestures (probability of failure and signal analysis) to achieve interesting results (good detection of faults).

- Paper [42] presented a fault detection system (in fact, a fault categorization algorithm) for renewable microgrids, derived from Clarke and S-transforms that analyse transients in three-phase current and voltage waveforms.

The advantage of the statistical methods are their ability to categorize and locate faults efficiently, without many mistakes, but their main drawback is that the quantification of the level of faults that occur is not so precise, residing on the analysis of fault residues (i.e. model-process mismatches).

Works with "stronger" results:

- In [43], the issue of high impedance (arcing) *FD* is studied, considering complex electrical distribution networks. By employing normalized dynamic features that are less dependent on the microgrid's operating conditions, very interesting results with high dependability are obtained. Moreover, such method only needs four cycles (sampling periods) of post-fault data to determine that a fault condition has occurred.

In the sequence, based on this global literature survey, possible (and practical) ways to design Fault Detection / Estimation schemes for modern microgrids (from the tertiary control level) are layed out, as well as possibilities on *FTC* policies. From these open threads, the global objectives of this Master dissertation will become evident.

1.2 OPEN RESEARCH THREADS

Note that, although there are only few works that effectively deal with the design of *FD/FE* for microgrids from the energy planning (third) layer, there are two clear paths of viable, pragmatic schemes that should certainly be further investigated: *i) LPV* observer-based methods; and *ii)* Moving Horizon fault estimation frameworks. Both are more deeply explained later on.

Remark 4. *The adaptation of the Fast Adaptive Fault Estimation (*FAFE*) method for microgrids, as well as the application of the robust observer proposed by [29] are interesting research routes, once they are both very robust techniques. Nonetheless, they are not dealt with in this work; they are to be studied in future works.*

Definition 2. *Tertiary Control Level The tertiary control level is understood as the planning layer of the control scheme. In the context of microgrids with multiple subsystems, this third level is concerned with long term (daily / monthly) energy generation goals, setting the set-points for local controllers in order to coordinate these subsystems,*

as well as being responsible for the supervision goals, raising alarms / warnings if variables escape from expected conditions.

Note that, in constrast, the primary (first) control level, in power systems, is concerned with current and voltage regulation, while the secondary (second) control level works towards power quality maintenance and economical operation (considering dynamics inside the range of some few minutes).

The three levels of control are illustrated by Figure 1.3.
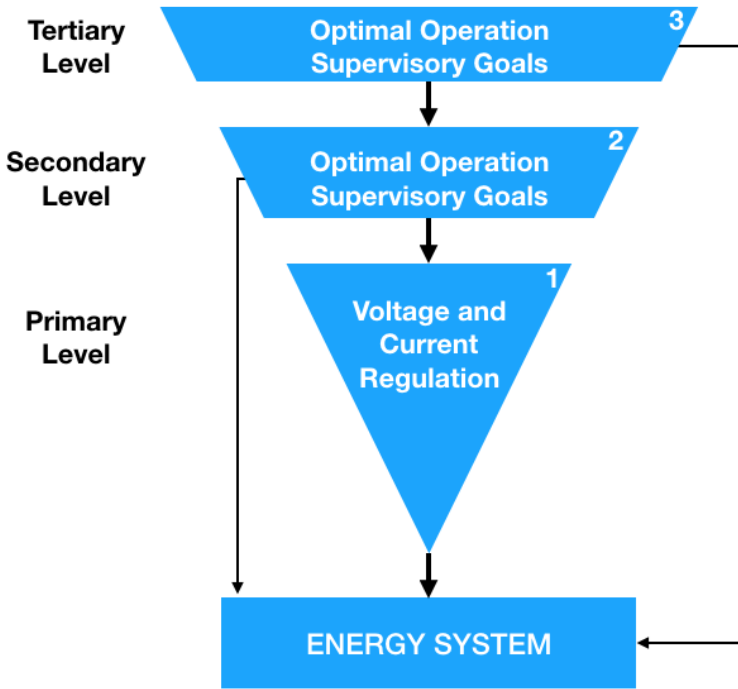
Figure 1.3: The Three Control Layers.

1.2.1 *LPV* Observers

Firstly proposed in [30] for the case of Electro-Rheological dampers in automotive suspensions, the use of *LPV* observer-based methods could be in fact applicable for real energy systems. Note

that to design these observers, one only needs to: *a)* have a **good model** of the observed system (from a tertiary/supervisory control-level point-of-view, derived, for instance, from the Energy Hubs method, later explained in Chapter 2); *b)* measure the **fault-related outputs** (in the case of microgrids, these should be the energy-generation outputs); *c)* compute **offline** observer laws, solving Linear Matrix Inequality (*LMI*) **problems**; *d)* implement simple (optimization free) **online observers**, that could be done (possibly) within the microgrid's distributed control system / PLCs (there is no need for complex online procedures).

The main drawback of this strategy is that, possibly, a single observer may have to be computed for each of the n subsystems of the supervised microgrids. This may lead to a harsh design procedure (yet offline), that certainly will take time to be correctly synthesized.

Anyhow, these observers point to a clear, simple path on how *FE* schemes for microgrids can be introduced in industry. The **open research threads include**: 1) Effectively designing and synthesizing them for the case of renewable energy systems; 2) Testing their performances, through realistic numerical simulation; 3) Checking their robustness guarantees, via Monte Carlo runs or μ-analysis; 4) Comparing them with other approaches in terms of computational effort and achieved performances (i.e. smoothness of fault estimative); 5) Assessing the observer performances through experimental validation, i.e. testing in real plant conditions.

Remark 5. *Note that if such* LPV *observer strategy effectively serves for the case of renewable microgrids, it will, most certainly, be useful for fault tolerant control goals of energy systems in the presence of faults, in order to preserve system stability, reliability and major performance goals (guarantee supply demand and others).*

1.2.2 Moving-Horizon Fault Estimators

The other method that possibly arises as an adequate, feasible way to implement a *FE* structure for microgrids derives from the Moving-Horizon Estimation framework, as proposed by [31].

The *MHE* method considers a backward estimation horizon comprised of past input and output information and, with this data, it is able to estimate the current and past states based on a good model of the plant [44]. Once again, this model must be a third-

level model, such as the ones derived from Energy Hubs methodologies.

This estimation scheme is formulated so to minimize the quadratic estimation error. Thereby, it solves an optimization problem, having a similar formulation to the Kalman Filter, but directly considering operational constraints. At each sampling instant k, the *MHE* optimization problem is solved and a current estimation for the states and faults becomes available for control and monitoring purposes.

Its main drawback is that the *MHE* online optimization procedure might be excessively costly, leading to the need of supervisory controllers with very good processors. **Open research threads** on the use of the *MHE* framework to collect faults on microgrids include the same topics pointed as open for the *LPV* method.

1.2.3 *FTC* Insights

Once adequate, feasible and accurate *FD/FE* for microgrids are made available, their global resilience (continuous stability, maintained operation and reduced maintenance) can be enhanced with the aid of *FTC* policies.
Two open *FTC* threads are discussed:

- **Shared *MHE* + *MPC* Optimization Loop:**

  Another very important advantage of the *MHE* scheme, apart from those listed above, is that it solves a (backward horizon) optimization problem. Therefore, if *FTC* goals are sought, the future control actions, that act on the supervision layer of microgrids, could be computed within the *MPC* framework which shares the same optimization formalism as the *MHE*. Thereby, a single optimization problem could be solved at every sampling instant: estimating faults and states and computing future (fault-tolerant) control actions. This **has not yet been tested for microgrids** in the literature and could certainly achieve interesting results in terms of fault-tolerance and performance maintenance.

- **Time-varying *MPC*:**

  Another option to design *MPC* supervisory controllers that act as *FTC*s for microgrids is to incorporate the estimated fault

terms (by whichever *FE* scheme works in parallel to it) to the model itself. This, in many cases, yields a nonlinear model. Then, a very simple idea consists in assuming the fault remains constant for the next prediction horizon, computing the *MPC* control law with a *frozen* fault + energy process model. This leads to a time-varying (scheduled) *MPC* policy, that adapts the optimization procedure according to the level of faults, which is **yet to be investigated**, and may also lead to interesting results.

1.3   OBJECTIVES

Over the past few years, there has been a growing interest in fault handling application for microgrids. Nonetheless, the available literature on *FD/FE* and *FTC* applied to microgrids is quite shallow, specially from a tertiary control point-of-view. Indeed, dealing with the faults that may arise on these energy plants should lead to a direct improvement on their resilience and maintained operation. Therefore, this Master dissertation investigates how to design such tools.

According to what has been layed out, there are some clear open paths in this field to be further researched: *LPV* observer *FE* methods[7], fault-tolerant *MPC* optimization procedures and works that assess the robustness guarantees of such strategies (w.r.t. model uncertainties, noise and disturbances).

From the above context and under the light of the bibliographical survey mentioned, the global (GO) and specific (SO) objectives of this work are listed below. Note that all these objectives are oriented to present novel results to the Control Systems scientific community.

GO 1) To propose an adequate model that incorporates the effects of faults that occur in renewable microgrids, from a tertiary level.

SO 1.1) To formalize, under the developed framework, the most common kinds of faults that occur in Brazilian sugarcane microgrids.

---

[7]*The Author also studied and proposed* MHE *schemes for fault estimation in microgrids. Nonetheless, they are not shown here due to scope restrictions, but rather in the conference paper [45].*

GO 2) To elaborate a novel technique to estimate such faults on microgrids, derived from *LPV* observers.

SO 2.1) To first validate this method on a specific, less complex case, such as one subsystem of a complete microgrid.

SO 2.2) To test this approach to the case of a complete Brazilian sugarcane microgrid, with all its subsystems.

GO 3) To develop an integrated approach for the fault-tolerant energy management of renewable microgrids, based on an *MPC* loop.

SO 3.1) To test the use of *LPV* feedback filters coupled with a linear *MPC* control law with a *frozen* fault energy generation model.

In addition to these objectives, complementary objectives (CO) are also layed out:
CO 1) To present a thorough and complete background review on the key topics of Control and Systems Theory, as well as a review of the *state-of-the-art* of control of energy plants, which is, in fact, presented in a separate document (this is discussed in Chapter 3).
CO 2) To check the robustness guarantees of the developed *FE* methods for microgrids, which can be done either via Monte Carlo runs or μ-analysis.

1.3.1 Methodology

This work is performed under rigorous scientific, bibliographical, documental and empirical research methodology. All developments were set inside the *GPER-UFSC*[8], project and research group. The methodological steps were divided in three project phases:

- Phase 1: Specifications - This phase, the backbone of the Master project, includes definition of functional requirements and the study of potential use-cases (faulty situations) of the sugarcane processing plants / microgrids.

    - *i)* Study and analysis of faults in renewable microgrids.
    - *ii)* Modelling of these faults inside an *LPV* paradigm.

---

[8]*Grupo de Pesquisa em Energias Renovavéis (Portuguese), Research Group on Renewable Energies.*

- Phase 2: Design methods- During the second phase, the methodological core of the project, theoretical developments were carried out, under the specifications of Phase 1.

  – *iii)* Study, development and implementation of *FDD/FE* algorithms.
  – *iv)* Study, development and implementation of *FTC* algorithms.

- Phase 3: Tests and Results - The final phase, comprises the campaign of tests and results analysis. The documentation was also included in this phase.

  – *v)* Discussing the *LPV-FDD* in terms of robustness and w.r.t. to other techniques inside the literature (such as the *MHE* scheme).
  – *vi)* Study, development and implementation of an *MPC-FTC* algorithm.
  – *viii)* Preparation of scientific papers

1.4 OUTLINE

A comment about the structure of this manuscript has to be made prior to the presentation of the content itself: this work is organized in a rather peculiar manner, with Chapters written in some kind of chronological order, pursuing the scientific arch in four main Parts:

(i) Part I stands for the preliminaries of this dissertation, introducing its global objectives, background literature and some essential tools for its thorough comprehension;

(ii) The main development is divided into two main Parts (II and III). The first is devoted to the achieved results in terms of Observation and Monitoring, while the latter is concerned with advances in Control. All the Chapters that comprise these two Parts are meant to be read independently, as standalone issues. This is done on purpose, by author, as he considers that this seems to be the fitter form to present a dissertation. Each and every one of these Chapters are just as scientific papers, to be presented to the Control Systems Community. A lot of effort was performed to reduce the amount of cross-references between these chapters.

(iii) Part IV is the denouement of this work, wherein the achieved results are summarized. Future work trends are also discussed in this Part.

It must be remarked that one should not necessarily read this document according to the progressive arch. In general, each chapter can be read individually and out of order, without having its meaning lost from the others. The content of each one of the Chapters is further explained:

- This Chapter (1) presented a formal introduction to this work, justifying why it was set out in the first place and what are its global and specific objectives. A complete literature survey of the related works was discussed and the available research gaps were identified.

- Chapter 2 presents the application example used throughout this work. The *state-of-the-art* and *state-of-practice* of Brazilian sugarcane-based plants are discussed, considering their applicability to the Brazilian sugarcane context.

- Chapter 3 presents the theoretical background of this work, rapidly recalling all the basic concepts that are used in the sequence.

- Chapter 4 shows the study of linear parameter varying-based approaches for the fault detection and diagnosis for the case of Brazilian sugarcane-based energy plants. In fact, the observer-based method is coupled with simple search algorithm for formalism. The complete methodology is applied to a grid-connected microgrid, with different renewable sources, such as photovoltaic panels, wind power generation and the use of biomass. This plant might present different possible faults, that can lead it to not comply with its operational constraints, such as communication failures, sensor malfunctions, vapor leakages and others. All these possible faults are carefully categorized based on empirical information from real plants in Brazil. The Fault Detection and Diagnosis system designed aims to estimate and categorize these faults and, to do so, the proposed *LPV* observers are derived from Linear Matrix Inequality computation of the mixed H_2/H_∞ norm minimization, in such way to reduce the effect of noise and external disturbances upon the fault estimation. Through high-fidelity

simulations, the benefits of the presented method are discussed. Results show the overall good behaviour of the proposed scheme.

- Chapter 5 analyses the robustness conditions in terms of stability and performance of the observers proposed in Chapter 4. As displayed in recent literature, Fault Estimation schemes can be designed for renewable microgrids considering the use of multiple Linear Parameter Varying observers, derived from *LMI* for the mixed H_2/H_∞ norm minimization. The study of such observers is extended: this given method is discussed in terms of Robustness, using the Small Gain Theorem and μ-analysis. Possible model uncertainties are carefully constructed, possibility present due to the assumptions from the modelling / identification phase. Via frequencal analysis, this Chapter also investigates the effect of noise and load disturbances upon fault estimation in the uncertain (model/plant-mismatch) situations. High-fidelity simulations are also presented to assess the robustness qualities of the observer method, whilst the noticeable performance deterioration is quantified.

- Chapter 6 presents the propositions of a novel approaches of fault-tolerant control method for faulty energy systems. The Chapter presents a Filtered Model-based Predictive Control method for the Fault-Tolerant Energy Management of a sugarcane microgrid. The proposed control policy ensures that the load demands are met at every iteration, despite the presence of faults, coordinating which energy source to use, maximizing the use of the available *renewables* according to contract rules. The proposed predictive controller is synthesized with a fault-free model of the plant and coupled with a *feedback* low-pass linear parameter varying filter that is scheduled according to the level of faults detected upon the system. Such system is compared to a standard predictive controller, displaying much improved behavior.

- Finally, Chapter 7 presents the conclusions to this Master Dissertation, summarizing the main contributions, achieved goals, concludes on the literature gaps that still remain and enumerates topics for future studies.

1.4.1   To Reader

Theoretical background and literature review are presented in a separate document. This is explained in Chapter 3. Please refer to this document (Theoretical Lexicon) whenever doubts appear on terms and technical knowledge. Once again, remark that each of the other chapters tries to express its goals and topics individually, in order to be able to be read detached from the whole document.

2 BRAZILIAN SUGARCANE MICROGRIDS

This Chapter details the *state-of-the-art* and *state-of-practice* in terms of Energy Management / Coordination technologies for renewable microgrids. Herein, the main case-study microgrid in this work is introduced and discussed.

2.1 RENEWABLE ENERGY SYSTEMS

As stated, the use and generation of energy in efficient ways are key elements for achieving more ambitious goals for sustainable and eco-friendly development. The current foundations on energy generation are about to change [46] in a profound way: the price of fossil fuels are rising each year (due to future scarcity, shortage and other factors - see [47]) whereas, at the same time, energy demands grow in every country and the search for viable renewable sources becomes evermore important [48].

There is a crescent of the smaller and more distributed energy plant structure [49] for generation of power and heat, and the highlights in the forthcoming years will be given to *clean*, renewable generation.

In sum, the biggest affair related with this kind of system is the unreliability and inconstant quality of the renewable energy sources, these being intermittent and inducing unpredictable fluctuations in the energy output. A practical solution to this matter is to include intermediate energy storage units / banks, such as batteries, super-capacitors, fly wheels and others, as it is proposed in [50].

Recent academic research has also given focus to generalized energy systems, with multiple generation and different energy carriers. The growing scope of research in this topic can be illustrated by some references: a large review of the *state-of-the-art* on multi-objective planning of these distributed plants is seen in [51]; a robust optimization approach to their management is seen in [52]; in [53], a real-time coordination of theses systems is considered for their control of frequencies.

Recent works have considered the integration of renewable sources w.r.t. the concept of microgrids [17]. The control of hybrid generation and storage plants (those systems that include renewable and non-renewable sources) is a significant issue to be studied in order to allow the optimal management and operation, carrying out a coordination between legal standards, minimal environmental standards and modern techniques [54]. Recent works have

brought to light *MPC*-based control structures used for energy management of microgrids. [12] shows an *MPC*-controlled hydrogen-based domestic microgrid; [15] also refer to optimal generation for renewable microgrid; [55] propose *MPC* structure for energy management of experimental microgrids, coupled with hydrogen storage systems; the work shown in [14] presents an economical *MPC* applied for the optimal production timing and power, considering biomass dispatch of an olive oil mill.

Solar radiation and wind speed exhibit frequent changes due to climatic issues, and their stochastic behavior becomes an additional challenge to energy management in renewable energy based power systems. Estimation of the future behavior of these variables is therefore a very important issue, as thoroughly discussed in [56, 57] and [11].

2.2   THE EXAMPLE MICROGRIDS

Still on this matter, one case that has to be mentioned is to consider a hybrid energy producer based on a sugarcane processing industrial plant. This plant considers biomass, biogas, solar and wind power energy as primary energy sources. This energy generation system was firstly presented in [58] and [2]. Then, in [9], a model-based predictive controller was designed and some other advanced control techniques, considering disturbance forecasting, were implemented in [59] and [11]. This system is now detailed:

Brazil is a country with an immensely diversified energy matrix [60], with over $43\,\%$ of it being renewable (considering primary generation). Solar energy can be considered as one of the possible energy sources to enlarge the renewable energy share, as the country has great potential for solar energy generation in several regions. The investment in this sector has vastly risen in the latter years, showing competitive costs (as it is seen in [61]).

The sugarcane distilleries are particularly significant to this study, since the sugarcane distillation process has a great amount of residue and waste that can be treated as *bio*-sources of energy. In sum, there are three important renewable sources from the canebrakes: the bagasse, the straw and the vinasse. In the Brazilian context, sugarcane is one of the main harvests of the country's economy; Brazil is the world's largest producer of sugarcane.

Given the importance of these sugar-ethanol plants in the

Brazilian energy setting[1] and knowing that these are mostly established in site with high levels of insolation, with low amounts of day-time rain during the harvest period, the sugar-ethanol plants are potential candidates to be managed as distributed microgrids [62]considering the use of biomass and *bio*-gas for *direct-to-electric-energy* generation and, also, auxiliary solar and wind power energy generation.

To detail the Brazilian industries that deal with sugarcane the overall processing of this plant to produce etanol and sugar has to be understood. This process is based on some main steps, schematized by Figure 2.1 and detailed below:

1. Firstly, the sugarcane is prepared and milled (where bagasse and straw appear as sub-products);

2. The sugarcane juice (*garapa*) is clarified and purified;

3. This treated juice is concentrated via evaporation;

To produce sugar:

(a) Crystallization of the concentrated, treated juice is done;

(b) Then, a centrifugation is done and sugar is dried and packed.

To produce bio-*etanol*:

(i) The remaining sugarcane juice is prepared into a must and fermented;

(ii) Then, the alcohol is distilled from this fermented must (vinasse is the main sub-product of this stage).

All these steps are very well detailed in [63].

From these procedures, the bagasse, the straw and the vinasse are the important residues that can become bio-fuels. In Figure 2.2, this sugarcane plant is presented as an energy producer (microgrid).

The bagasse is the main residue from sugarcane processing. This residue is very polluting when improperly discarded. It is often used in the industry as burn fuel for boilers, as explained in [64]; an assessment on the different technological routes for energy generation derived from the sugarcane bagasse is seen in [65].

---

[1]17.2 *% of Brazilian (primary) Energy comes from processed Sugarcane!*
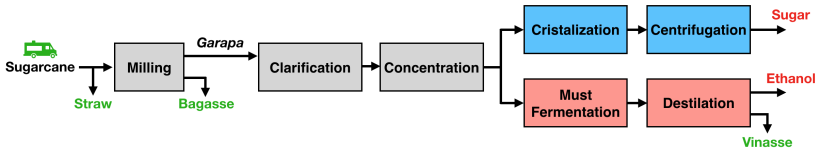
Figure 2.1: Sugarcane Processing Flow Chart.
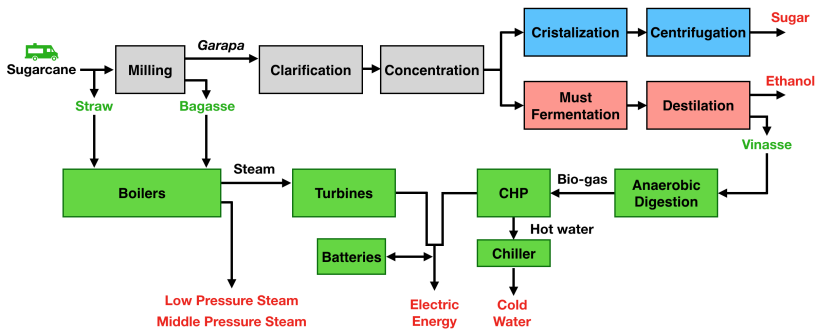
Figure 2.2: Sugarcane Processing Industry as Energy Producer.

It is important to remark that the stockage of bagasse residue is a very common practice on canebrakes. In Figure 2.3, taken from [66], the stockage of bagasse on outdoor piles is seen. These piles can have up to $300\,\mathrm{m}$ of length, $100\,\mathrm{m}$ of width and $40\,\mathrm{m}$ of height, as detailed in [67], stocking up to $100000\,\mathrm{Mg}$ of this kind of biomass. Therefore, from here onwards, it is assumed that each sugarcane-based microgrid has its own bagasse stockage area.

The sugarcane straw is composed of unseasoned leafs, dry leafs and by the sugarcane pointer. It is responsible for approximately one third of total primary energy source from the sugarcane, as detailed in [68], although it is not yet explored in its plenitude, given that, in Brazil, it is mostly left on the ground or burned, for a common practice is to pre-burn the canebrakes during the pre-harvest period. As these residues are either discarded or burned, new legislation (dating 2013) has been introduced[2] to avoid this is-

---

[2]*See: Brazilian Legislation from the state of São Paulo: Lei 11241/02 | Lei n. 11.241, from 19 September 2002.*

Figure 2.3: Bagasse Waste Stockage on a Sugarcane Processing Plant.

sue and, as an outcome, novel ways to re-use this residues have to be considered.

Finally, there is the vinasse [69], a destillation residue from the sugarcane juice (*garapa*), that can be transformed into biogas with the technology of anaerobic digestion [70]; the economic feasibility, energy potential and avoided CO_2 emissions with the use of vinasse biogas is discussed on [71].

In terms of quantification of these wasted residues: for every ton of processed sugarcane for the production of ethanol, around 730 kg of *garapa* and 250 kg of bagasse are obtained, see [72]. For every liter of ethanol produced in the distillation units, 12 liters of vinasse are obtained.

A complete discussion on the use of some of these sources as *biofuel* possibilities and some future projections are seen in [73]. This work, on the other hand, is interested in the possibility of this sources for the *direct-to-electric-energy* generation, but it has to be clear that the sugar-cane processing plants produce sugar and, also, ethanol (*biofuel*).

2.2.1 Control Goals

Most of the current industrial Brazilian sugarcane processing plants have a similar structure. Therefore, these plants have similar kinds of internal demands:

1. to produce steam in different pressures (used to boost water pumps, spray pumps, exhausters, chippers, shredders and other equipments);

2. to produce cold water, for internal refrigeration needs (used to cool down generators, oil tanks from the distillery process and other systems present on the plant);

3. to produce electric power to sustain the plant, which corresponds, in average, to $8000\ kW$ of internal needs.

4. Apart from these three internal demands, most sugarcane processing plants also sell the excedent electric energy to a local Distribution Network Operator (*DNO*, i.e. the external network). In average, this corresponds to a contract of $753\ MWh$ per day of energy-generation. This power generation can be continuous, maintaining a constant value, or time-varying, with different values at each hour of the day.

Remark 6. *Satisfying one of these three demands alone is not adequate, as they are inextricably linked. As an example: increasing the amount of power supplied by the turbines also increases the amount of steam that is produced.*

As detailed in [74] and [66], a maximization of the calorific power can be achieved when mixing bagasse with straw leftovers. The straw has a high calorific power when compared to the bagasse, but it is normally very humid. For this, an appropriate choice of misture, given the average moistures of the collected bagasse and straw, can lead to a boost in the flow-to-steam gain of the boilers. As discussed in [2], the energetic potencial of these boilers can be increased when mixing bagasse and straw. It is important to remark that the amount of straw leftover from a sugarcane harvest is smaller than the residual bagasse amount and that, usually, the straw cannot boost boilers alone, due to its high moisture, and too much straw on a biomass mixture causes problems with the ignition of the boilers.

In average, the best possible mixture of bagasse and straw to boost boilers is 50% of each, as justified in [75], [76] and [77]. In fact, the optimal percentage varies according to the moistness of the collected straw and bagasse. Therefore, the mixture factor α_{mix} can be chosen as a function of the moistness of each input, i.e. $\alpha_{mix} = \alpha_{mix}(\text{moisture}_{Bag}, \text{moisture}_{Str})$.

2.2.2 Global Structure

The global structure of the considered (Brazilian) sugarcane-based microgrid is illustrated by the block-diagram in Figure 2.4, where Q_E^A and Q_E^B represent biomass mixture (bagasse plus straw) flows ($\frac{Mg}{h}$); the rest of the notation/nomenclature is given in Table 2.1. This microgrid is composed of the following subsystems: two boilers, with different efficiencies; two steam turbines, with different efficiencies; a combined heat and power system, hereafter denoted as *CHP*; a water chiller; photovoltaic panels; water heating solar panels (*WHS*); a wind turbine; two pressure reduction valves; one heat exchanger; stocks of bagasse, straw and compressed *bio-gas*; a hot water tank; and a battery bank.
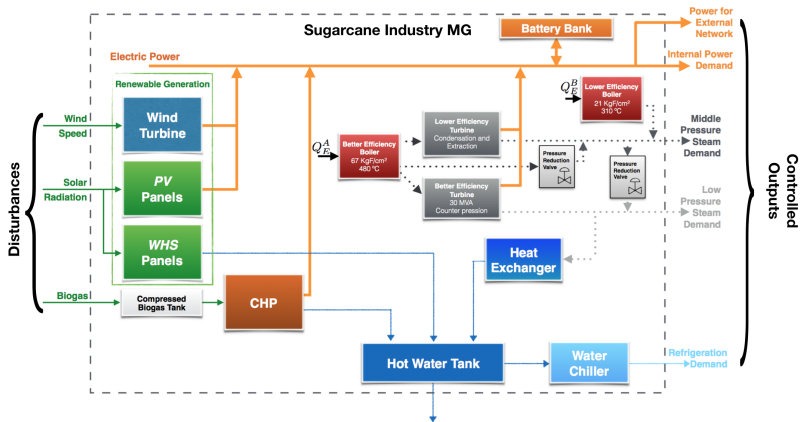
Figure 2.4: Sugarcane MG.

Table 2.2 further details the operational constraints of each of the microgrid subsystems. Note that if control performances are sought, these should always be respected.

Table 2.1: Sugarcane MG: Nomenclature.

Symbology	Manipulated Variable	Unit
SP_{TU}^{A}	Higher Eff. Turbine's SP	(kW)
SP_{TU}^{B}	Lower Eff. Turbine's SP	(kW)
Pot_{Net}	Power to the Ext. Net.	(kW)
SP_{C}^{B}	Boiler's SP	$\left(\frac{Mg}{h}\right)$
Q_{V}^{Out}	High-Mid. Press. Red. Valve's SP	$\left(\frac{Mg}{h}\right)$
Q_{Esc}^{M}	Mid. Press. Steam Escape Flow	$\left(\frac{Mg}{h}\right)$
Q_{Esc}^{B}	Low Pressure Steam Escape Flow	$\left(\frac{Mg}{h}\right)$
SP_{CHP}	*CHP*'s Set-point	(kW)
SP_{Ch}	Water Chiller's SP	$\left(\frac{m^3}{h}\right)$
SP_{TC}	Heat Exchanger's SP	$\left(\frac{m^3}{h}\right)$
Pot_{Bat}	Energy Flow to the Battery Bank	(kW)
Q_{V}^{MB}	Mid.-Low Press. Red. Valve's SP	$\left(\frac{Mg}{h}\right)$
Q_{Esc}^{Tank}	Hot Water Escape Flow	$\left(\frac{m^3}{h}\right)$

2.2.3 System Modelling

Now, the mathematical methodology used to model this system is detailed. In this work, the Energy Hubs methodology (see [78]) is followed.

An energy hub can be used to describe the interface between energy producers, consumers and the transmission line. From the system's outlook, a hub can be identified as a black box unit that comprises the following requirements: (1) input and output of electric power; (2) energy conversion; (3) energy storage.

The intermediate storage units present in the studied microgrid, the biomass stocks, tanks and the battery bank, are considered to be composed of an interface and an internal storage. The interface can be understood as an energy flow converter; the converted energy is stored in an ideal internal stage. Slightly adapted from the described methodology, the internal storage state of a hub, x_s evolves as follows:

$$\dot{x}_s(t) = A_s x_s(t) + \breve{u}_s^E(t) \qquad (2.1)$$

where the storage input flow $\breve{u}_s^E(t)$ stands for $\breve{u}_s^E(t) = e_s(t)u_s^E(t)$, being $u_s^E(t)$ the generic input flow to the storage and A_s an appropriate matrix. The efficiency of the hub's interface is represented by $e_s(t)$; notice that this factor depends on the direction of the ex-

j	Subsystem	Efficiency	Minimal Operating Point	Maximal Operating Point
1	Low Eff. Turbine	70 %	1000 kW	20000 kW
2	High. Eff. Turbine	65 %	1000 kW	27000 kW
3	Power House $\rightarrow$ *DNO*	–	0 MW	17 MW
4	Low Eff. Boiler	76.5 %	1 Mg/h	250 Mg/h
5	High-Mid. Pressure Red. Valve	25 %	0 Mg/h	550 Mg/h
6	Mid. Pressure Escape Valve	–	0 Mg/h	–
7	Low. Pressure Escape Valve	–	0 Mg/h	–
8	*CHP*	90 %	800 kW	8000 kW
9	Water Chiller ($200\,\text{m}^2$, $1.8\,\text{MW}_{peak}$)	78 %	$10\,\text{m}^3/\text{h}$	$110\,\text{m}^3/\text{h}$
10	Heat Exchanger	60 %	$130\,\text{m}^3/\text{h}$	$1.5\,10^4\,\text{m}^3/\text{h}$
11	Battery Bank	$\approx \pm 93\,\%$	-2500 kW	5000 kW
12	Mid.-Low Pressure Red. Valve	20 %	0 Mg/h	450 Mg/h
13	Water Tank Escape Valve	–	0 Mg/h	–

Table 2.2: Technical Information for Each Subsystem.

changed flow, if the storage unit is either being "*charged*" or "*discharged*".

    As described in [79], the continuous *state-space* representation model of the studied plant can be put as in (2.2). This mathematical model was obtained and validated through simulation based on experimental data; for full details refer to [2]. This model comprises the dynamics of the system's internal states (x), measured outputs (y) and controlled outputs (z). With this representation, the controlled outputs are those outputs that have some control perfomance specification, as settling time constraints, reference tracking, *etc*. Note that these are not necessarily all measured: $z \neq y$.

$$\Sigma_{\text{MG}} := \begin{cases} \dot{x}(t) &=& Ax(t) + B_1w(t) + B_2u(t) \\ z(t) &=& C_1x(t) + D_{11}w(t) + D_{12}u(t) \\ y(t) &=& C_2x(t) + D_{21}w(t) + D_{22}u(t) \end{cases} \quad (2.2)$$

    The system state vector is defined by Eq. (2.3), where each entry represents the normalized percentage of each stock: battery bank, bagasse stock, straw stock, *bio*-gas stock and hot water tank.

$$\begin{aligned} x(t) &= \begin{bmatrix} X_{Bat}(t) & X_{Bag}(t) & \dots \\ X_{Str}(t) & X_{Bg}(t) & X_T(t) \end{bmatrix}^T. \end{aligned} \quad (2.3)$$

    The complete manipulated variables, input vector is given by Eq. (2.4).

Remark 7. *Considering the control-oriented works [9], [59] and [11] that have dealt with this plant,* MPC *laws were developed with sampling periods of $\Delta T = 1\,h$. This means that the system's control inputs are zero-order-held continuous variables. These manipulated variables are defined individually in Table 2.1.*

Assumption 1. *Notice that the control signals $u(t)$ are set-points to the lower-level subsystems, to be treated by their internal controllers. As the Energy Hubs methodology is used for a third-level control point-of-view, this means that, if no fault occurs in the subsystems, the set-points have been accurately tracked by the internal controllers and the actuation to the plant is given by $u(t)$.*

$$u(t) \quad = \quad [\; SP_{TU}^A(t) \quad SP_{TU}^B(t) \quad Pot_{Net}(t) \quad \ldots \tag{2.4}$$
$$SP_C^B(t) \quad Q_V^{Out}(t) \quad Q_{Esc}^M(t) \quad \ldots$$
$$Q_{Esc}^B(t) \quad SP_{CHP}(t) \quad SP_{Ch}(t) \quad \ldots$$
$$SP_{TC}(t) \quad Pot_{Bat}(t) \quad Q_V^{MB}(t) \quad Q_{Esc}^T(t) \;]^T .$$

In terms of the system's controlled outputs, the output vector is defined by Eq. (2.5), being P_{Proc} the electric power produced due to the sugar cane processing demand (kW); Q_V^M the flow of middle pressure steam $(\frac{Mg}{h})$; Q_V^L the flow of low pressure steam $(\frac{Mg}{h})$; Q_{CW} the flow of chilled water required by the distillery process $(\frac{m^3}{h})$; finally, P_{Sale} represents the electric power made available to the external network (kW). These are the controlled outputs given that they are those that have to be controlled in order to attend the plant's demands.

$$z(t) \quad = \quad [\; P_{Proc}(t) \quad Q_V^M(t) \quad \ldots \tag{2.5}$$
$$Q_V^L(t) \quad Q_{CW}(t) \quad P_{Sale}(t) \;]^T .$$

The system's measured outputs are given by the internal states. As of this, one has:

$$y(t) \quad = \quad x(t) . \tag{2.6}$$

The external disturbances to the system are herein defined by Eq. (2.7), being Wnd_{in} the wind speed $(\frac{km}{h})$ present in the microgrid's area, used by the wind turbines to generate electric power; $Irrd_{in}$ the amount of solar irradiance $(\frac{W}{m^2})$ on the microgrid's solar panels; Bag_{in}, Str_{in} and Bg_{in} represent the input rate / intake $(\frac{Mg}{h})$ of bagasse, straw and (compressed) *bio*-gas in their stocks, respectively.

Remark 8. *The bagasse, straw and bio-gas incomes are proportional to the sugar cane crop harvest. This means that these curves are completely known and do not have to be estimated. Nonetheless, both wind speed (Wnd_{in}) and solar irradiance $(Irrd_{in})$ curves are unknown, with only registered historical data being available, although they can be estimated if accurate weather information is available.*

$$w(t) \quad = \quad [\; Wnd_{in}(t) \quad Irrd_{in}(t) \quad \ldots \tag{2.7}$$
$$Bag_{in}(t) \quad Str_{in}(t) \quad Bg_{in}(t) \;]^T$$

Remark 9. *Given that the considered sugarcane-based microgrid is modelled from a tertiary control level, it has **no dynamics**, but those of the integrator nodes (stocks). This model has 13 control inputs (set-points for the lower levels of control) and 5 controlled outputs, which means controllability is obviously guaranteed. As extensively discussed in [2], the control problem herein is not the usual stability / reference tracking / disturbance rejection performance enhancement, but how to coordinate this plant (choosing which energy system to use) in the most sustainable and profitable manner possible, knowing the availability of resources.*

Remark 10. *This state-space model can be given in a discrete-time version. This is done using $t = k\Delta T$, which implies, of course, on different matrices A to D_{22}. Throughout this work, the discrete-time versions of this model are taken with $\Delta T = 1\,h$, as done previously and justified in [9].*

2.3   FAULT MANAGEMENT

It has to be remarked that, up to the author's best knowledge, only few works have presented studies on Fault Detection for energy generation systems; these have been listed through the Introduction. For the case of sugarcane-based microgrids, such tools do not exist. In industrial practice, what is done is that, basically, some alarms are activated to indicate whenever a controlled subsystem escapes an operational range. This work hopes to point out pragmatic ways to develop such tool, which is done from Part II onwards.

3 THEORETICAL BACKGROUND

There are some essential theoretical concepts, theorems, lemmas, propositions, conjectures and mathematical unwindings that serve as background for what is presented in this Master Dissertation, in the sequel.

Due to lack of space (the Author does not seek for this document to be excessively long), an online Theoretical Lexicon is found in this Google Drive Link[1]. This Theoretical Lexicon is also included by the end of this Dissertation (after Bibliography, by the Appendixes, Part V).

Therefore, this Chapter will only list the essential concepts the reader must know to continue onto the developments of Part II. These concepts are:

1. Linear Algebra: notions of Singular Values (and decomposition), Vector Spaces, Signal Norms, System Norms.

2. Dynamic Systems: notions of *LTI* Control, Controllability, Observability, Closed-Loop Pole Placement and Asymptotical *LTI* Observers.

3. Linear Matrix Inequalities: Strict Linear Matrix Inequality constraints, Semi-Definite Programming, Quadratic Stability via Linear Matrix Inequalities, the Bounded Real Lemma and Schur Lemma.

4. H_∞ and H_2 Performances: via static state-feedback, dynamical output feedback and *LMI* procedures.

5. Robustness: notions of uncertainty modelling, *LFT*s and *LFR*s, robustness stability analysis, $M - \Delta$ representation, robust control design methods, μ-analysis.

6. Linear Parameter Varying Systems: basic representation, Nonlinear and Linear Differential Inclusion, *LPV* Classes and Models, *LPV* Control and Observation, Polytopic Approaches.

7. Stability: notions on well-posedness, BIBO stability, Lyapunov Stability, Stability of Linear Time-Invariant Systems, Stability of Linear Parameter Varying Systems, Nonlinear stability and Small Gain Theorem.

---

[1]<https://drive.google.com/file/d/
1gW-VPsRHfN1LIpu4L5ujSuf6kiZPhVRx/view?usp=sharing>

8. Optimal and Predictive Control: notions on Model Predictive Control, Process Models, Free and Forces Responses.

9. Fault-Tolerant Control: notions on Passive and Active approaches, *FDD* and *FE* schemes, reconfiguration mechanisms.

10. Modelling and Identification for Microgrids: notions on Energy Hubs and their state-space representation.

Part II

Central Development:
Observation and Monitoring

4 FAULT DETECTION FOR HYBRID ENERGY GENERATION SYSTEMS IN THE SUGARCANE INDUSTRY

4.1 ABOUT CHAPTER

The previous Chapters were introductory to this work. Now, this Chapter presents the first results that concern with the issue of estimating faults that occur in a renewable microgrid. These faults are estimated by an *LPV* observer that only measures the available outputs and control signals.

Global Objective GO 1 and GO 2 are tackled by this Chapter. Specific Objectives SO 1.1, 2.1 and 2.2 are also tackled herein.

Keywords: Fault Detection and Diagnosis; LPV systems; Energy mangament; Mixed H_2/H_∞ performance; Renewable sources.

The content of this Chapter derived the following work:

- [80] Morato, M. M., Mendes, P. R. C., Normey-Rico, J. E., Bordons, Carlos. *LPV-H_∞* **Fault Estimation for Boilers in Sugarcane Processing Plants**, presented in the 2nd *IFAC* Workshop on Linear Parameter Varying Systems, Florianópolis, Brazil, 2018. This publication tackled SO 2.1.

- [81] Morato, M. M., Mendes, P. R. C., Normey-Rico, J. E.. **Dealing with Faults to Improve Resilience of Microgrids**, submitted to the 2019 IEEE PES Innovative Smart Grid Technology Latin America (ISGT LA), Gramado, Brazil, 2019.

- [82] Morato, M. M., Regner, D. J., Mendes, P. R. C., Normey-Rico, J. E., Bordons, Carlos. **Fault Analysis, Detection and Estimation for a Microgrid via H_2/H_∞ *LPV* Observers**, published in the International Journal of Electrical Power & Energy Systems, 2019.

4.2 INTRODUCTION

As thoroughly discussed in the Introduction, the Control Systems community has given, in recent years, certain attention to the following question of prime importance: how can *renewables* be adequately integrated to modern grids. The concept of microgrids has been brought to focus, since it facilitates the modelling and control of (multi-source) energy plants, as well as the model integration of renewable sources to energy systems. This methodology is applied in [83] and [54], for example.

The optimal control of microgrids that include renewable and non-renewable sources, in order to maximize the use of *renewables* and economic profit, while complying with operational demands, has been treated, specially, with Model Predictive Control (*MPC*) based control schemes. This has been seen in a diverse set of works: [12] presents an *MPC*-controlled hydrogen-based domestic microgrid; papers [15] and [13] also deal with optimal generation for renewable microgrids; [84] presents an *MPC*-based framework for distributed energy management; [55] shows an *MPC* structure for energy management of experimental microgrids, coupled with hydrogen storage systems.

Note that the discussion of the effect of faults on this energy system is yet to be researched. Real instrumented systems present evermore an increase on complexity and become more vulnerable to faults and failures. This is also very true for energy systems and power microgrids. Possible faults on these systems may lead these plants to not comply with their operational constraints, which might result in economic deprivation and in a lack of the available power to the external network. To ensure sufficient measures of reliability and safety, fault detection methodologies have been sought. A fault detection system has been schematized by Figure 1.1, in the Introduction.

The detection of faults and failures in these energy systems can elevate internal system stability, safety and also enable the better management of energy. If a controller has accurate and timely knowledge about faulty situations, an active Fault Tolerant Control (*FTC*) scheme can be designed, as discussed in [85], to overcome the fault outcomes so that the energy production can be immune to faults, offering increased process availability, avoiding breakdowns from simple fault events.

An accurate Fault Detection and Diagnosis system is, then, of most importance for an *FTC* in order to provide it with timely information on the condition, subsystem (location), magnitude and type of fault event that occurs on the controlled plant (in this case, microgrid). In terms of *FDD* systems, some works opt for nonlinear model-based approaches, as those in [86], [87], [88] and [89]. Anyhow, a great deal of works suppose linear time-invariance system characteristics (*LTI* systems) and resort to parity-space and residual analysis, as those seen in [90], [18] and [91].

This usual *LTI* model-based *FDD* design method presents some troubles when dealing with operational point changes, once (false) fault alarms may appear. One key issue that has to be noticed is that

most of the cited works (both nonlinear and *LTI*) make use of the redundant availability of sensors in order to determine if the system is healthy or not. This issue can be overlapped, for instance, with the use of an observer-based *FDD*, as it has been deeply discussed in [27]. Thus, from the beginning of the 2000's, works have proposed gain-scheduled *FDD* design to extend the scope of the linear *FDD* methods to nonlinear systems. A natural idea is to extend *LTI* system models to *LPV* ones. Such models can be used to accurately describe some complex nonlinear plants, as demonstrate [92] and [93].

In comparison to the Linear Time-Invariant state-space representation, the *LPV* representation encompasses matrices that are dependent on known, bounded scheduling parameters. Therefore, an *LPV*-based fault estimation system can, in an autonomous manner, re-adjust and schedule itself depending on the observed plant's operating point, according to the scheduling parameter. Choosing an *LPV* system representation is an interesting option, as it represents something in between the full nonlinear designs and *LTI* methods based on a fixed operating condition, since most of the conveniencies of *LTI* synthesis are present and, still, good performance and stability conditions can be guaranteed over a broader operating set.

In terms of *LPV* design, the Control Systems community has given attention mostly to controller synthesis, as in [94] and [95], although literature on *LPV*-based *FDD* is still slightly limited. Anyhow, the *LPV*-based observer design method to estimate faults is quite advantageous, as it can present good results with somewhat easy implementation and not needing any additional sensors. This Chapter opts for this kind of approach.

A few of these recent *LPV-FDD* works have presented strong results that also include some experimental validation. These are: the paper [96] shows the application of model-based *LPV FDD* to an industrial benchmark; an *FTC* strategy for actuator faults on helicopters is seen in [97]; an adaptive fault estimation scheme is also applied to helicopter models in [98]; recently, [99] showed fault estimation for discrete *LPV* systems, with the use of switched observers; in [100], where a method is presented for the synthesis of *FDD* filters based on an *LMI* solution for polytopic *LPV* systems and in [101], where an *LMI*-based pole-placement robust *LPV* estimator is presented.

4.2.1 Studied Problem

Given the presented context, the following novel discussion is the main purpose of this work: how to analyse, detect, diagnose faults on hybrid energy generation plants with a broader view, focusing on all possible faults on all subsystems from a higher (supervisory) level, without any additional sensors? This Chapter discusses the use of *LPV*-based *FDD* to detect and estimate these faults, that usually stand for sensor malfunctions, gain decrease on boilers and turbines due to accumulated dirt and many others.

4.2.2 Main Contributions

This Chapter aims to unravel a solid framework on how to detect and diagnose faults on a hybrid power plant. The main contributions are listed next :

(i) First of all, based on real data, this Chapter tries to mangle out all the possible faults that might occur on the studied microgrid, categorizing and sorting them out in terms of magnitude, location, type, reason and effect. Then, the faults are modelled as different multiplicative factors;

(ii) Secondly, a bank of *LPV* observers is designed to detect and diagnose each of these faults, considering a mixed H_2/H_∞ synthesis.

(iii) Also, a simple search algorithm is presented in order to categorize the estimated faults.

(iv) With the aid of a high-fidelity simulation model, results are delivered to enlighten the effectiveness of the proposed approach.

This Chapter is organized as follows: in Section 4.3, the discussion of all possible faults on the studied (Brazilian sugarcane-based) microgrid is shown, leading to a faulty system representation; then, in Section 4.4, the proposed *LPV* Fault Detection and Diagnosis system is designed; finally, Section 4.5 presents results in terms of simulation and a thorough discussion is drawn; the chapter ends with conclusions.

4.3 FAULT ANALYSIS AND MODELLING

With respect to the context detailed in Chapter 2, the micro-grid under investigation is based on a sugarcane processing plant, considering biomass, *bio*-gas, solar and wind power energy as primary energy sources. Since this system has been previously (thoroughly) explained, this Section goes into details about all the possible faulty situations that might occur upon this microgrid and each of its subsystems.

To model the possible faults on a given subsystem j, this work follows a multiplicative fault representation with accordingly *loss of effectiveness* time-varying factors λ_j. This solid fault representation framework has been introduced in [102] and, in short, it is assumed that the real, faulty actuation to the energy system, given by $u_f(t)$, is proportionally dependent on the expected, faultless actuation $u(t)$. This is represented in Figure 4.1. The loss of effectiveness factors of $\lambda_j(t) = 1$ stand for faultless situations, while $\lambda_j(t) = 0$ represents that subsystem j has a complete failure or breakdown;
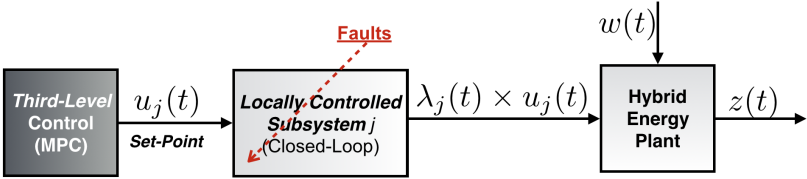
Figure 4.1: Fault Representation on Local Subsystem j.

In mathematical terms, whenever one subsystem j is faulty, despite the possibility of the others also being faulty, the whole energy system's state-space representation (2.2) changes to:

$$\Sigma_{\text{MG}}^{\text{faulty}} := \begin{cases} \dot{x}(t) &= & Ax(t) &+ & B_1 w(t) \\ & & + & B_2^j u_j^{\text{f}}(t) &+ & B_2^{j\star} u_{ot}^j(t) \\ z(t) &= & C_1 x(t) &+ & D_{11} w(t) \\ & & + & D_{12}^j u_j^{\text{f}}(t) &+ & D_{12}^{j\star} u_{ot}^j(t) \\ y(t) &= & C_2 x(t) &+ & D_{21} w(t) \\ & & + & D_{22}^j u_j^{\text{f}}(t) &+ & D_{22}^{j\star} u_{ot}^j(t) \end{cases}, \tag{4.1}$$

where the (faulty) actuation of subsystem j is given by:

$$u_j^{\text{f}}(t) = \lambda_j(t) u_j(t), \tag{4.2}$$

with n_x, n_u, n_y and n_z standing, respectively, for the number of states, control inputs, measured outputs and controlled outputs. And, finally, with:

$$
\begin{aligned}
u_{ot}^j(t) &= \mathrm{col}\{u_m^{\mathrm{f}}\} \\
\text{for } m &\in \{1, 2, \ldots, j-1\} \cup \{j+1, j+2, \ldots, n_u\}.
\end{aligned}
\tag{4.3}
$$

Synthetically, the notation $\mathcal{M}^j$ stands for the j-column of matrix $\mathcal{M}$, while $\mathcal{M}^{j\star}$ stands for matrix $\mathcal{M}$ with the j-column suppressed. And, thus, $u_{ot}^j(t)$ is the vector of all other (possibly faulty) control inputs, not considering $u_j^{\mathrm{f}}(t)$. An example of the used notation is given below.

Example 1.

$$
u = \begin{bmatrix} u_1 & u_2 & u_3 \end{bmatrix}, \tag{4.4}
$$

$$
u_2^f = \begin{bmatrix} \lambda_2 u_2 \end{bmatrix} \tag{4.5}
$$

$$
u_{ot}^2 = \begin{bmatrix} \lambda_1 u_1 & \lambda_3 u_3 \end{bmatrix}, \tag{4.6}
$$

$$
\mathcal{M} = \begin{bmatrix} m_{11} & m_{12} & m_{13} \\ m_{21} & m_{22} & m_{23} \\ m_{31} & m_{32} & m_{33} \end{bmatrix}, \tag{4.7}
$$

$$
\mathcal{M}^2 = \begin{bmatrix} m_{12} \\ m_{22} \\ m_{32} \end{bmatrix}, \tag{4.8}
$$

$$
\mathcal{M}^{2\star} = \begin{bmatrix} m_{11} & m_{13} \\ m_{21} & m_{23} \\ m_{31} & m_{33} \end{bmatrix}. \tag{4.9}
$$

Remark 11. *The multiplicative commutative property is valid for both variables λ_j and u because, at a given instant $t = t_1$, they are both scalars.*

Now that the used fault modeling framework has been detailed, the focus is given to categorize which types of faults occur on each subsystem and what do they represent in terms of magnitude ($||\lambda_j||_2$), average time duration and periodicity. The following development was done based on real information and empirical study of two different sugarcane processing plants that burn biomass to sell their excedent energy to local *DNOs*, located in the states of *Paraná* and *São Paulo*, in Brazil. The whole sugarcane treatment process is carefully detailed in [63].

Remark 12. *Readers must bear in mind that the operation of sugar-ethanol power plants is as follows: for* 200 *days of the year (during the harvest), the operation is non-stop; while for the remaining months, the whole systems is manually put in rest for revisioning, conservation and maintenance services, as stated in [2]. This means that most faults that occur on the plant are only corrected after the whole harvest period, without being detected and revisioned while the energy is generated. As of this, the following detailed faults are, mainly, those that lead to a subsystem's (light) gain decrease and that would only be actually noted with maintenance and that, if detected, could be overlapped by a supervisory controller's operation.*

4.3.1   Subsystems 1-2: Turbines

Considering the energy-generation steam turbines present in the plant, two kinds of faults may occur. These are:

1. The burnt biomass on the boilers heats water and, thus, produces steam that rotates the turbines. Sometimes, the turbines' shovels may get stuck on the inner wall. In practice, if the shovels are not released quickly and the sheer stress does not decrease, the turbines stop their operation. This kind of event is rare but, once a shovel begins to halt its movement, the energy generation rapidly ends (at most, two hours later). In terms of the turbines' effectiveness, this can be represented by a fast-decaying exponential curve, going from 1 to 0 in a period of 2 h.

2. If a manual stop is imposed to the turbines, the output produced energy becomes null, instantaneously. This is represented by the use of a step function, going to zero.

4.3.2   Subsystem 3: Power House

In terms of the power house station, some faults may occur when providing the external network (*DNO*) with energy. The Reader should bear in mind that the power house has many relays, converters, transformers, rectifiers and inverters.

1. Firstly, a very usual fault that occurs is the faulty operations of the main relays. This means that the output power to the external network fluctuates over the expected value, with up to 10 % loss. Globally, this can be represented by a fast-decaying

(within one hour) sinusoidal curve going from 1 to 0.9 with amplitude of $\pm 0.3\,\%$, in terms of the effectiveness of the output power.

2. Also, a complete failure in the connection to the outside network (in the inverters or transformers) may occur, leading the output power to zero within an hour. One hour is considered because there occurs an incipient delay when inverters and transformers fail (due to electromagnetic issues) - they are not instantaneous.

3. Finally, the circuit breaker may be disarmed by a local operator, meaning that the output power goes null instantaneously. This is represented by the use of a step function, once more.

4.3.3   Subsystem 4: Biomass Boiler

Upon the steam-generation biomass-burning boiler, three main kinds of faults may occur. These are:

1. Of frequent happening, the debris and the residues from the burnt biomass accumulate on the burning reservoir. This prevents the total income volume of biomass and leads, bit by bit, to a *biomass-to-steam* gain decrease. The volume of debris and residues that gets stuck on the reservoir can lead up to a $25\,\%$ decrease on the boiler's gain. This phenomenon occurs slowly, during an interval of three to five days (up to $120\,\mathrm{h}$). Normally, it is corrected by the emptying of the reservoir. The mathematical model that can accurately represent this fault situation is a slow-decaying exponential curve.

2. If the (controlled) conveyor belt that brings the biomass to the burning reservoir gets stuck (this can happen for many different reasons) and does not move on, the entire operation of this subsystem is compromised. This is: within a very short interval (assumed as $1\,\mathrm{h}$), the boiler's gain goes null. Once again, a (fast) exponential decaying curve can model this phenomenon.

3. Likewise, if a manual stop is imposed to this subsystem, the same kind of fault event occurs, although instantly. This can be represented with the use of a step function, going to zero.

4.3.4   Subsystems $5, 6, 7 \& 12$: Pressure Valves

In terms of the (steam) pressure reduction valves, two kinds of faults are considered. These are:

1. A manual stop at the valves, from manual operators, that instantly close the passage of steam. This leads the output to go instantly null and can be represented by a step function.

2. Leakages of the steam might also occur, which implies in a loss of mass flow. This means that the output steam flow coming from the valves, when there is leakage, has less mass than the input flow. This leakages usually are of, at most, 15% and can be represented by a decaying exponential curve, with period of $2\,\text{h}$.

4.3.5   Subsystem 8: *CHP* Unit

The *CHP* Unit is a combined system that produces, simultaneously, hot water and electric power. It is powered by compressed *bio-gas* and has a very high efficiency in terms of input energy exploitation, as it uses the lost thermal energy from the burnt gas to heat water. In terms of faults, three main kinds may occur:

1. Although not so often, gas leakages might happen on these units. This prevents the expected amount of *biogas* to be present inside the *CHP*'s crankshaft chamber. Gradually, this implies in a *biogas-to-power* gain decrease. These leakages do not represent a completely opened duct, but small losses, of around 10%. This phenomenon occurs slowly, during a period of two to three days (up to $72\,\text{h}$). Normally, it is corrected by the replacement of the corrupted gas pipe. Once again, a mathematical model that can accurately represent this fault situation is, of course, a exponetially decaying curve.

2. Partial clogging may occur inside the hot water flow duct, which may be caused due to unexpected, small, unfiltered objects that appear inside the duct. In these units, usually, only light clogging occurs (of around 5% of lost water), over the course of three or four hours. The used mathematical model is an exponential function.

3. As in the other systems, if a manual stop is imposed to this subsystem, both its outputs (hot water and electric power) go instantly null. This is emulated by a step function.

4.3.6 Subsystem 9: Water Chiller

Considering the water chiller, that converts income hot water into refrigerated water, in order to attend to the microgrid's demands, only a manual (emergency) stop fault is considered. This subsystem is very robust and other process-related faults are either very slow or of very rare happening.

4.3.7 Subsystem 10: Heat Exchanger

In terms of the heat exchanger, that converts low pressure steam into hot water, two possible faulty situations are of interest:

1. Firstly, there might exist corrosion (oxidation given presence of steam) of its internal plates, leading to slow wear of its performance. This means that the effectiveness of the heat exchanger will decrease according to the degree of corrosion. This corrosion leads, at most, to a 20 % loss in up to three months. This is represented by an exponential function.

2. Also, a manual stop can be imposed to this subsystem, leading the hot water output flow to cease. This is emulated by a step function.

4.3.8 Subsystem 11: Battery Bank

The battery bank present in the studied plant is a robust Lithium-ion storage used to compensate the microgrid's internal energy fluctuations. In terms of the possible faults, these are listed below:

1. The battery bank's capacity is directly influenced by the outside room temperature. If a battery provides 100 % of its storage capacity at ambient temperature of 25 ℃, it (typically) only manages to deliver 50 % of its storage capacity at colder temperatures of −20 ℃. As the studied microgrid is set in a tropical country, the problem is faced when there is excessive heat. At 40 ℃, the loss on the batteries life-cycle can decrease up to 40 % [1]. Li-ion batteries suffer from stress when exposed to prolonged heating and, of course, this will be considered

---

[1]*This is just an example and these characteristic vary according to the battery's internal chemical dynamics.*

as a plausible faulty situation in this study. The mathematical model that can accurately represent this over-heating situation is a decaying exponential curve of up to $40\,\%$ with a period of $6\,h$ (assuming that the peak-temperatures in Brazil occur just after midday until the beginning of twilight).

2. As in the other systems, if a manual stop is imposed to the battery bank, its operation completely stops - mathematically, a step function, going to zero.

4.3.9   Subsystem 13: Tank's Water Valve

The faults considered to occur on the water valve are the same as those that appear on pressure reduction valve ($j = 5, 6, 7$ or 12), the only difference is that the ullage is of hot water, instead of steam.

4.3.10   Overview of Possible Faults

Given the chosen multiplicative representation of faults on the studied energy system and the analysis of each subsystem, Table 4.1 presents a synthetic overview of where each fault may occur at, its magnitude, its model and time-wise behaviour. In terms of the operational constraints of every (possibly faulty) subsystem, these are given by Table 2.2 (in Chapter 2). In the paper [82], some simulations are presented in order to illustrate the time-wise characteristics of these faults ($\lambda_j(t)$).

Remark 13. *The aim herein is not to understand the underlaying physics of each fault event (what happens in lower control layers), but to estimate them from a tertiary viewpoint, as loss of effectiveness factors.*

4.4   THE FAULT DETECTION AND DIAGNOSIS PROBLEM

Now that the system and its possible faults have been described, the main problem of this Chapter can, finally, be presented. How can faults on the studied microgrid be (accurately and efficiently) detected and diagnosed ? Answering this question can later on be used for surveillance and safety goals or even as a paradigm for a fault tolerant control strategy.

Considering the chosen fault modelling, the objective of this Chapter, then, is to estimate accurately each fault term $\lambda_j(t)$. To do

Subsystem	Type	λ_j	Model	Max. Period
$j = 1, 2$ Turbines	Stuck Shovel	$\lambda_{1,2} \to 0$	Decreasing Exp.	1 h
	Manual Stop	$\lambda_{1,2} \to 0$	Step	Instantaneous
$j = 3$ Power House	Relay Malfunc.	$0.87 < \lambda_3 < 1$	Decreasing Sine	1 h
	Connect. Fail.	$0 < \lambda_3 < 1$	Decreasing Exp.	1 h
	Manual Stop	$\lambda_3 \to 0$	Step	Instantaneous
$j = 4$ Biomass Boiler	Debris Acc.	$0.75 < \lambda_4 < 1$	Decreasing Exp.	120 h
	Conveyor Belt	$0 < \lambda_4 < 1$	Decreasing Exp.	1 h
	Manual Stop	$\lambda_4 \to 0$	Step	Instantaneous
$j = 5, 6, 7$ & 12 Valves	Leak.	$0.85 < \lambda_j < 1$	Decreasing Exp.	2 h
	Manual Stop	$\lambda_j \to 0$	Step	Instantaneous
$j = 8$ CHP Unit	Gas Leak	$0.90 < \lambda_8 < 1$	Decreasing Exp.	72 h
	Water Clog.	$0.95 < \lambda_8 < 1$	Decreasing Exp.	3 h
	Manual Stop	$\lambda_8 \to 0$	Step	Instantaneous
$j = 9$ Chiller	Stop	$\lambda_9 \to 1$	Step	Instantaneous
$j = 10$ Heat Exchanger	Oxidation of Plates Stop	$0.8 < \lambda_j < 1$	Decreasing Exp.	2160 h
	Stop	$\lambda_{10} \to 1$	Step	Instantaneous
$j = 11$ Battery Bank	High Temp.	$0.6 < \lambda_{11} < 1$	Decreasing Exp.	6 h
	Manual Stop	$\lambda_{11} \to 0$	Step	Instantaneous
$j = 13$ Water Valve	Leak.	$0.85 < \lambda_j < 1$	Decreasing Exp.	2 h
	Manual Stop	$\lambda_j \to 0$	Step	Instantaneous

Table 4.1: Fault Analysis: Type, Subsystems, Magnitude & Model.

so, the *FDD* system must be able to compute a good estimate of these terms given known manipulated variables $u(t)$ and measured outputs $y(t)$. This paradigm is represented by Figure 4.2.

Remark 14. *From a supervisory standpoint, the set-points $u(t)$ will be chosen by some optimal control scheme, as the one proposed in [59]. The lower-level local controllers will track these references in avid time such that the outputs of these subsystems (actuation to the energy generation system) is given by $u(t)$. Thus, there is still the need to detect possible faults on these subsystems, so that this fault information can be passed onto the higher-level controllers that (re-)adjust the set-points $u(t)$ correspondingly.*
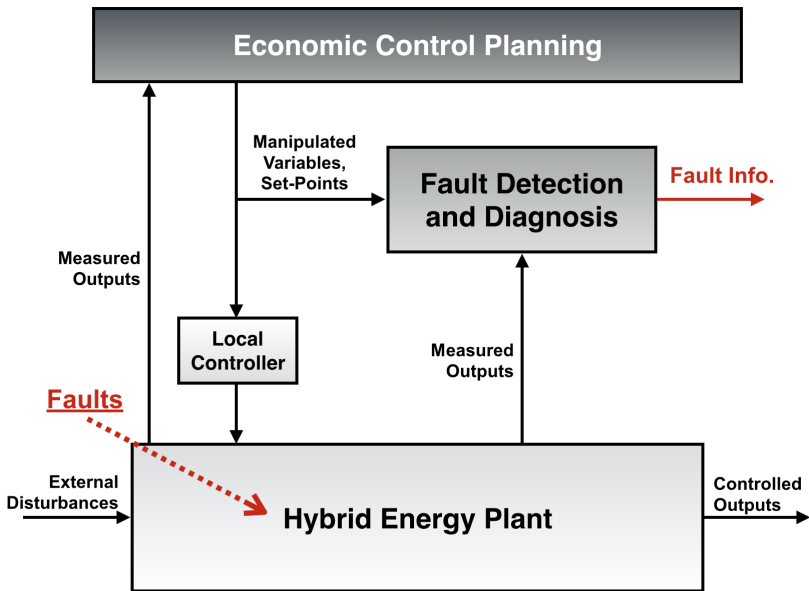
Figure 4.2: Fault Detection Paradigm.

4.4.1 External Disturbances & Measurement Noise

To further guarantee truthfulness to this study, two issues have to be taken into account, in terms of disturbance handling:

the effect of (measurement, instrumentation) noise and of external disturbances $w(t)$.

4.4.1.1 Measurement Noise

Considering that there always exists some high-frequency measurement noise ($\nu(t)$) associated to the measured outputs $y(t)$, the studied system (4.1) can be re-written as:

$$
\Sigma_{\text{MG}}^{\text{faulty}} := \left\{
\begin{array}{rclclcl}
\dot{x}(t) & = & Ax(t) & + & B_1 w(t) \\
+B_2^j u_j^{\text{f}}(t) & + & B_2^{j\star} u_{ot}^j(t) & + & B_\nu \nu(t) \\
y(t) & = & C_2 x(t) & + & D_{21} w(t) \\
+D_{22}^j u_j^{\text{f}}(t) & + & D_{22}^{j\star} u_{ot}^j(t) & + & D_\nu \nu(t)
\end{array}
\right. ,
\qquad (4.10)
$$

where B_ν and D_ν are adequate noise distribution matrices.

4.4.1.2 Renewable Disturbances

As described, three of the five disturbances to the system are well-known at every instant t, these are the incomes of bagasse, straw and *bio*-gas, that derive from the sugar cane income. Nonetheless, the solar irradiance and wind speed present on the field are completely unknown, a part from historical data.

Nonetheless, these two external, non-dispatchable disturbances can be partially estimated. This has been previously done in [59], where a Double Exponential Smoothing technique was applied, and also in [11], where Non-linear Auto-Regressive (*NAR*) Neural Networks (*NN*) were used. In both of these works, obviously, there always exists some prediction error. Synthetically, this means that $w(t)$ can be written as a sum of estimated and deviance (prediction error) parts, namely $\hat{w}(t)$ and $\epsilon(t)$:

$$
w(t) = \overbrace{
\begin{bmatrix}
\hat{Wnd}_{in}(t) \\
\hat{Irrd}_{in}(t) \\
Bag_{in}(t) \\
Str_{in}(t) \\
Bg_{in}(t)
\end{bmatrix}}^{\hat{w}(t)}
+ \overbrace{
\begin{bmatrix}
\epsilon_{Wnd}(t) \\
\epsilon_{Irrd}(t) \\
0 \\
0 \\
0
\end{bmatrix}}^{\epsilon(t)} .
\qquad (4.11)
$$

The method used in this Chapter to predict these non-dispatchable disturbances is based on *NAR NN* with time-delays, as done by

the Author in [11]. All background and mathematical formulation about this methodology can be found therein.

It is very important to state that the predictions were done for each disturbance with a $N_H = 12$ h-ahead horizon. These predictions are updated every $\Delta T = 1$ h. The considered Neural Networks for each of these two disturbances are detailed in Table 4.2.

Table 4.2: Neural Networks - Hourly Predictions.

	1 h - Wind S.	1 h - Solar Ir.
Layers	2	1
Neurons	[2 , 1]	1
Delay	[48 , 48]	288

The computation and training algorithm for each neural network was done through *MATLAB* [103] using *Levenberg-Marquardt* optimization algorithm [104], that settles the bias and weights for each neural network.

Below, in Figures 4.3 and 4.4, the prediction of Wind Speed and Solar Irradiance in a 12 h horizon are given, compared to real data.
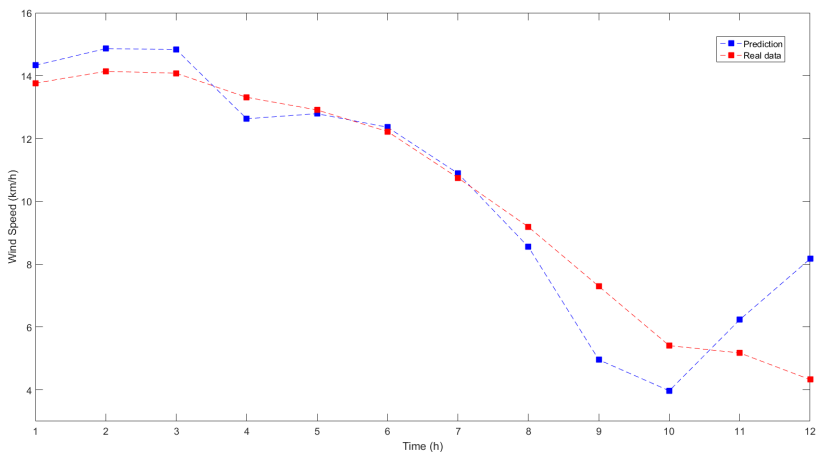
Figure 4.3: *NN* Estimated Curves: Wind Speed.
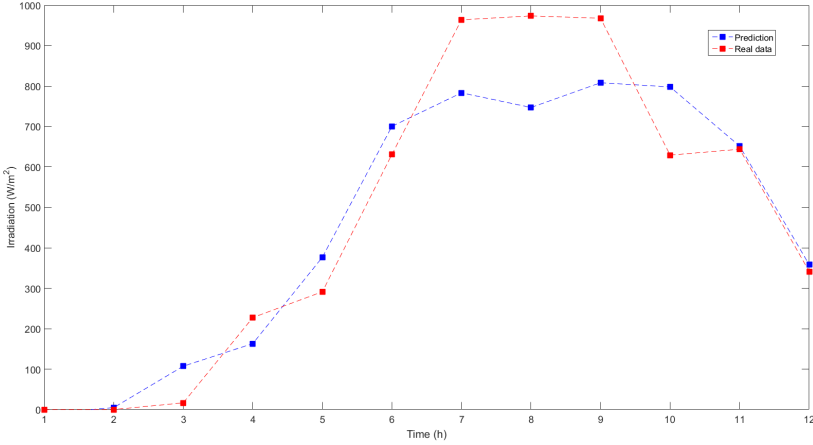
Figure 4.4: *NN* Estimated Curves: Solar Irradiance.

Table 4.3 also elucidates the efficiency of the presented estimation results, where the mean relative error,

$$MRE \quad = \quad \frac{\sum_{k=0}^{N_H}\left(|w_i(t)-\hat{w}_i(t)|/w_i(t)\right)}{N_H}, \qquad (4.12)$$

of these predictions is presented. Obviously, the prediction errors ($\epsilon_{Wnd}(t)$ and $\epsilon_{Irrd}(t)$) exist and have to be dealt with.

Table 4.3: Disturbance Estimates: Mean Relative Error.

Horizon	Wind Speed	Solar Rad Irrad.
1 h	17.8 %	16.5 %

4.4.2 *LPV* Extended-State Representation

In this Chapter, the first step towards the design of the *FDD* system is to describe the faulty energy generation system (4.1) inside n_u different polytopes $\mathcal{P}^j$. This will, further on, facilitate the design of an observer to asymptotically track each fault term λ_j.

Assumption 2. *Thanks to the multiplicative fault representation, the dynamics of each fault term $\lambda_j(t)$ can be assumed to be constant or*

slow-varying, this is: $\dot{\lambda}_j = 0$. Of course, this is a simplification, as each fault term can be more accurately represented by some model, as those summarized in Table 4.1. Nonetheless, as stated in [105], it is worth noting that even if $\lambda_j(t)$ is assumed to be constant, the corresponding additive fault magnitude to the energy system is given by $f_j(t) = [(1 - \lambda_j(t))u_j(t)]$, which is a time-varying signal that depends on the value of the expected actuation $u_j(t)$. Thus, this simplification is quite reasonable, considering the nature of the detailed faults, as put in Table 4.1.

Taking $x_a^j(t)$ as an augmented-state, the following representation is obtained:

$$
\overbrace{\begin{bmatrix} \dot{x}(t) \\ \dot{\lambda}_j(t) \end{bmatrix}}^{\dot{x}_a^j(t)} = \overbrace{\begin{bmatrix} A & \underbrace{B_2^j u_j(t)}_{B_\lambda^j} \\ 0 & 0 \end{bmatrix}}^{A_a^j} \overbrace{\begin{bmatrix} x(t) \\ \lambda_j(t) \end{bmatrix}}^{x_a^j(t)}
\tag{4.13}
$$

$$
+ \overbrace{\begin{bmatrix} B_\nu \\ 0 \end{bmatrix}}^{B_{\nu a}} \nu(t) + \overbrace{\begin{bmatrix} B_1 \\ 0 \end{bmatrix}}^{B_{1a}} \hat{w}(t)
$$

$$
+ \overbrace{\begin{bmatrix} B_2^{j\star} & B_1 \\ 0 & 0 \end{bmatrix}}^{B_q^j} \overbrace{\begin{bmatrix} u_{ot}^j(t) \\ \epsilon(t) \end{bmatrix}}^{q^j(t)},
$$

$$
y(t) = \overbrace{\begin{bmatrix} C_2 & \underbrace{D_{22}^j u_j(t)}_{D_\lambda^j} \end{bmatrix}}^{C_a^j} x_a^j(t)
\tag{4.14}
$$

$$
+ D_{21}\hat{w}(t) + D_\nu \nu(t)
$$

$$
+ \overbrace{\begin{bmatrix} D_{22}^{j\star} & D_{21} \end{bmatrix}}^{D_q^j} q^j(t).
$$

Remark 15. *In the augmented representation (4.13)-(4.14), the evolution of augmented-states x_a^j can be seen, in terms of estimated disturbances $\hat{w}$, measurement noise ν and compacted (all other) variables q^j. Then, if there exists some asymptotical tracking of x_a^j, the estimation of $\lambda^j(t)$ is explicit and direct.*

Remark 16. *It is important to notice that the matrices A_a^j and C_a^j are affine on $u_j(t)$, due to the terms (respectively) B_λ^j and D_λ^j.*

From this point, an *LPV* approach can be used to represent this extended system (4.13)-(4.14). Bearing in mind that each $u_j(t)$ represents a *set-point* to be passed to the j subsystem, that is essentially a known variable and, also, bounded, due to physical saturation constraints of the given subsystem j. Refer to Table 2.2 for the maximal and minimal values for each u_j (saturation limits). Then, it is imposed that:

$$u_j(t) \quad \in \quad \mathcal{P}^j\,, \tag{4.15}$$

$$\mathcal{P}^j \quad = \quad \{u_j^{min} \le u_j(t) \le u_j^{max}\}\,. \tag{4.16}$$

Thus, for every j augmented system representation x_a^j, a bounded scheduling parameter $\rho^j = u^j(t)$ is chosen so that, as matrices A_a^j and C_a^j are affine on ρ^j, system (4.13)-(4.14) can be re-written as a polytopic *LPV* system, defined inside the polytope $\mathcal{P}^j$.

This polytopic representation is given by the linear combination of two frozen *LTI* systems, at each vertex k of $\mathcal{P}^j$. This is:

$$\dot{x}_a^j(t) \quad = \quad \mathcal{F}^{min}(\rho^j)\mathcal{S}_{x_a}^{min}(\cdot) \tag{4.17}$$

$$+ \quad \mathcal{F}^{max}(\rho^j)\mathcal{S}_{x_a}^{max}(\cdot)\,,$$

$$y \quad = \quad \mathcal{F}^{min}(\rho^j)\mathcal{S}_y^{min}(\cdot) \tag{4.18}$$

$$+ \quad \mathcal{F}^{max}(\rho^j)\mathcal{S}_y^{max}(\cdot)\,,$$

with:

$$\mathcal{F}^{min}(\rho^j) \quad = \quad \frac{u_j^{max} - \rho^j}{u_j^{max} - u_j^{min}}\,, \tag{4.19}$$

$$\mathcal{F}^{max}(\rho^j) \quad = \quad \frac{\rho^j - u_j^{min}}{u_j^{max} - u_j^{min}}\,. \tag{4.20}$$

And:

$$
\begin{aligned}
\mathcal{S}_{x_a}^{min}(\cdot) &= A_a^j(u_j^{min})x_a^j(t) + B_{\nu a}\nu(t) \quad\quad\quad (4.21)\\
&+ B_{1a}\hat{w}(t) + B_q^j q^j(t)\,,\\
\mathcal{S}_{x_a}^{max}(\cdot) &= A_a^j(u_j^{max})x_a^j(t) + B_{\nu a}\nu(t) \quad\quad\quad (4.22)\\
&+ B_{1a}\hat{w}(t) + B_q^j q^j(t)\,,\\
\mathcal{S}_y^{min}(\cdot) &= C_a^j(u_j^{min}) + D_q^j q^j(t) + D_\nu\nu(t)\,, \quad (4.23)\\
\mathcal{S}_y^{min}(\cdot) &= C_a^j(u_j^{min}) + D_q^j q^j(t) + D_\nu\nu(t)\,. \quad (4.24)
\end{aligned}
$$

4.4.3   Bank of *LPV* Observers

The faulty system has been represented through an augmented framework in n_u different systems of states $x_a^j(t)$ that, each, contains the information on the possible faults of subsystem j, given by $\lambda_j(t)$. Then, synthetically, the problem is to identify each loss of effectiveness factor term $\lambda_j(t)$, that represents the studied faults on the hybrid power plant, only through the available measurements of $y(t)$. This fault detection paradigm has been presented in Figure 4.1 and can be done by an observer-based approach, as it is proposed next.

Similarly to what is seen in [106] and [100], n_u polytopic *LPV* observers can be designed to asymptotically track the states $x_a^j(t)$, each defined as:

$$
\begin{aligned}
\frac{d\hat{x}_a^j}{dt}(t) &= [A_a^j(\rho^j) - L^j(\rho^j)C_a^j(\rho^j)]\hat{x}_a^j(t) \quad\quad (4.25)\\
&+ L^j(\rho^j)[y(t) - D_{21}\hat{w}(t)]\\
&+ B_{1a}^j\hat{w}(t)\,,\\
\hat{\lambda}^j(t) &= \underbrace{\left[\begin{array}{cc} 0_{1\times n_x} & 1 \end{array}\right]}_{E^j}\hat{x}_a^j(t)\,, \quad\quad\quad (4.26)
\end{aligned}
$$

where $\hat{x}_a^j(t)$ and $\hat{\lambda}^j(t)$ stand, respectively, for the estimation of the augmented states and the loss of effectiveness term on subsystem j.

Considering the extended estimation error ($e^j(t) = x_a^j(t) - \hat{x}_a^j(t)$) and the fault estimation error ($e_\lambda^j(t) = \lambda_j(t) - \hat{\lambda}_j(t)$), the following dynamics are found:

$$\dot{e}^j(t) = [A_a^j(\rho^j) - L^j(\rho^j)C_a^j(\rho^j)]e^j(t) \qquad (4.27)$$
$$+ [B_q^j - L^j(\rho^j)D_q^j]q^j(t)$$
$$+ [B_{\nu a} - L^j(\rho^j)D_\nu]\nu(t),$$
$$e_\lambda^j(t) = E^j e^j(t). \qquad (4.28)$$

Remark 17. *To further ensure good results, term $[B_q^j - L^j(\rho^j)D_q^j]\hat{q}^j(t)$ can be added to the observer law (4.25), considering $\hat{q}^j(t)$ as a rough estimative of $q^j(t)$. This leads to a modification on the estimation error dynamics. Notice that the term*

$$[B_q^j - L^j(\rho^j)D_q^j]q^j(t)$$

becomes

$$[B_q^j - L^j(\rho^j)D_q^j][q^j(t) - \hat{q}^j(t)].$$

If the estimate is good, $[q^j(t) - \hat{q}^j(t)]$ is small enough and this term becomes null. To do so, the estimate is taken as follows:

$$\hat{q}^j(t) = [\; col\{u_m(t)\}^T \quad 0_{1,5} \;]^T, \qquad (4.29)$$

for $m \in \{1, 2, \ldots, j-1\} \cup \{j+1, j+2, \ldots, n_u\}$ - this is :for all other control inputs except u_j.

In fact, this is a close estimate to the actual $q^j(t)$, which is given by:

$$q^j(t) = [\; col\{\lambda_m(t)u_m(t)\}^T \quad \ldots \qquad (4.30)$$
$$[\; \epsilon_{Wnd}(t) \quad \epsilon_{Irrd}(t) \quad 0 \quad 0 \quad 0 \;] \;]^T,$$

with $\epsilon_{Wnd}(t)$ and $\epsilon_{Irrd}(t)$ non-null, but small.

Figure 4.5 illustrates the proposed approach to estimate faults on the studied hybrid microgrid, given by a bank of n_u LPV observers. Notice how there is no need for additional (redundant) sensors with this methodology, and the faults will be estimated solely based on $u(t)$, $y(t)$ and the known model of the microgrid.

4.4.3.1 Disturbance Handling

The estimation error dynamics (4.27) are influenced by the external disturbances q^j, given by the renewable prediction error
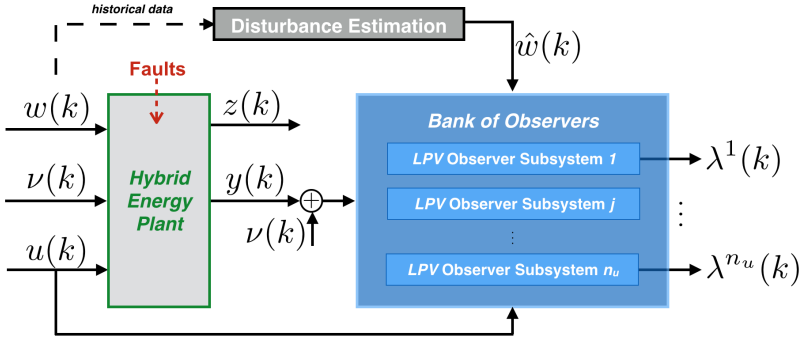
Figure 4.5: *FDD*: Bank of Observers.

(ϵ) and the actuation from other subsystem (u_{ot}^j), and by the measurement noise ν. To reduce the effect of these disturbances, when estimating each fault term λ^j, this study follows a mixed H_2/H_∞ sensitivity approach for the synthesis of the observers (4.25), as done in [107] and [108].

The H_2 norm of a system, through a stochastic point-of-view, is equal to the square-root of the asymptotic variance of the output when the input is a white noise. This means that, with this normed synthesis, in terms of the observer's performance, the measurement noise ν effect will be diminished when estimating $\lambda_j(t)$ - *impulse-to-energy* gain minimization.

On the other hand, the H_∞ norm of a system can be understood as the induced *energy-to-energy* gain, being the worst case attenuation level of a system to a given input. This means that, with this normed synthesis, in terms of the observer's performance, the influence of the additive disturbance q^j upon the estimation of λ^j will be minimized. Mathematically, the H_∞ norm definition of the error system (taking $q^j(t)$ as input) is given by:

$$||T_{e_\lambda^j q^j}||_\infty \quad = \quad \sup_{q^j \in \mathcal{H}_2} \frac{||e_\lambda^j||_2}{||q^j||_2}. \qquad (4.31)$$

It is explained in literature that the H_2 norm cannot ensure any reasonable degree of robustness. Also, it is well-known that the H_∞ norm cannot cope well with noise sensitivity, as some poor detection performances has already been seen, see [109]. Roughly

speaking, unknown inputs can be handled as bounded-power inputs (H_∞ approach) or fixed spectral density ones (H_2 approach). Nonetheless, in real situations, unknown inputs are of both types, as clearly seen in Eq. (4.27). So, the obvious synthesis is mixed H_2/H_∞ one, aiming to minimize, in the H_2 sense, the effect of ν on e_λ^j and, also, the effect of q^j on e_λ^j, in the H_∞ sense. This is: noise filtering *plus* additive disturbance attenuation. Thus, the following problem is detailed, adapted from [110] and [111].

Problem 1. *The mixed H_2/H_∞ LPV observer problem is defined as follows: Find a gain matrix $L^j(\rho^j)$, affine on the scheduling parameter ρ^j and defined within the polytope $\mathcal{P}^j$ so that the estimation error dynamics, given by Equation (4.27), are exponentially stable (considering $\nu(t)$ and $q^j(t)$ are null) and that the two following objective functions are minimized:*

$$J_{H_2} \quad = \quad ||\tfrac{e_\lambda^j}{\nu}||_2 \quad \leq \quad \gamma_{H_2}^j \qquad (4.32)$$

under $\quad e(t)|_{t=0} = 0 \quad$ *and* $\quad q^j(t) \equiv 0$,

$$J_{H_\infty} \quad = \quad ||\tfrac{e_\lambda^j}{q^j}||_\infty \quad \leq \quad \gamma_{H_\infty} \qquad (4.33)$$

under $\quad e(t)|_{t=0} = 0 \quad$ *and* $\quad \nu(t) \equiv 0$.

4.4.3.2 Problem Solution

The solution to this polytopic *LPV* observer with a H_2/H_∞ criterion is presented by the following Lemma. This solution represents, after all, the key to the proposed *FDD* scheme, that is based on n_u observers, as depicted by Figure 4.5.

A widely explored control design framework is the mixed H_2/H_∞ criterion, that ensures robustness (H_∞ property), while minimizing signal energy (H_2 property). The H_∞ approach is essentially based on the worst case performance analysis, therefore it provides lower performances with bigger robustness margins. Nonetheless, the H_2 approach stands for an average performance, although providing smaller robustness margins. Since both these criteria share the same formalism, they can be associated in an unified synthesis.

Lemma 1. *The mixed H_2/H_∞ synthesis consists in imposing Equations (4.32) and (4.33). This criterion to compute the polytopic LPV observer matrix gain L^j is obtained by minimizing the scalars $\gamma_{H_2}^j$ and*

$\gamma_{H_\infty}^j$ and solving the following Linear Matrix Inequalities (LMIs), exposed in Equations (4.34)-(4.38), taking $Q^j(\rho) = P^j L^j(\rho)$, with P^j and N^j being two positive definite matrices. All matrices dependent on ρ^j are affine-dependent.

$$Tr(N^j) \leq \gamma_{H_2}^j, \tag{4.34}$$

$$\begin{bmatrix} (\mathcal{K}^j)_{11}^1 & (\mathcal{K}^j)_{12}^1 \\ \star & (\mathcal{K}^j)_{22}^1 \end{bmatrix} < 0, \tag{4.35}$$

$$(\mathcal{K}^j)^2 < 0, \tag{4.36}$$

$$\begin{bmatrix} (\mathcal{K}^j)_{11}^3 & (\mathcal{K}^j)_{12}^3 \\ \star & (\mathcal{K}^j)_{22}^3 \end{bmatrix} > 0, \tag{4.37}$$

$$\begin{bmatrix} (\mathcal{K}^j)_{11}^4 & (\mathcal{K}^j)_{12}^4 & (E^j)^T \\ \star & -\mathbb{I}\gamma_{H_\infty}^j & 0 \\ \star & \star & -\mathbb{I}\gamma_{H_\infty}^j \end{bmatrix} < 0. \tag{4.38}$$

$$\begin{aligned}
(\mathcal{K}^j)_{11}^1 &= (A_a^j(\rho^j))^T P^j + P^j A_a^j(\rho^j) & (4.39) \\
&\quad - (C_a^j(\rho^j))^T (Q^j(\rho^j))^T - Q^j(\rho^j) C_a^j(\rho^j), \\
(\mathcal{K}^j)_{12}^1 &= -Q^j(\rho^j), & (4.40) \\
(\mathcal{K}^j)_{22}^1 &= -(E^j)^T E^j, & (4.41) \\
(\mathcal{K}^j)^2 &= 2\phi^j P^j + (A_a^j(\rho^j))^T P^j & (4.42) \\
&\quad + P^j A_a^j(\rho^j) \\
&\quad - (C_a^j(\rho^j))^T (Q^j(\rho^j))^T - Q^j(\rho^j) C_a^j(\rho^j), \\
(\mathcal{K}^j)_{11}^3 &= N^j, & (4.43) \\
(\mathcal{K}^j)_{12}^3 &= B_{\nu a}^T P^j - D_\nu^T (Q^j(\rho^j))^T, & (4.44) \\
(\mathcal{K}^j)_{13}^3 &= P^j, & (4.45) \\
(\mathcal{K}^j)_{11}^4 &= (A_a^j(\rho^j))^T P^j + P^j A_a^j(\rho^j) & (4.46) \\
&\quad - (C_a^j(\rho^j))^T (Q^j(\rho^j))^T - Q^j(\rho^j) C_a^j(\rho^j), \\
(\mathcal{K}^j)_{12}^4 &= P^j B_q^j - Q^j(\rho^j) D_q^j. & (4.47)
\end{aligned}$$

Proof. To solve Problem 1 and guarantee that the objective functions J_{H_2} and J_{H_∞} are minimized, the four conditions listed below have to be satisfied. Note that $T_{e_\lambda^j \nu}(s)$ stands for the transfer function from $\nu(t)$ to $e_\lambda^j(t)$, neglecting q^j, and $T_{e_\lambda^j q^j}(s)$ stands for the transfer function from $q^j(t)$ to $e_\lambda^j(t)$, neglecting ν.

(i) The stability of $T_{e_\lambda^j \nu}(s)$;

(ii) The maximum bound (H_2 sense) upon $||T_{e^j \nu}(s)||_2$ to be given by $\gamma_{H_2}^j$.

(iii) The stability of $T_{e_\lambda^j q^j}(s)$;

(iv) The maximum bound (H_∞ sense) upon $||T_{e^j q^j}(s)||_\infty$ to be given by $\gamma_{H_\infty}^j$.

Note, beforehand, that for the H_2 criterion conditions (*i-ii*), q^j is neglected while ν is taken as the sole input to the error system (4.27) and, likewise, for the H_∞ criterion conditions (*iii-iv*), ν is neglected while q^j is taken as the sole input to the error system (4.27). This is an obvious path.

Condition *i*:

The stability of $T_{e^j \nu}(s)$ can be achieved using the Ricatti equation, if there exists some positive definite symmetric matrix P^j such that:

$$
\begin{aligned}
(A_a^j - L^j C_a^j(\rho^j))^T P^j &+ \\
P^j (A_a^j - L^j C_a^j)(\rho^j) + (E^j)^T E^j &< 0
\end{aligned}
\tag{4.48}
$$

With the Schur complement[2], Equation (4.48) can be equivalently converted to:

$$
\begin{bmatrix} (\mathcal{K}^j)_{11}^5 & (\mathcal{K}^j)_{12}^5 \\ \star & (\mathcal{K}^j)_{22}^5 \end{bmatrix} < 0
\tag{4.49}
$$

$$
\begin{aligned}
(\mathcal{K}_{11}^j)^5 &= (A_a^j - L^j C_a^j(\rho^j))^T P^j \\
&+ P^j (A_a^j - L^j C_a^j)(\rho^j)
\end{aligned}
\tag{4.50}
$$

$$
\begin{aligned}
(\mathcal{K}_{12}^j)^5 &= -(L^j C_a^j(\rho^j))^T P(\rho^j) \\
&+ P(\rho^j)(-L^j C_a^j)(\rho^j)
\end{aligned}
\tag{4.51}
$$

$$
(\mathcal{K}^j)_{22}^5 = -(E^j)^T E^j
\tag{4.52}
$$

The above matrix inequality is nonlinear in terms of $L^j(\rho^j)$ and P^j. Then, taking $L^j(\rho^j) = (P^j)^{-1} Q^j(\rho^j)$, it can be reformulated as *LMI* (4.35).

---

[2]Refer to [112].

Condition *ii*:
Moving on to the H_2 upper bound, one aims:

$$||T_{e^j\nu}(s)||_2 \leq \gamma_{H_2}^j \tag{4.53}$$

The following development:

$$||T_{e^j\nu}(s)||_2 = \int_0^{+\infty} \text{Tr}\{\mathcal{T}\}dt, \tag{4.54}$$

$$\mathcal{T} = (B_{\mathcal{T}}(\rho^j))^T e^{(A_a^j(\rho^j))^T t}(E^j)^T E^j e^{A_a^j(\rho^j)t} B_{\mathcal{T}}(\rho^j), \tag{4.55}$$

$$B_{\mathcal{T}}(\rho^j) = B_{\nu a} - L^j(\rho^j)D_\nu, \tag{4.56}$$

$$P_0 = \int_0^{+\infty} e^{(A_a^j)^T(\rho^j)t}(E^j)^T E^j e^{A_a^j(\rho^j)t}dt. \tag{4.57}$$

leads to:

$$||T_{e^j\nu}(s)||_2 = \text{Tr}\{(B_{\mathcal{T}}(\rho^j))^T P_0 B_{\mathcal{T}}(\rho^j)\}. \tag{4.58}$$

Then, suppose that there exists a positive definite symmetric matrix P^j such that:

$$\text{Tr}\{(B_{\mathcal{T}}(\rho^j))^T P B_{\mathcal{T}}(\rho^j)\} > \tag{4.59}$$
$$\text{Tr}\{(B_{\mathcal{T}}(\rho^j))^T P_0 B_{\mathcal{T}}(\rho^j)\},$$

As

$$\text{Tr}\{(B_{\mathcal{T}}(\rho^j))^T P_0 B_{\mathcal{T}}(\rho^j)\} = ||T_{e^j\nu}(s)||_2, \tag{4.60}$$

it is true that:

$$\text{Tr}\{(B_{\mathcal{T}}(\rho^j))^T P B_{\mathcal{T}}(\rho^j)\} > ||T_{e^j\nu}(s)||_2. \tag{4.61}$$

Then, suppose there exist another positive definite symmetric matrix $N^j \geq 0$ that satisfies:

$$N^j - (B_{\mathcal{T}}(\rho^j))^T P^j B_{\mathcal{T}}(\rho^j) \geq 0 \tag{4.62}$$

and

$$\text{Tr}\{N^j\} \geq \gamma_{H_2}^j. \tag{4.63}$$

This implies that:

$$\text{Tr}\{(B_{\mathcal{T}}(\rho^j))^T P^j B_{\mathcal{T}}(\rho^j)\} \leq \text{Tr}\{N^j\}. \tag{4.64}$$

Using the Schur complement, this is equivalently expressed as:

$$
\begin{bmatrix} N^j & (B_\mathcal{T}(\rho^j))^T P^j \\ \star & P^j \end{bmatrix} \quad < \quad 0 \tag{4.65}
$$

The above matrix inequality is nonlinear in terms of $L^j(\rho^j)$ and P^j. Then, taking $L^j(\rho^j) = (P^j)^{-1} Q^j(\rho^j)$, it can be reformulated as *LMI* (4.37).

Notice that as $\text{Tr}\{N^j\} \geq \gamma_{H_2}^j$, the H_2 norm upper bound on $||\frac{e_\lambda^j}{\nu}||_2$ is given by $\gamma_{H_2}^j$.

Conditions *iii* and *iv*:

Both these conditions can be expressed quite directly by the used of Bounded Real Lemma[3] upon the error system (4.27). This is: system (4.27) is internally stable and with $||T_{e^j q^j}(s)||_\infty \leq \gamma_{H_\infty}$ if and only if there exists a positive definite symmetric matrix P^j such that the following matrix inequality holds:

$$
\begin{bmatrix} (\mathcal{K}^j)_{11}^6 & (\mathcal{K}^j)_{12}^6 & (\mathcal{K}^j)_{13}^6 \\ \star & -\mathbb{I}\gamma_{H_\infty}^j & 0 \\ \star & \star & -\mathbb{I}\gamma_{H_\infty}^j \end{bmatrix} \quad < \quad 0 \tag{4.66}
$$

$$
\begin{aligned}
(\mathcal{K}^j)_{11}^6 &= (A_a^j - L^j C_a^j(\rho^j))^T P^j \tag{4.67} \\
&+ P^j(A_a^j(\rho^j) - L^j(\rho^j) C_a^j(\rho^j)) \\
(\mathcal{K}^j)_{12}^6 &= P^j(B_q^j - L^j(\rho^j) D_q^j) \tag{4.68} \\
(\mathcal{K}^j)_{13}^6 &= (E^j)^T \tag{4.69}
\end{aligned}
$$

Reader must notice how the above inequality is nonlinear in terms of $L^j(\rho^j)$ and P^j. To overcome this problem, a change of variables is introduced, $L^j(\rho^j) = (P^j)^{-1} Q^j(\rho^j)$. After some algebrae, this non-convex problem can be easily reformulated as the convex *LMI* (4.38).

Solution:

Then, to solve Problem 1 and guarantee conditions *i* to *iv*, the following *LMIs* have to be solved:

(i) Condition (*i*) is guaranteed if *LMI* (4.35) holds;

(ii) Condition (*ii*) is guaranteed if *LMIs* (4.34) and (4.37) hold;

---

[3]Refer to [113].

(iii) Conditions *(iii)*-*(iv)* is guaranteed if *LMI* (4.38) holds.

And, for them to hold, there must exist adequate positive definite symmetric matrices P^j and N^j and block matrix $Q^j(\rho^j)$. These adequate matrices can be found with the aid of semi-definite programming softwares. These softwares resort to solving the optimization problem described above under the constraint of minimizing parameters $\gamma_{H_2}^j$ and $\gamma_{H\infty}^j$. This is: finding matrices P^j, Q^j and N^j in such way that the four *LMIs* hold and that the two parameters are the minimal possible.

This concludes proof.   □

Remark 18. *About the* LMI*s:*

1. *A weighting function can be appropriately introduced to specify the frequency range within which sensor noises should be attenuated. Besides, (obviously) sensor noise is considered as a high frequency signal (matrices B_ν and D_ν);*

2. *The scalar ϕ^j in the* LMI *(4.36) is a root-locus condition imposed upon the eigenvalues of $(A_a^j(\rho^j) - L^j(\rho^j)C_a^j(\rho^j))$: their real part must be greater, in module, than ϕ^j (chosen according to the settling time restrictions of each subsystem) $Re\{eigenvalues\} \leq \phi^j$ - this comes from the Ricatti condition;*

3. *The maximal variance of the estimation error, due to the presence of measurement noise $\nu(t)$, with this solution, is given by $Tr(N^j) = \gamma_{H_2}^j$. The maximal amplification of the estimation error, with this solution, due to the presence of the additive disturbance $q^j(t)$ is given by $\gamma_{H\infty}^j$.*

The interest of this polytopic *LPV* approach is that the *LMIs* (4.34)-(4.37) are computed *offline*, at the two vertices of each polytope $\mathcal{P}^j$. Then, each observer gain matrix $L^j(\rho)$ is given by a linear combination of $(L^j)^{max}$ (at $u_j = u_j^{max}$) and $(L^j)^{min}$ (at $u_j = u_j^{min}$), with $L^j(\rho)$ being affine on the scheduling vector ρ^j and guaranteeing the exponential stability of the estimation error dynamics (4.27). This is demonstrated by Equation (4.70). This means that, in finite time, each fault term $\lambda_j(t)$ will be accurately determined by its respective observer. Furthermore, there is no need for extra sensors with the proposed approach, as it is needed by many *FDD* techniques.

$$L^j(\rho^j) = \mathcal{F}^{min}(\rho^j)(L^j)^{min} \qquad (4.70)$$
$$+ \mathcal{F}^{max}(\rho^j)(L^j)^{max}.$$

4.4.4   Solution Analysis

Table 4.4 presents the achieved (H_2, H_∞) bounds in terms of the computation of the *LMI* problem, given by (4.34)-(4.38) and presented in Lemma 1. Therein, $\gamma^j_{H_2}$ and $\gamma^j_{H_\infty}$ stand, respectively, for the maximal singular values of $||\frac{e^j_\lambda}{\nu}||_2$, at u^{min}_j and u^{max}_j and the maximal singular values of $||\frac{e^j_\lambda}{q^j}||_\infty$, at u^{min}_j and u^{max}_j. The H_2 norm parameters $\gamma^j_{H_2}$ were fixed at 10^{-3} to overcome the non-convexitivity of the *LMIs*.

Remark 19. *The above* LMI *problem is non-convex problem because both scalars $\gamma^j_{H_2}$ and $\gamma^j_{H_\infty}$ are sought to be minimized. In order for it to be properly solved, $\gamma^j_{H_2}$ is fixed, whereas $\gamma^j_{H_\infty}$ is minimized. This procedure is detailed in [116]. If a trade-off between H_2 and H_∞ performances is sought, an adequate approach would be to solve the* LMI *problem minimizing the convex sum $\mathcal{S}(\gamma^j_{H_2}, \gamma^j_{H_\infty}) = \theta^j \gamma^j_{H_2} + (1 - \theta^j)\gamma^j_{H_\infty}$ with $\theta^j \in [0, 1]$, as detailed in [110]. This compromise, well known in economy and game theory, is also called the "Pareto optimality". For more details on this topic, reader is invited to refer to [117]. Another approach would be to determine an upper-level optimizer, in such way to find the optimal minimal pair $(\gamma^j_{H_2}, \gamma^j_{H_\infty})$.*

Also, Table 4.4 points out the used values for ϕ^j, for the *LMI* synthesis, and the consequent slower eigenvalue of the fault term estimation error dynamics. These values represent sufficient bounds for the *LMI* solutions, considering this Chapter's application. Bear in mind that $\gamma^j_{H_2}$ is related to the noise upon the estimation error (*impulse-to-energy* gain minimization), while $\gamma^j_{H_\infty}$ is related to the additive disturbances influence upon the estimation error (*energy-to-energy* gain minimization).

Note that, as of what is discussed in Remark 17, the additive term of $(q^j - \hat{q}^j)$, with the proposed estimate $\hat{q}^j$, has an average norm in the magnitude order of 10^{-1}. This means that, with the achieved H_∞ bounds, their influence on the estimation of each λ_j will be very small, which is what is expected within the scope of

this study. As evidenced, the effect of measurement noise ν on these estimations will also be small, as the H_2 bounds are sufficient.

     Figures 4.6 and 4.7 show the frequency H_∞ and H_2 (*Bode*) plots for each $e_\lambda^j(t)$, taken at the two vertices of each polytope $\mathcal{P}^j$ - this is, at u_j^{min} and u_j^{max}. The achieved performances are good, as the H_2 plots behave as low-pass filters and the H_∞ plots present small maximal peak. Note that ν represents instrumentation noise, which is intrinsically of higher frequencies and thus their effect on the estimations will be small. Also, good estimation results can be expected in terms of disturbance attenuation, given that their influence can be measured in terms of the *energy-to-energy* behaviour (maximal singular value, *Bode* peak). The worst performance, in terms of disturbance attenuation, can be expected at $j = 5$, which has an upper bound of $-2.125\,\text{dB} \approx 0.783$.

Remark 20. *Note that both Figures 4.6 and 4.7 present $2^1\,n_u = 26$ curves. Some of these curves are overlayed, on top of each other, but this does not compromise their understandment as only the peak values of the H_∞ curve and the high-frequency behaviour of the H_2 curve have to be read.*
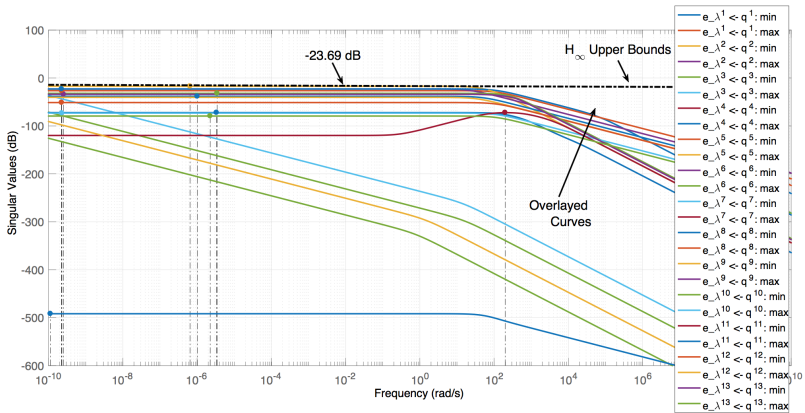
Figure 4.6: Additive Disturbance Effect.

Subsystem (j)	H_2 Bound ($\gamma_{H_2}^j$)	H_∞ Bound ($\gamma_{H_\infty}^j$)	ϕ^j	Slowest pole
1	10^{-3}	5.4160×10^{-2}	5	-9.82
2	10^{-3}	11.50×10^{-2}	9	-9.29
3	10^{-3}	5.011×10^{-18}	0.10	-0.20
4	10^{-3}	4.103×10^{-1}	7	-8.23
5	10^{-3}	7.892×10^{-1}	7	-9.75
6	10^{-3}	7.647×10^{-18}	0.15	-0.27
7	10^{-3}	6.554×10^{-18}	0.10	-0.20
8	10^{-3}	8.608×10^{-2}	5	-7.64
9	10^{-3}	9.883×10^{-2}	5	-7.57
10	10^{-3}	4.100×10^{-2}	10	-15.50
11	10^{-3}	2.262×10^{-4}	5	-6.42
12	10^{-3}	4.661×10^{-18}	0.2	-0.21
13	10^{-3}	5.743×10^{-2}	5	-10.81

Table 4.4: Achieved *LMI* Bounds.
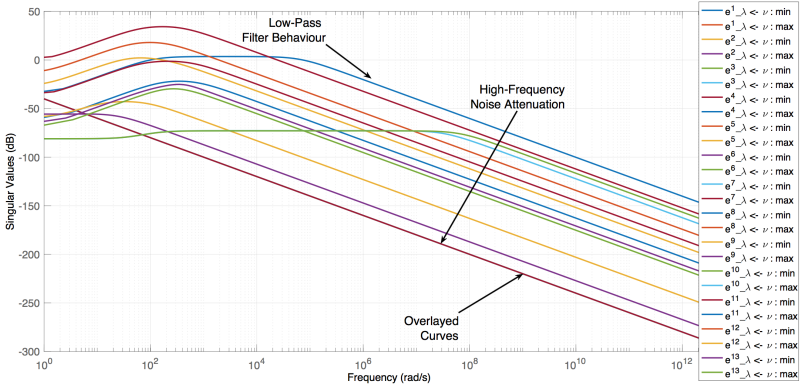
Figure 4.7: Noise Effect.

4.4.5 The Diagnosis Algorithm

To ensure better results, a diagnosis algorithm is coupled to each of the *LPV* observers in Figure 4.5. This algorithm has the goal to categorize which kind of fault occurs on the analysed subsystem j, into the possibilities presented in Table 4.1.

To do so, this algorithm is based on a fast computation of a simple search algorithm, that analyses three characteristics of the fault term estimated by the respective *LPV* observer ($\hat{\lambda}_j$). These are: *i)* Magnitude Analysis; *ii)* Period Analysis; *iii)* Maximal Fault Analysis.

Synthetically, the idea behind the algorithm is to sort out $\hat{\lambda}_j$ as done in Table 4.1. The algorithm considers that $\hat{\lambda}_j(t)$ is a time-wise function defined as $\hat{\lambda}_j(t) : (t_0^f, t_{end}^f) \rightarrow (\lambda_j^{min}, \lambda_j^{max})$, where t_0^f, t_{end}^f, λ_j^{min} and λ_j^{max} are, respectively, the (known) initial and final instants (after stabilization) of the fault event, and the minimal and maximal magnitude of the fault. The algorithm firstly (state $S0$) analyses the magnitude of the fault terms, given by $||\hat{\lambda}_j(t_{end}^f) - \hat{\lambda}_j(t_0^f)||_2$. If the fault can be already categorized (logical condition c_0), the algorithm goes to state $S3$. Else, the period analysis is done (state $S1$), categorizing the fault in respect to $(t_{end}^f - t_0^f)$. Once again, if the fault is categorized (logical condition c_1), the algorithm goes to state $S3$. Finally, a maximal fault analysis is realized (state $S2$), categorizing the fault according to

$||\hat{\lambda}_j(t_{end}^f)||_2$. When this step is done, all possibilities of sorting have been searched (logical condition c_2), and the algorithm goes to state $S3$. State $S3$ stands for the fault term being diagnosed by the algorithm. In this state, an alarm is ringed, stating to the supervisory system (or *SCADA*) which kind of fault has occurred upon subsystem j.

Figure 4.8 illustrates how this diagnosis algorithm works, with the aid of a *Grafcet* representation.
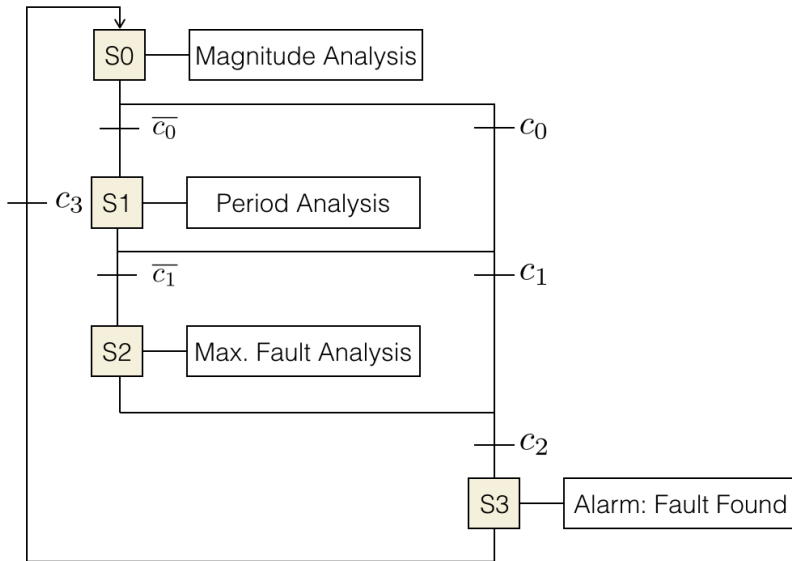
Figure 4.8: Diagnosis Algorithm: *Grafcet* Representation.

An example is given below to illustrate the algorithm's operation. Note that this algorithm has been verified to work for all considered fault cases empirically. Further assessments considering its operation are topic of future (separate) works[4]. This is not the main contribution of this Chapter, but a small sideway appendix. Please refer to [82] for more details on this matter.

---

[4]*Algorithms considering the use of genetic tools or neural networks could serve for the same purpose.*

Example 2. *Consider the following detected fault, a gas leakage that occurs on the* CHP *unit. This leakage occurs at* $t_0^f = 72\,h$, *ending at* $t_{end}^f = 144\,h$, *with* λ_8 *going from* 1 *to* 0.95, *as illustrated by Figure 4.9.*
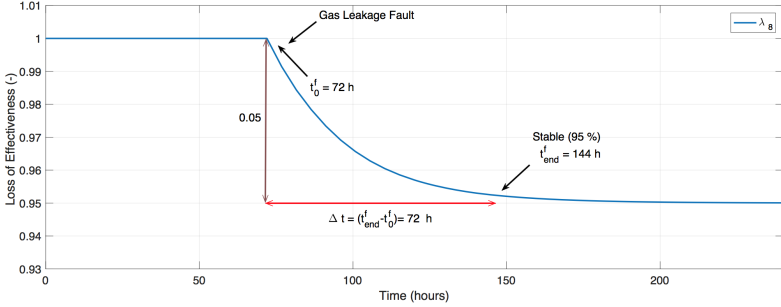
Figure 4.9: Gas Leakage Fault on the *CHP* Unit.

1. *Firstly, the algorithm detects, in state* $S0$, *that the magnitude of* 0.05 *can represent, as reads Table 4.1, either a "Gas Leakage" fault or a "Clogged Water" fault. A Manual stop fault is discarded. The logical condition* $\overline{c_0}$ *is set. Algorithm goes to state* $S1$.

2. *Then, the algorithm analyses the fault's period of* $72\,h$. *A "Clogged Water" fault is discarded. The logical condition* c_1 *is set. Algorithm goes to state* $S3$, *having no more option of faults but "Gas Leakage".*

3. *In state* $S3$, *an alarm is sound: the fault has been categorized (correctly) as a "Gas Leakage" fault.*

4.5   RESULTS

4.5.1   Simulation Results

As carefully detailed in Section 4.3, various faulty situations are considered in this Chapter. These faults occur upon the different subsystems of the hybrid microgrid and present different behaviours (models). Now, results are presented considering: *i)* individual, separate fault scenario and *ii)* a concomitant, multiple fault scenario. Some complementary results are presented in [82].

Remark 21. *Considering the following results, this Chapter used the softwares: MATLAB [103], Yalmip toolbox [114] and SDPT3 solver [115]. These results were obtained using a high-fidelity plant model (refer to [9]), controlled by a supervisory control scheme (refer to Remark 14), responsible for determining the manipulated vector $u(t)$ inside its feasible region, that aims, only, to make sure the load demands are met at every instant t. The control vector $u(t)$ is given by Figure 4.10. For simplicity, these signals repeat periodically each $24\,h$, as do the load demands. Bear in mind that these signals are used as the scheduling parameters of each observer of the proposed* FDD *scheme.*

Also, for the following results, the used disturbances w are taken as real (historical) data of bagasse, straw and bio-gas income to a sugarcane processing plant and as real meterological data of solar irradiance and wind speed present in the state of Paraná, Brazil. As explained, these last two curves are estimated by a NN *technique. The prediction error of solar irradiance and wind speed are overlapped by the sufficient H_∞ norm upper bound. Figure 4.11 shows the external disturbances scenario (and the predictions) for an interval of ten days. Once again, for simplicity, these signals repeat periodically each $24\,h$.*

4.5.1.1   Separate Fault Events

Given each of the signals $u_j(t)$, it is considered that the real (faulty) actuation to the hybrid power plant is given by $u_j^{\mathrm{f}}(t) = \lambda_j(t) \times u_j(t)$. Then, seven different simulations were retrieved (all considering the scenario depicted by Figures 4.10 ($u(t)$) and 4.11 ($w(t)$), for each of the faulty situations listed below. Therein, the "alarm" activated by the diagnosis algorithm when it finished categorizing the fault is represented by the vertical ⋄-line.

1. The continuous accumulation of debris and residues occurs on the boiler, $j = 4$. This leads to a *direct-to-energy* gain decrease of up to $25\,\%$ during the period three days. Also, a manual (emergency) stop is imposed to this subsystem, just after the beginning of the eighth day of simulation. The detection and estimation of the respective loss of effectiveness term $\lambda_4(t)$ is seen in Figure 4.12.

2. An unpredicted change on the weather conditions leads to peak on the batteries' room temperature. This leads to a decrease in the bank's capacity and a loss of effectiveness of $35\,\%$. The detection and estimation of the respective faut term $\lambda_{11}(t)$ is seen in Figure 4.13.

Bear in mind that each of these Figures 4.12 and 4.13 represent different simulation runs, wherein faults were simulated separately.

4.5.1.2 Concomitant Fault Events

In terms of concomitant faulty simulation, it is important to state that the computation of the fault terms λ_J is much harder in mathematical terms. This happens because the estimation $\hat{q}^j(t)$ is worse than before, with more terms λ_j being different than 1 (refer to Remark 17).

Various concomitant fault events were tested by the Author. In order to illustrate the results, the following test is presented: At a given instant, debris start to accumulate on the boiler when, after some hours, a gas leakage fault occurs on *CHP*, leading to a loss on the supplied hot water flow. This implies that the loss of effectiveness factors $\lambda_4(t)$ and $\lambda_8(t)$ are non-null during a same period $t \in [t_{f1}, t_{f2}]$. Then, results containing the estimated faults by the proposed bank of *LPV* observers approach towards *FDD* are seen in Figure 5.9. Clearly, detection is still very accurate and efficient and there is a decoupling between the detection of individual fault events.

The performance of the diagnosis algorithm, in terms of its computational time, is given by Table 4.5. Comparisons between the faulty and real control signals (u_j^{f}, u_j), for each of the presented scenarios, are given in the paper [82].

Table 4.5: Diagnosis Algorithm: Performance.

Scenario	Fault	Computational Time
1	Debris Acc.	62.50 ms
	Manual Stop	62.50 ms
2	High Temp.	46.90 ms
$C1$	Debris Acc.	78.10 ms
	Gas Leak.	281.30 ms

4.5.2 Overall Analysis

As proved by the realistic simulation results and the *LMI* solution analysis, the proposed *FDD* approach, given by a bank of *LPV*

observers coupled with simple categorization algorithms, is very accurate in terms of estimating, detecting and diagnosing faulty situations on a hybrid microgrid. Of course, the proposed technique has been adapted to the studied power plant but it can also be used for other plants - changing the number of subsystems, and, thus, observers. Some smooth estimation results in terms of fault estimation for energy system were seen, considering a higher-level supervisory scheme, which is rather novel in literature.

4.6 CONCLUSIONS

This Chapter presented the issue of Fault Detection and Diagnosis for hybrid generation power system, based on a sugarcane power plant. This work proposed a bank of *LPV* observers strategy to estimate fault terms, coupled with simple search algorithms that categorize what kind of fault occurs. As showed by simulation results, the proposed scheme is able to efficiently (and accurately) collect information on possible faults. The chosen mixed H_2/H_∞ norm synthesis for the observers allowed the effect of noise and additive disturbances to be sufficiently reduced, and, thus, the estimation of fault terms to be very smooth.

Such accurate *FDD* scheme can be used for fault tolerant control goals of hybrid energy systems in the presence of faults, in order to preserve the system stability, reliability and major performance goals (supply demand and others).

The *state-of-practice* of Fault Detection and Diagnosis in the industry is very limited. Most energy management systems for microgrids are based on *PLCs* with some alarms that indicate operating point escapes from the controlled subsystems[5]. This Chapter hopes to have pointed out a clear,simple path on how this topic can be introduced in industry.

What remains as open investigation threads from this development is: 1) analysing and surveying other possible fault detection techniques for multiplicative faults on microgrids and 2) compare and further analyse the application of fault tolerant model predictive control with the proposed method used to determine the controlled plant's state (healthy or faulty).

---

[5]*See these industrial solutions:* *<https://iot.telefonica.com/blog/>*, *<http://prod.sandia.gov/techlib/>*.
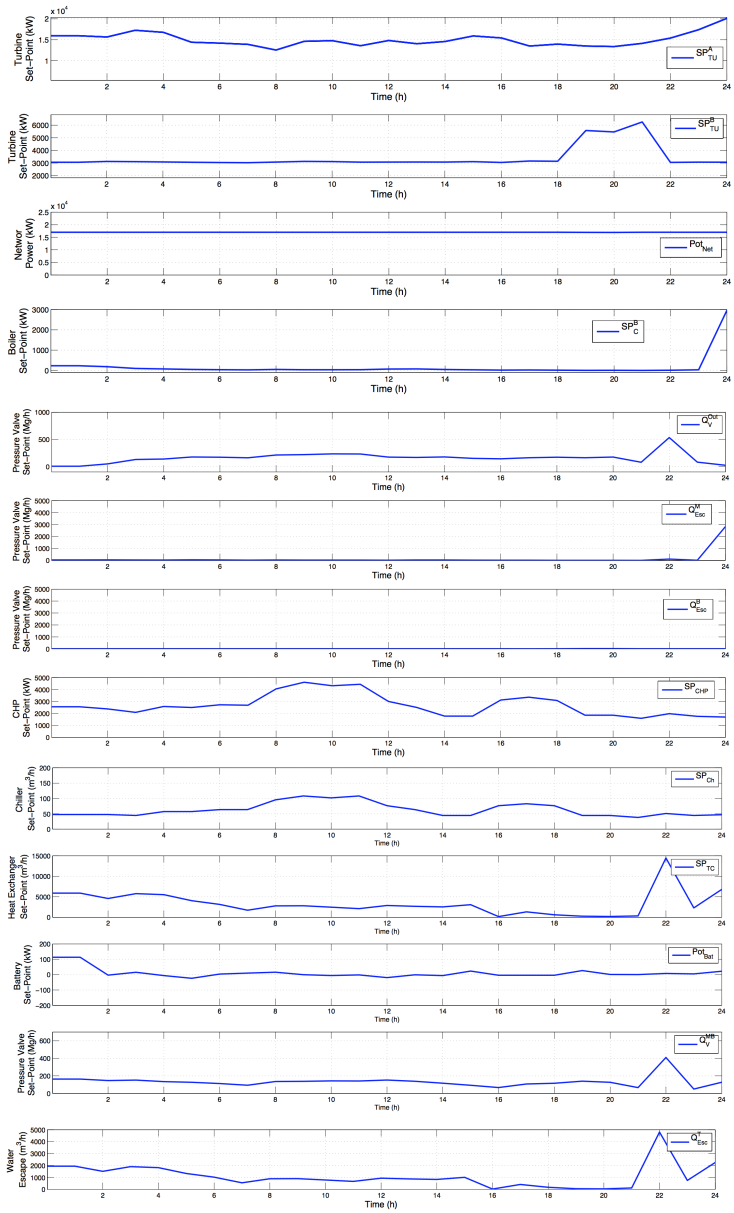
Figure 4.10: Supervisory Control: *Set-Points* $u(t)$.
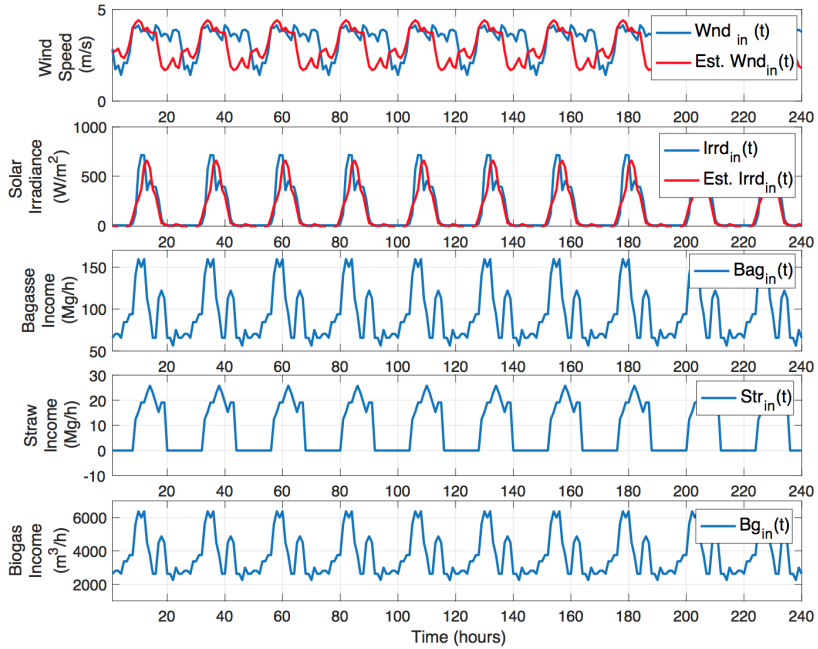
Figure 4.11: External Disturbances: Wind Speed, Solar Irradiance, Bagasse, Straw and *Bio*-gas Incomes.
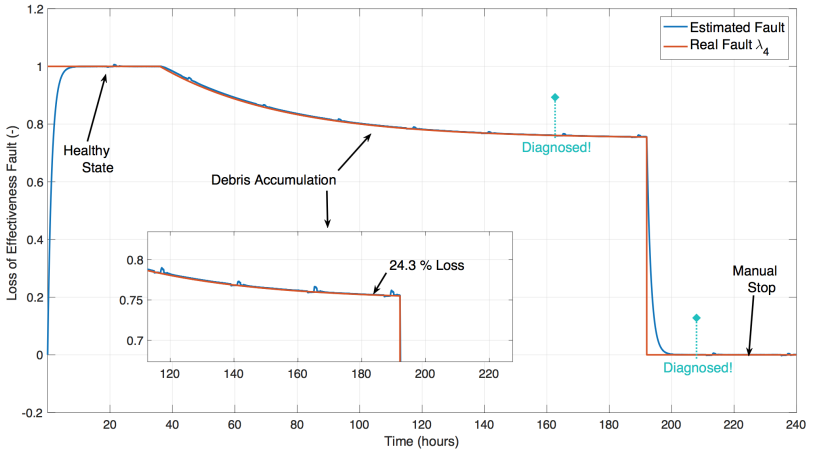
Figure 4.12: Scenario 1: Debris accumulation and Manual Stop, Boiler $j = 4$.
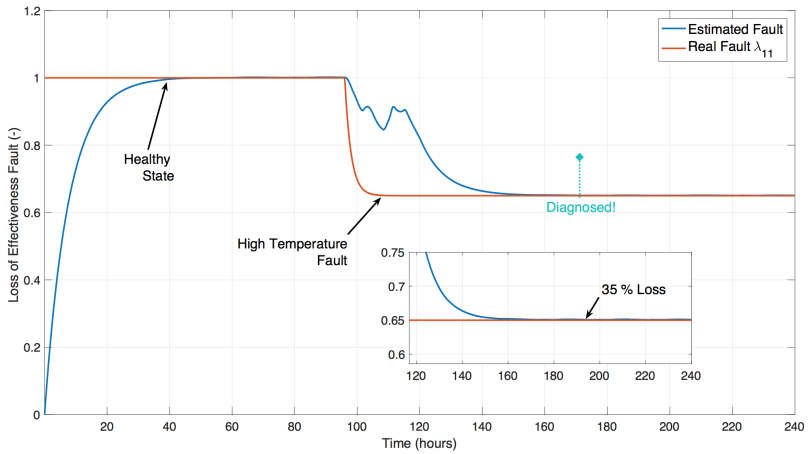
Figure 4.13: Scenario 2: High Temperature on Battery Bank $j = 11$.
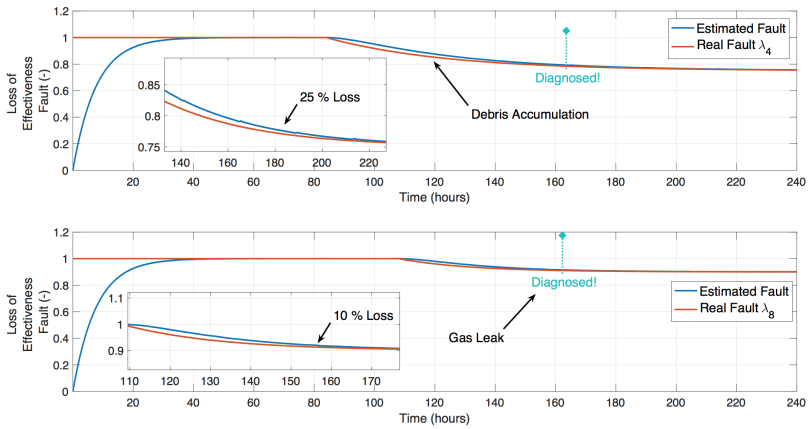
Figure 4.14: Scenario $C1$: Faults on Boiler ($j = 4$) and *CHP* ($j = 8$).

5 ROBUSTNESS CONDITIONS OF *LPV* FAULT ESTIMATION SYSTEMS FOR RENEWABLE MICROGRIDS

5.1 ABOUT CHAPTER

This Chapter continues to investigate the bank-of-*LPV*-observers proposed in Chapter 4. Now, the robustness conditions of these proposed observers are scrutinized. By doing so, the complementary objective CO 2 is tackled.

Keywords: Robustness Analysis; μ-Analysis; Fault Estimation; *LPV* Observers; Mixed H_2/H_∞ Performance.

The content of this Chapter derived the following works:

- [45] Lima, B. M., Morato, M. M., Mendes, P. R. C., Normey-Rico, J. E..**Moving Horizon Estimation of Faults in Renewable Microgrids**, presented in the 12th *IFAC* Symposium on Dynamic and Control of Process Systems, including Biosystems, Florianópolis, Brazil, 2019.

- [118] Morato, M. M., Mendes, P. R. C., Normey-Rico, J. E., Bordons, Carlos. **Robustness Conditions of *LPV* Fault Estimation Systems for Renewable Microgrids**, published in the International Journal of Electrical Power & Energy Systems, 2019.

5.2 CONTEXT

This Chapter is a direct continuation of Chapter 4, which presented the issue of Fault Detection and Diagnosis for a hybrid generation power system. To do so, a bank of *LPV* observers strategy was proposed to estimate fault terms, coupled with simple search algorithms that categorize what kind of fault occurs. Via realistic simulation, the Chapter showed that the proposed scheme is able to efficiently collect information on possible faults. The used mixed H_2 / H_∞ norm synthesis for the observers allows the effect of noise and additive disturbances to be strongly reduced, and, therefore, very smooth results can be achieved. Remark that the microgrid considered as a study case therein is the energy producer based on a sugarcane power plant, considering biomass, *bio*-gas, solar and wind power energy as primary energy sources, as introduced in Chapter 2.

The *LPV FE* bank-of-observers strategy proposed in Chapter 4 has some main novelties, w.r.t. the (*state-of-the-art*) microgrid *FDD* works, which are:

- It is in fact applicable for real energy systems and can be easily adapted to many other energy plants, once it is based on a very simple, intuitive modelling methodology (the Energy Hubs framework);

- It can serve, in the future, for fault tolerant control goals of hybrid energy systems in the presence of faults, in order to preserve system stability, reliability and major performance goals (guarantee supply demand and others). Indeed, it is reasonably robust to noise and disturbance (due to the mixed H_2 / H_∞ synthesis).

- To design it, one only needs to *i)* have a good plant model (from a tertiary / supervisory control-level point-of-view); *ii)* measure the energy-related outputs; *iii)* compute *offline* observer laws, solving Linear Matrix Inequality (*LMI*) problems; *iv)* implement simple (optimization-free) online observers, that can be done within the microgird's distributed control system / *PLC* (there is no need for complex online procedures).

As open threads of Chapter 4, these were:

(i) Surveying other possible fault detection / fault estimation techniques for multiplicative faults on hybrid energy systems, which has already been developed alongside, in the conference paper [45].

(ii) Investigate the robustness conditions of such bank of *LPV* observers technique, which is the scope of this Chapter.

5.2.1 Problem Statement and Contributions

As extensively discussed (over the last Chapters!), in the very near future, the renewable energy share will vastly increase. The foundations of energy systems will no longer rely on a single technology, but will incorporate multiple sources. Therefore, advanced Control techniques, as well as reliable, robust Fault Estimation systems must be available to ensure the successful integration of these renewables.

Thereby, the main motivation of this Chapter is to test, discuss and assess the bank-of-*LPV*-observers *FE* technique proposed in Chapter 4, in terms of robustness in the face of uncertainties. The main contributions, in respect to this matter, are summarized below:

(i) Firstly, possible uncertainties on the supervised plant's model are raised and discussed, due to incorrect modelling / identification hypothesis (Section 5.3);

(ii) From this point, Robustness conditions are derived for the proposed *LPV FE* method in terms of Stability and Performance (see Section 5.4). This is realized using the Structured Singular Value and Small Gain Theorem, i.e. μ-analysis;

(iii) Finally, realistic simulation results are presented in order to analyse the robustness / performance degradation trade-off of such *FE* method, illustrating the obtained performance in uncertain plants in constrast to a nominal situation (Section 5.5).

Synthetically, this Chapter enhances the analysis of *LPV*-observers *FE* technique for microgrids, from the viewpoints of robustness guarantees. A debate on the achieved results is presented in Section 5.6.

5.3   UNCERTAINTY MODELLING

This Section discusses where do the possible model uncertainties arise from and why to consider them is of paramount importance when estimating faults. Before further development, nonetheless, one should recall some basic notions of Robust Stability (*RS*).

First of all, note that Eq. (4.27) stands for an *LPV* system with a single scheduling parameter ρ^j. Hence, one can take the scheduling parameter a min. / max. bounds, which leads to two frozen *LTI* systems:

At $\rho^j = u^j_{min}$:

$$e^j(s) \quad \equiv \quad \mathcal{O}^j_{min}(s)i(s) \ , \tag{5.1}$$

At $\rho^j = u^j_{max}$:

$$e^j(s) \quad \equiv \quad \mathcal{O}^j_{max}(s)i(s) \ , \tag{5.2}$$

where both $\mathcal{O}^j_{min}(s)$ and $\mathcal{O}^j_{max}(s)$ are stable *LTI* transfer matrices w.r.t. $i(s)$, which is an input vector that comprises the concatenated inputs, i.e. measured outputs y, control inputs u, disturbances q^j and noise ν.

5.3.1 Robust Stability Conditions

Say, for simplicity, that the observed energy plant can be described via linear transfer functions such as the one below:

$$G(s) \;=\; G_n(s)\left[\mathbb{I} + W_g(s)\Delta_g(s)\right] \;, \tag{5.3}$$

where $y(s) \triangleq G(s)i(s)$ is the complete plant input / output representation, $G_n(s)$ is some nominal model (used for control / observation goals) and $W_g(s)\Delta_g(s)$ stand for multiplicative uncertainties, with W_g as some arbitrary transfer function and $||\Delta_g||_\infty \leq 1$.

Then, one can also write the *FE* estimation error laws (once again with simplifications) quite similarly, just as:

$$\mathcal{O}(s) \;=\; \mathcal{O}_n(s)\left[\mathbb{I} + W_o(s)\Delta(s)\right] \;, \tag{5.4}$$

where $e^j(s) \triangleq \mathcal{O}(s)i(s)$ is the complete j-th observer input / output representation (being $e^j(s)$ its estimation errors). Note that $\mathcal{O}_n(s)$ derives from the use of the nominal plat model $G_n(s)$ and the uncertainties $W_o(s)\Delta(s)$ are a direct consequence of $W_g(s)\Delta_g(s)$. Note that Eq. (5.4) is not so far from the actual representation of the studied *FE* observers (with frozen scheduling parameters), as given in Eqs. (5.1)-(5.2).

As one has an output multiplicative uncertainty description, the complete uncertain *FE* system can be written as an $M - \Delta$ representation structure (see [119]), as shown in Figure 5.1. The above steps were, in fact, first ones towards an unified representation of uncertainties, by using the upper Linear Fractional Transformation (*LFT*), which gives a transfer matrix from i to e^j:

$$F_u(M, \Delta) \;=\; M_{22} + M_{21}\Delta\left(\mathbb{I} - M_{11}\Delta\right)^{-1} M_{12} \;. \tag{5.5}$$

The transformation above accounts for:

$$\begin{bmatrix} y_\Delta(s) \\ e^j(s) \end{bmatrix} = \overbrace{\begin{bmatrix} M_{11} & M_{12} \\ M_{21} & M_{22} \end{bmatrix}}^{M(s)} \begin{bmatrix} u_\Delta(s) \\ i(s) \end{bmatrix} \;, \tag{5.6}$$

and, ultimately:

$$\hat{x}_a^j(s) \;=\; F_u(M, \Delta)i(s) \;. \tag{5.7}$$

Thence, it is direct to notice that Robust Stability is guaranteed if M_{11} is stable for all Δ with $||\Delta||_\infty < 1$, with nominal stability being *a priori* guaranteed (of course this is no absurd hypothesis
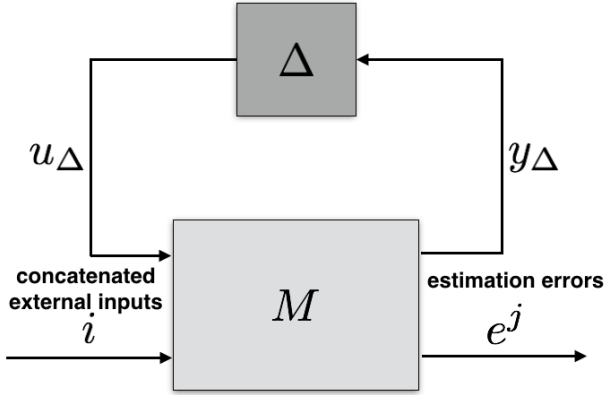
Figure 5.1: General M-Δ Formulation.

once the observers must present Lyapunov-stable error dynamics such that the estimation of faults is adequate; unstable dynamics would be of no use). This leads to the following well-known Robust Stability Theorem:

Theorem 1. *Small Gain Theorem*
Suppose $M \in \mathcal{RH}_\infty$. Then, the closed-loop system given in Figure 5.1 is well-posed and internally stable for all $\Delta \in \mathcal{RH}_\infty$ such that:

$$||\Delta||_\infty \leq \delta \quad \textit{if and only if} \quad ||M_{11}||_\infty < \frac{1}{\delta}. \qquad (5.8)$$

Of course, the above Theorem retains Robust Stability essentially because the only term in Eq. (5.5) that may lead to the appearance of an unstable pole is $(\mathbb{I} - M_{11}\Delta)^{-1}$.

Now, to handle in a direct manner parametric uncertainties, the structured singular value is defined:

Definition 3. μ
For $M \in \mathbb{C}^{n \times n}$, the structured singular value is given by:

$$\mu(M) \triangleq \frac{1}{\min\{\overline{\sigma}(\overline{\Delta}) : \overline{\Delta} \in \Delta,\, det(\mathbb{I} - \overline{\Delta}M) \neq 0\}}. \qquad (5.9)$$

In simpler words, this tool allows to find the smallest structured $\overline{\Delta}$ which makes the determinant of $(\mathbb{I} - \overline{\Delta}M)$ null.

Finally, the last important point to be recalled is the Small Gain Theorem adapted to the use of μ:

Theorem 2. *Structured Small Gain Theorem*
Let $M(s)$ be a stable LTI system and Δ an uncertain LTI block, then the system in Fig. 5.1 is stable for all Δ if and only if the structured singular value of M ($\mu(M)$) is smaller than 1 for $||\Delta||_{\infty} \leq 1$.

5.3.2   Possible Uncertainties

Once the structured *RS* criterion has been thoroughly detailed, one must qualify and quantify the possible model uncertainties Δ upon the studied nominal plant model, given by Equation (2.2).

Following this direction, one must remark that such nominal model for the sugar-ethanol energy plant, firstly presented in [2], derives from an Energy Hubs mathematical modelling kit. Such methodology considers two main assumptions. Indeed, if this assumptions are not really true, then the considered model may indeed be different from the actual process itself, which leads to an uncertainty that must be handled by the proposed *FE* observers. These two hypothesis are:

(a) The energy system is described in steady-state. This means all transitory dynamics have already converged and that all process variables stay within their bounds (either with constant behaviour or uniform variations);

(b) Energy losses only occur when storing or converting energy. Losses in trasmission lines and other are disregarded.

Thereby, one can conclude that the possible uncertainties (model-process mismatch) that derive from the above assumptions are:

1. Unmodeled dynamics due to transitory behaviour of conversion units, nonlinearities and start-up/shut-down events inside the decision-making sampling period;

2. Disregarded energy losses in transmission line. These can be treated, roughly, as input-to-output gain uncertainties.

Recalling the (fault-free) plant model Σ_{MG}, given in Eq. (2.2), these uncertainties might meddle with matrices A to D_{22}. Therefore, one considers an uncertain microgrid model set given by:

$$\Sigma_{\text{MG}}^{Unc} = \left\{ \begin{array}{rcl} \dot{x}(t) & = & A^{Unc}x(t) + B_1^{Unc}w(t) + B_2^{Unc}u(t), \\ y(t) & = & C_2^{Unc}x(t) + D_{21}^{Unc}w(t) + D_{22}^{Unc}u(t), \end{array} \right. \quad (5.10)$$

where:

$$\begin{array}{rcl} A^{Unc} & = & A + \Delta A, \quad\quad\quad (5.11) \\ B_1^{Unc} & = & B_1 + \Delta B_1, \\ \vdots & = & \vdots \\ D_{22}^{Unc} & = & B_{22} + \Delta B_{22}. \end{array}$$

Then, one must quantify how much do these uncertainties in fact represent:

- Due to the physical properties of the system (energy / mass balance on the states, which are stocks) A^{Unc} must always have an integrator property, i.e. A as a null block, and, hence, ΔA is taken as a diagonal block with stable eigenvalues. This is:

$$\Delta A \;=\; \text{diag}\{ \; -a_1 \;\; \ldots \;\; -a_{n_x} \; \}, \quad\quad (5.12)$$

with each a_i being stable (and fast) poles. Note that the piecewise constant control policy u, that acts each hour, is determined by some *MPC* scheme, and, furthermore, that the converter units of microgrids always present *fast* conversion dynamics [2]. Therefore, the settling period of these poles are assumed to be, at most, of 3 hours, which means they will converge within three sampling periods. This is coherent with any real / industrial energy-conversion application [120, 54, 80]. Each parameter a_i is then taken as, as most, bounded by 1, i.e.:

$$a_i \;\; \leq \;\; 1\,h^{-1} \; . \quad\quad\quad\quad (5.13)$$

- Matrix B_1^{Unc} stands for the disturbance-to-state relationship. Given that the disturbances $w(t)$ are the renewable incomes,

B_1^{Unc} is, roughly speaking, the efficiency of the plant's renewable subsystems (i.e. photovoltaic panels, *CHP* unit *etc*). Thus, one can consider ΔB_1 as some renewable conversion efficiency model-plant mismatch. As discussed in [121], for instance, the effect of dust on *PV / solar* panel can lead to up to 18% of performance deterioration; similar assessments have been made for wind turbines [122]. Therefore, it is adequate to consider:

$$\Delta B_1 \leq \delta b_1 B_1 \text{ , with: } |\delta b_1| \leq 0.18 \text{ .} \qquad (5.14)$$

- Given that B_2^{Unc} describes the energetic-inputs-to-state relationship, one can consider a similar assumption as of the previous case, of B_1^{Unc}. The plant model in Eq. (2.2) was conceived in [2], with extra care given to the development of this matrix. Herein, a 20% model-mismatch in the case of B_1^{Unc} is taken. Indeed, this is already a slight exaggeration, since boilers, turbines and other may present efficiency deterioration due several different factor (humidity of biomass for the boilers [123], dirt accumulation for the turbines [124] *etc*), but these losses are usually not more than 10%. This leads to:

$$\Delta B_2 \leq \delta b_2 B_2 \text{ , with: } |\delta b_2| \leq 0.2 \text{ .} \qquad (5.15)$$

- Matrices D_{21}^{Unc} and D_{22}^{Unc} are null by definition. Note that the measured outputs are the actual states, upon which there are no direct transfers from $w(t)$ and $u(t)$.

- Finally, given that the measured outputs are the system states, i.e. $y(t) = x(t)$, then, uncertainties upon C_2^{Unc} may derive from badly adjusted sensors. Therefore, one takes:

$$\Delta C_2 \leq \delta c_2 \mathbb{I}_5 \text{ , with: } |\delta c_2| \leq 0.25 \text{ .} \qquad (5.16)$$

This hypothesis assumes that one sensor can actually measure 25% wrong information.

In order to illustrate the differences between the nominal model and the complete uncertain model, Figure 5.2 shows the frequency H_∞ plot for the nominal case and sampled models taken within the uncertain model set Σ_{MG}^{Unc}. Note that this model is stable and low-pass by definition, despite the considered uncertainties.
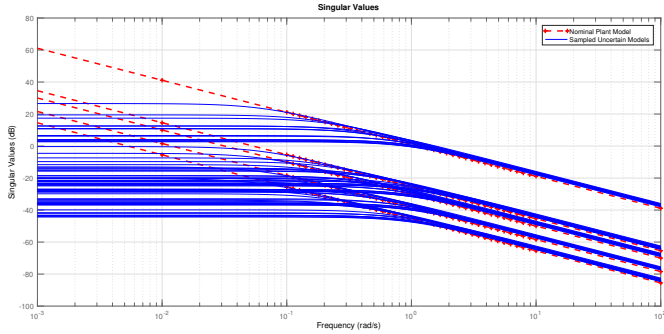
Figure 5.2: H_∞ Plot: Nominal model vs. Uncertain Plant.

5.4 ROBUSTNESS ANALYSIS

Once the possible uncertainties have been qualified and quantified, arriving at the uncertain model set $\Sigma_{\mathrm{MG}}^{Unc}$, this Section discusses the Robust Stability (*RS*) and Robustness Performance (*RP*) conditions of the analysed bank-of-*LPV*-observers *FE* strategy.

Recall that a control system is robust if it is insensitive to the differences between the actual system and the model used for the control design procedure. Likewise, such *FE* strategy is said to be robust if the estimation of faults remains accurate despite plant-model mismatches, i.e. for whichever plant inside the model set $\Sigma_{\mathrm{MG}}^{Unc}$. Therefore, once model uncertainties are known, one aims to check Robust Stability and Robust Performance conditions of the *FE* scheme. To do so, *RS* is checked considering the law (state estimates) derived from each observer, verifying whether $e^j(t)$ is Lyapunov-sense stable despite uncertainties, while *RP* is checked considering that the stability conditions and performance goals of the estimation errors are maintained, despite uncertainties.

Remark 22. *If one aims to resort to the design of a robust controller / robust* FE *scheme, for which the synthesis actually accounts for the uncertainties, the most common procedures seen in literature are either Monte-Carlo runs or μ-synthesis. In this Master dissertation, a very adequate* FE *scheme has already been proposed and synthesized, considering a mixed H_2 / H_∞ performance goal. Bearing in mind that the H_∞ norm, by definition, already imposes a reasonable degree*

*of robustness, neither of these robust synthesis methods will be used
in this chapter. Herein, one does not aim to quantify how much the
observer is robust to but **if it is robust towards the quantified un-
certainties** Δ described in Section 5.3; and such condition is derived
from the Small Gain Theorem, via Structured Singular Value analysis
(i.e. μ-analysis), see [119].*

One aims, thence, to write each one of the thirteen observers'
estimation errors ($e^j(t) = x_a^j(t) - \hat{x}_a^j(t)$) within the $M - \Delta$ represen-
tation form (illustrated by Fig. 5.1), when considering the complete
uncertain model set of Eq. (5.10).

Firstly, one must recall that matrices A_a^j and C_a^j are depen-
dent on the nominal plant model:

$$
\begin{aligned}
A_a^j(\rho^j) &= \begin{bmatrix} A & B_2^j \rho^j \\ 0 & 0 \end{bmatrix} , \\
C_a^j(\rho^j) &= \begin{bmatrix} C_2 & D_{22}^j \rho^j \end{bmatrix} .
\end{aligned}
\tag{5.17}
$$

Considering the use of the uncertain model, one arrives at:

$$
\begin{aligned}
A_a^j(\rho^j) &= \overbrace{\begin{bmatrix} A & B_2^j \rho^j \\ 0 & 0 \end{bmatrix}}^{\overline{A_a^j}(\rho^j)} + \overbrace{\begin{bmatrix} \Delta A & \Delta B_2^j \rho^j \\ 0 & 0 \end{bmatrix}}^{\Delta A_a^j(\rho^j)} , \\
C_a^j(\rho^j) &= \underbrace{\begin{bmatrix} C_2 & D_{22}^j \rho^j \end{bmatrix}}_{\overline{C_a^j}(\rho^j)} + \underbrace{\begin{bmatrix} \Delta C_2 & 0 \end{bmatrix}}_{\Delta C_a^j} .
\end{aligned}
\tag{5.18}
$$

Secondly, one defines:

$$
\begin{aligned}
B_q^j &= \overbrace{\begin{bmatrix} B_2^{j\star} & B_1 \\ 0 & 0 \end{bmatrix}}^{\overline{B_q^j}} + \overbrace{\begin{bmatrix} \delta b_2 B_2^{j\star} & \delta b_1 B_1 \\ 0 & 0 \end{bmatrix}}^{\Delta B_q^j}
\tag{5.19}
\\
D_q^j &= \underbrace{\begin{bmatrix} D_{22}^{j\star} & D_{21} \end{bmatrix}}_{\overline{D_q^j}} + \underbrace{\begin{bmatrix} \delta c_2 D_{22}^{j\star} & \delta c_2 D_{21} \end{bmatrix}}_{\Delta D_q^j}
\tag{5.20}
\end{aligned}
$$

$x_a^j(t)$ stands for the uncertain dynamics of the process itself,
given by the model set Σ_{MG}^{Unc}, while $\hat{x}_a^j(t)$ is the fixed estimation dy-
namics, having been previously synthesized with the nominal plant

model Σ_{MG}. Therefore, each (uncertain) estimation error dynamics, given by $e^j(t) = x_a^j(t) - \hat{x}_a^j(t)$ can be re-written as follows:

$$
\frac{d\hat{x}_a^j}{dt}(t) = \overbrace{[A_a^j(\rho^j) - L^j(\rho^j)\overline{C_a^j}(\rho^j)]}^{\overline{\mathcal{A}^j}(\rho^j)} \hat{x}_a^j(t) \tag{5.21}
$$
$$
+ \; L^j y(t) + (B_{1a} - L^j D_{21})\hat{w}(t) \;,
$$

$$
\frac{dx_a^j}{dt}(t) = \overline{A_a^j}(\rho^j)x_a^j(t) + B_{\nu a}\nu(t) \tag{5.22}
$$
$$
+ \; B_{1a}\hat{w}(t) + B_q^j q^j(t)
$$
$$
+ \; \Delta A_a^j(\rho^j)x_a^j(t) + \delta b_1 B_{\nu a}\nu(t)
$$
$$
+ \; \delta b_1 B_{1a}\hat{w}(t) + \Delta B_q^j q^j(t) \;,
$$

$$
y(t) = \overline{C_a^j}(\rho^j)x_a^j(t) + D_\nu \nu(t) + D_q^j q^j(t) \tag{5.23}
$$
$$
+ \; \Delta C_a^j(\rho^j)x_a^j(t) + \delta c_2 D_\nu \nu(t)\Delta D_q^j q^j(t) \;,
$$

$$
\frac{de^j}{dt}(t) = \mathcal{A}^j e^j(t) \tag{5.24}
$$
$$
+ \; (\Delta A_a^j(\rho^j) - L^j(\rho^j)\Delta C_a^j(\rho^j))x_a^j(t)
$$
$$
+ \; (B_{\nu a} - L^j(\rho^j)D_\nu)\nu(t)
$$
$$
+ \; (\delta b_1 B_{\nu a} - L^j(\rho^j)\delta c_2 D_\nu)\nu(t)
$$
$$
+ \; \delta b_1 B_{1a}\hat{w}(t)
$$
$$
+ \; (B_q^j - L^j(\rho^j)D_q^j)q^j(t)
$$
$$
+ \; (\Delta B_q^j - L^j(\rho^j)\Delta D_q^j)q^j(t) \;,
$$

which, obviously, yields an *LPV* system of form similar to the scheme in Figure 5.1, that is satisfied if the scheduling parameter ρ^j is frozen (becomes *LTI*). Such system can be equivalently expressed as:

$$
\frac{de^j}{dt}(t) = \mathcal{A}^j e^j(t) + \mathcal{B}^j i(t) \tag{5.25}
$$
$$
+ \; \Delta\mathcal{A}^j e^j(t) + \Delta\mathcal{B}^j i(t) \;.
$$

To further explain the above development, Figure 5.3 illustrates the complete $M - \Delta$ representation of each *FE* scheme. Notice that M is the block transfer from external inputs to estimation errors; moreover, the lower loop, namely O, stands for the observer law (synthesized with a nominal plant model) and N stands for the block transfer for the uncertain energy plant itself (defined by the set Σ_{MG}^{Unc}), as gives:

$$
\begin{bmatrix} e^j(s) \\ y(s) \end{bmatrix} = \overbrace{\begin{bmatrix} N_{11} & N_{12} \\ N_{21} & N_{22} \end{bmatrix}}^{N(s)} \begin{bmatrix} i(s) \\ \hat{x}_a^j(s) \end{bmatrix} \tag{5.26}
$$

One can compute M directly by using the lower *LFT*, with N and O as *LTI* transfer matrices:

$$
\begin{aligned}
M = F_\ell(N, O) &= N_{11} \\
&+ N_{12} O \left(\mathbb{I} - N_{22} O \right)^{-1} N_{21} .
\end{aligned} \tag{5.27}
$$

Thereby, after computing M (with uncertainties included in Δ), *RS* and *RP* properties can be concluded, as developed in the sequence.

5.4.1 Robust Stability (*RS*)

To re-affirm the general $M - \Delta$ formulation, the observer law of Equation (5.21), one considers **frozen scheduling parameters** $\rho^j = \rho_{\text{frozen}}^j$; to simplify notation, such frozen *LPV* systems appear, from this point onwards, with ρ^j suppressed.

Note that if one aims to guarantee *RS* and *RP* of a polytopic *LPV* system, that evolves inside polytope $\mathcal{P}^j$, it does not suffice to analyse the nominal vertices of this polytope. As discussed extensively in [125, 126], when uncertainties are present in a polytopic *LPV* system, to guarantee *RS* and *RP* properties, one must consider a dilated polytope $\mathcal{P}_D^j$ and, then, it suffices to take frozen scheduling parameters in the two vertices of this new polytope.

Theorem 1 presented in [127] proposes a robust state-feedback control approach for uncertain polytopic *LPV* systems. Its basic idea is to use a double-layer polytopic description in order to take into account both the variability of the system due to the parameter vector (nominal polytope) and the variability due to the uncertainties
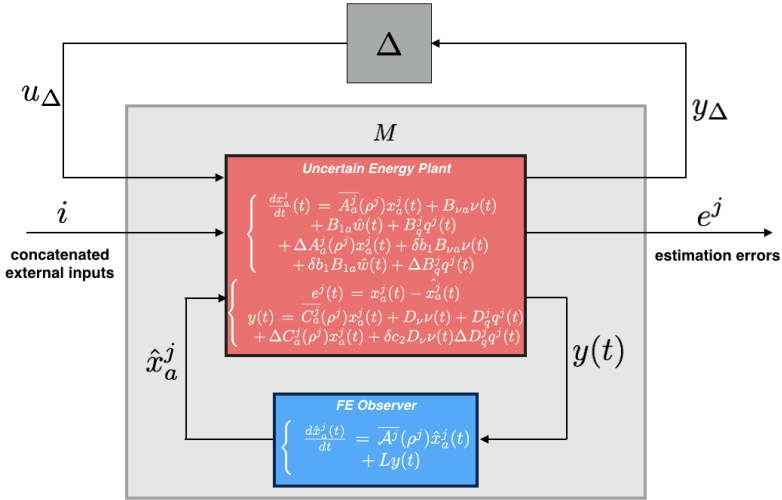
Figure 5.3: Complete $M - \Delta$ Representation of each *FE* Observer.

(dilated polytope). One can use the first *LMIs* of such Theorem (first layer) to obtain the new vertices of the dilated polytope of the uncertain system. In the studied *LPV* system given by Eq. (4.25), as there is only one scheduling parameter, finding $\mathcal{P}_D^j$ is straightforward and, therefore, the complete *LMI* formulation used to find $\mathcal{P}_D^j$ is not presented herein.

To represent the *FE* observer from Equation (5.21) in such form as in Fig. 5.3 one takes the law in Equation (5.25) and couples it with the quantified uncertainties (detailed in Section 5.3), thereby finding[1] Δ, y_Δ (with $u_\Delta(s) = \Delta(s)y_\Delta(s)$) and $M(s)$ as in Equation (5.6). It is direct to deduce that $\Delta(s)$ derives directly from the weights a_i, δb_1, δb_2 and δc_2, considering their respective upper limits, which characterizes the magnitude of Δ; note that its sparsity comes from the form of matrices ΔA_a^j, ΔC_a^j, ΔB_q^j and ΔD_q^j.

Finally, to conclude on *RS*, one only needs to perform μ-analysis,

---

[1]*The complete mathematical development is not presented herein, given that it is exhaustive and heavily algebraic. It suffices to say there will be some uncertain output y_Δ that holds for the necessity of the Structured Small Gain Theorem.*

i.e. Structured Small Gain Theorem, assuring, for $||\Delta||_\infty < 1/\overline{\mu}$, that the following inequality holds[2]:

$$\mu(M(jw)) \leq \overline{\mu} \quad \forall\, w \in \mathbb{R} \ . \tag{5.28}$$

This procedure was realized numerically using the Robust Control toolbox (i.e. with `sysic`, `robuststab`) of the Matlab software package. Table 5.1 synthesizes the obtained results for all the thirteen *LPV* observers from Chapter 4, $j = 1, \ldots, 13$, at both extremities of each delated polytope $\mathcal{P}_D^j$ (min. / max.).

Figure 5.4 illustrates the achieved frequency-domain result for $j = 1$ in terms of $\mu(M(jw))$ for the considered uncertainties, with scheduling parameters frozen at min. / max. bounds of $\mathcal{P}_D^j$. Note that it is verified that $\mu(M(j\omega)) < 1$ for all frequencies ω. The results for the other twelve *FE* observers are found in the paper [118]. Note that in these plots, the navy line stands for the maximal $\mu(\omega)$ at the the min. vertex of $\mathcal{P}_D^j$, the cyan dotted line stands for the minimal $\mu(\omega)$ at this same vertex, the red line stands for the maximal $\mu(\omega)$ at the the max. vertex of $\mathcal{P}_D^j$, while, finally, the pink dotted line stands for the minimal $\mu(\omega)$ at this second vertex.

From these presented frequency results (Figures and Table 5.1), it is direct to conclude that **Robust Stability is guaranteed for all observers**, which is a very **strong** result, given that the considered uncertainty set is quite large. The reason for such good results resides, basically, in the nice robustness qualities implied by the H_∞-norm minimization synthesis, solved in an *LMI* formulation presented in Chapter 4 (i.e. the Bounded Real Lemma *LMI*).

5.4.2 Robust Performance (*RP*)

Now that *RS* has been mathematically guaranteed, via Small Gain Theorem, what can one conclude on *RP*? Well, the performance goals set for each *FE* observer of Chapter 4[3] were clear:

1. To present Lyapunov-sense stable estimation error dynamics $\dot{e}^j(t)$, which has in fact just been verified by *RS*;

2. To achieve the minimal possible H_∞ norm from the additive disturbances $q^j(t)$ to $e^j(t)$;

---

[2]*Note that in this work, $\Delta(s)$ is parametrized s.t. $||\Delta||_\infty < 1$, i.e. $\overline{\mu} = 1$.*
[3]*Refer to Table 4.4.*

Table 5.1: μ-analysis: *RS* Guarantees.

FE Observer (j)	$\rho^j \in \mathcal{P}_D^j$	$\max\{\mu(M(jw))\}\ (10^{-4})$	Eq. (5.28) ?
1	min. vertex	1.9999	Yes
	max. vertex	1.9999	Yes
2	min. vertex	4.6719	Yes
	max. vertex	1.9999	Yes
3	min. vertex	5.8246	Yes
	max. vertex	5.8246	Yes
4	min. vertex	5.9999	Yes
	max. vertex	5.9999	Yes
5	min. vertex	1.9999	Yes
	max. vertex	1.9999	Yes
6	min. vertex	2.1273	Yes
	max. vertex	2.1273	Yes
7	min. vertex	2.1274	Yes
	max. vertex	2.1274	Yes
8	min. vertex	8.6369	Yes
	max. vertex	8.6369	Yes
9	min. vertex	4.6724	Yes
	max. vertex	1.9999	Yes
10	min. vertex	1.9999	Yes
	max. vertex	8.6369	Yes
11	min. vertex	4.8557	Yes
	max. vertex	4.8557	Yes
12	min. vertex	6.0538	Yes
	max. vertex	6.0538	Yes
13	min. vertex	8.6369	Yes
	max. vertex	1.9999	Yes

3. To preserve the H_2 bound of 10^{-3} from the measurement noise $\nu(t)$ to $e^j(t)$.

These two later objectives can be verified by using the same $M - \Delta$ representation of Figure 5.3, by certifying that the outputs of M (which are in fact the estimation errors e^j) obey such conditions by maintaining the expected H_2 and H_∞ bounds despite the uncertainties - or, at least, admissible bounds: respectively close to 10^{-3} and to the minimal found in Chapter 4, respectively.
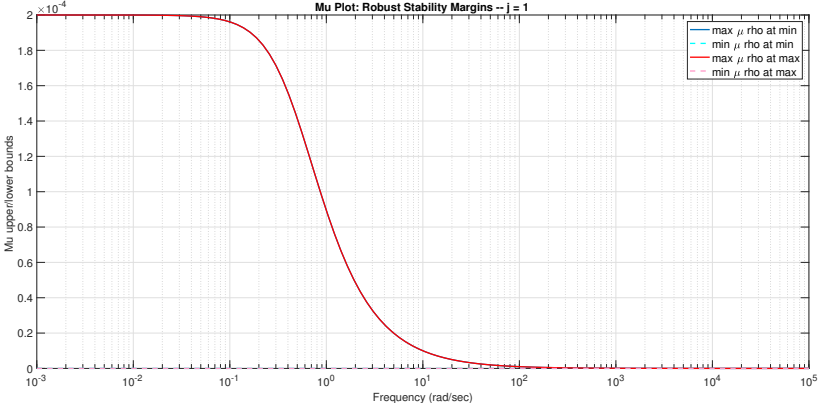
Figure 5.4: μ-analysis: *FE* Observer $j = 1$.

Via μ-analysis one does in fact verify this point. But, to do so, two fictive outputs of M must be introduced[4]:

$$k_2^j(s) = W_2^j(s)e^j(s) \ , \tag{5.29}$$
$$k_\infty^j(s) = W_\infty^j(s)e^j(s) \ . \tag{5.30}$$

$W_2^j(s)$ and $W_\infty^j(s)$ are stable transfer matrix templates (weights) taken to impose the performance specifications on the error dynamics. $[W_2^j(s)]^{-1}$ is defined as a diagonal low-pass filter, with 10^{-3} gain in high frequencies (H_2 specification), while $[W_\infty^j(s)]^{-1}$ is a diagonal gain equivalent to the specified H_∞ norm.

Then, one only needs to check if each of these two fictive outputs k_2^j and k_∞^j present their H_∞ norms smaller than 1 for the whole uncertainty set (using μ-analysis, once again). Note that once $||k_i^j||_\infty = ||W_i^j e^j||_\infty$, if $||k_i^j||_\infty \leq 1$, it is directly implied that $||e^j||_\infty \leq ||\frac{1}{W_i^j}||_\infty$. In such condition, e^j falls within these defined frequency templates, guaranteeing that the sought performance specifications are attained, despite the uncertainties.

For all the thirteen outputs j, such conditions are verified. These results are presented in Table 5.2, that recalls the maximal

---

[4]*Once again, the following development considers frozen values of the scheduling parameter $\rho_{frozen}^j \in \mathcal{P}_D^j$.*

obtained values (either found on the min. or max. vertex of the dilated polytope $\mathcal{P}_D^j$) for the H_2 and H_∞ norms of transfers $\nu \rightarrow e^j$ and $q^j \rightarrow e^j$, respectively, inside the uncertainty set, compared to values at nominal conditions. Note that the achieved bounds are in accordance with the expected norms for the nominal case, with some deterioration. μ-analysis was performed considering the dilated polytope $\mathcal{P}_D^j$, analyzing the polytopic *LPV* model in the polytope's two extremities (two *LTI* models). Notice that this Table (5.2) presents a qualitative analysis, concluding on *RP* whether the min. / max. norms are given inside a good / sufficient range of values (i.e. small deterioration shall be noticed when the *FE* observers are tested in real plants different from the nominal model within the uncertainty set Σ_{MG}^{Unc}).

To illustrate these frequency results, Figure 5.5 shows the max. singular-values frequency plots[5] of e^1 for the $j = 1$ *FE* observer when it is applied to 15 different randomly sampled plants from the uncertain model set Σ_{MG}^{Unc}, compared to the respective frequency templates W_2^j and W_∞^j. The results for the other twelve *FE* observers are found in the paper [118]. In these Figures, the bold **black** lines stand for the performance templates, the +-line and +-line stand, respectively, for the nominal plant at the max. vertex of $\mathcal{P}^j$, while the blue and cyan lines stand for sampled models from the uncertain set with ρ taken, respectively, at the min. and max. vertices of $\mathcal{P}_D^j$. Also note that, in these Figures, the lines are superimposed for the reasons given: for each *LTI* system (*LPV* system with frozen scheduling parameter) the singular value decomposition gives 5 singular values for each frequency; moreover, when 15 sampled plants from the uncertain set are taken, 75 lines are plotted in such graph.

Such Figures are able to demonstrate how the performance objectives are overall maintained, once all estimation errors e^j are always constrained inside their respective templates. Moreover, it must be remarked that the H_2 norm condition is always very closely satisfied, given that the monitored energy-generation process is naturally low-pass by itself (see Figure 5.2).

---

[5]*A Bode (H_2) plot is shown for $\nu \rightarrow e_\lambda^j$, and an H_∞ frequency plot for $q^j \rightarrow e_\lambda^j$.*

j	H_2 norm of $\nu \rightarrow e^j$	**nominal** H_2	Deterioration	
1	$9.9999 \cdot 10^{-4}$	10^{-3}	$\approx$ none	
2	0.001	10^{-3}	None	
3	$9.9999 \cdot 10^{-4}$	10^{-3}	$\approx$ none	
4	0.001	10^{-3}	None	
5	0.001	10^{-3}	None	
6	$9.9999 \cdot 10^{-4}$	10^{-3}	$\approx$ none	
7	$9.9999 \cdot 10^{-4}$	10^{-3}	$\approx$ none	
8	10^{-3}	10^{-3}	None	
9	10^{-3}	10^{-3}	None	
10	$9.9999 \cdot 10^{-4}$	10^{-3}	$\approx$ none	
11	10^{-3}	10^{-3}	None	
12	$9.9999 \cdot 10^{-4}$	10^{-3}	$\approx$ none	
13	10^{-3}	10^{-3}	None	
j	H_∞ norm of $q^j \rightarrow e^j$	**nominal** H_∞	Deterioration	*RP*?
1	0.125	$5.4160 \cdot 10^{-2}$	Small	Yes
2	0.7874	$11.50 \cdot 10^{-2}$	Small	Yes
3	$< 10^{-5}$	$< 10^{-5}$	Small	Yes
4	0.6249	0.4103	Very Small	Yes
5	0.9333	0.7892	Very Small	Yes
6	$< 10^{-5}$	$< 10^{-5}$	Small	Yes
7	$< 10^{-5}$	$< 10^{-5}$	Small	Yes
8	$10.2158 \cdot 10^{-2}$	$8.608 \cdot 10^{-2}$	Very Small	Yes
9	$13.079 \cdot 10^{-2}$	$9.883 \cdot 10^{-2}$	Very Small	Yes
10	$8.7345 \cdot 10^{-2}$	$4.100 \cdot 10^{-2}$	Small	Yes
11	$2.4876 \cdot 10^{-4}$	$2.262 \cdot 10^{-4}$	Very Small	Yes
12	$< 10^{-5}$	$< 10^{-5}$	Small	Yes
13	$6.8368 \cdot 10^{-2}$	$5.743 \cdot 10^{-2}$	Very Small	Yes

Table 5.2: μ-analysis: *RP* Guarantees.
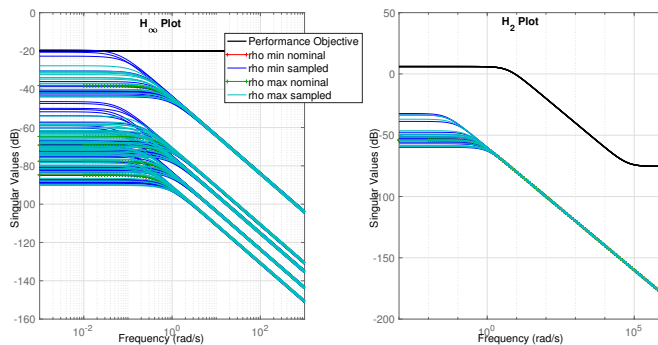
Figure 5.5: Robust Performance: *FE* Observer $j = 1$.

5.5 SIMULATION RESULTS

This Section shows numerical simulation examples to corroborate with the frequency results, comparing a nominal situation with an uncertain one and assessing the deterioration in terms of performances.

Remark 23. *Some comments must be made:*

- *Considering the following results, this Chapter used the software packages: MATLAB, Yalmip toolbox and SDPT3 solver [103], [114], [115].*

- *These results were obtained using a high-fidelity plant model [2], controlled by a supervisory control scheme, responsible for determining the manipulated vector $u(t)$ inside its feasible region, that aims, only, to make sure the load demands are met at every instant t. Such kind of control policy ($u(t)$) has been previously presented in [9]. For simplicity, these signals repeat periodically each $24\,h$, as do the plant's load demands.*

- *The used disturbances w are taken as real (historical) data of bagasse, straw and bio-gas income to a sugarcane processing plant and as real meterological data of solar irradiance and wind speed present in the state of Paraná, Brazil. Such curves are presented in Figure 4.11.*

Two simulation plant models are considered: the nominal
one, given by Σ_{MG}, from [2], and a disturbed one (with uncertainties). For this later model, it is assumed that a very dry period occurred just prior to the simulation run. This implies that dirt accumulated on the solar panels and the biomass became much less
humid than usual. One assumes this leads to a 10% gain change
in matrices B_1 and B_2. Moreover, one assumes the sensors were
badly calibrated, presenting 5% biased measurements. Such kind
of situation is very common, as discussed in [2, 65]. Figure 5.6
displays the differences between the nominal plant model used for
the original *FE* scheme design and the actual (disturbed) model, in
terms of a singular-values frequency plot. Note that fast internal
energy-conversion dynamics are also considered, instead of simple
integrator nodes.
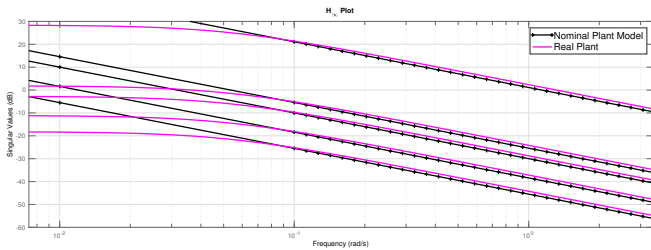
Figure 5.6: H_∞ Plot: Nominal model vs. Real Plant.

Then, considering these two plants (nominal and disturbed),
the following simulation scenarios are tested:

1. An unpredicted change on the weather conditions leads to
   peak on the batteries' room temperature, leading to a decrease
   in the battery bank's capacity and a consequent loss of effectiveness of 35%. Li-ion batteries suffer from stress when exposed to prolonged heating. As the studied microgrid is set
   in a tropical country, this kind of issue does in fact happen
   frequently, when there is excessive heat in the battery room.
   For instance, at $40\,^oC$, the loss on the batteries life-cycle can
   decrease up to 40%.

2. A sudden steam leakage occurs in the middle-low pressure
   reduction valve, $j = 5$. This leads to a decrease in the valve's

effectiveness of up to 15%, given that some portion of the steam is lost.

3. At a given instant, debris start to accumulate on the boiler when, after some hours, a gas leakage fault occurs in *CHP,* leading to a 10% loss on the supplied hot water flow. This is a concomitant fault scenario, but, to be synthetic, one aims solely to analyze the *FE* in terms of the *CHP*. Remark that in a concomitant fault scenario, the estimation of faults is harder, once u_{ot}^j increases and thereby the magnitude of the external disturbances q^j also enlarges.

Below, in Figure 5.7, one sees the estimation of fault term $\lambda_1(t)$ for the first scenario by the proposed bank-of-*LPV*-observers technique, comparing the estimation in a nominal condition and in the disturbed plant case. Clearly, the estimation of faults in the battery bank remains sufficiently good with the observers synthesized in Chapter 4, despite the uncertainties.
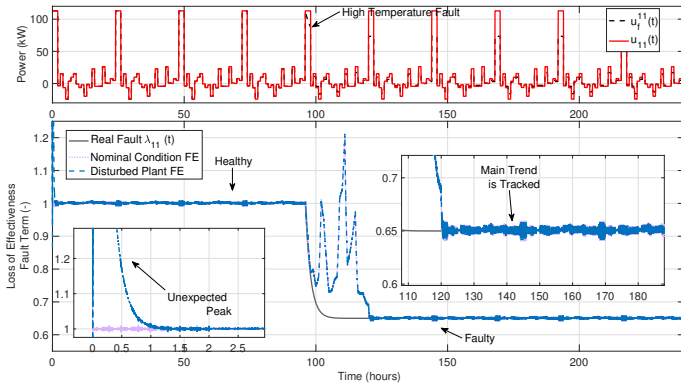
Figure 5.7: Simulation Scenario: Battery Bank Temperature Fault $(j = 11)$.

Figure 5.9 shows the estimation of fault term $\lambda_5(t)$ for the second scenario, which also yields apparently good results.

Finally, Figure 5.9 shows the estimation of fault term $\lambda_8(t)$ for the third scenario, comparing the estimation in a nominal condition and in the uncertain case. There is small performance deterioration, as expected, but this does not meddle much with the accurateness of
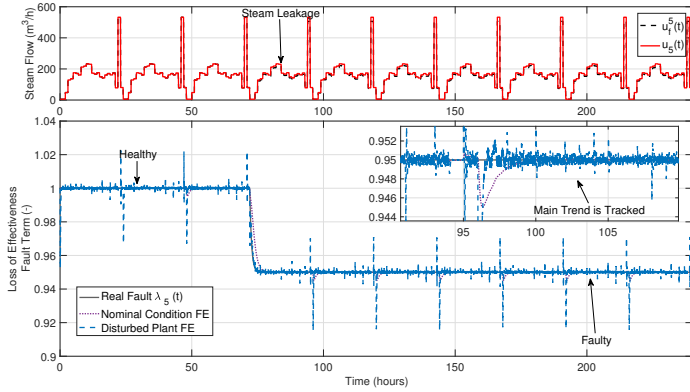
Figure 5.8: Simulation Scenario: Valve Steam Leakage Fault ($j = 5$).

the method, as predicted by the frequency analysis given in Section 5.4. Notice that the effect of noise and external disturbances is very small (as pointed out by the *RP* analysis).
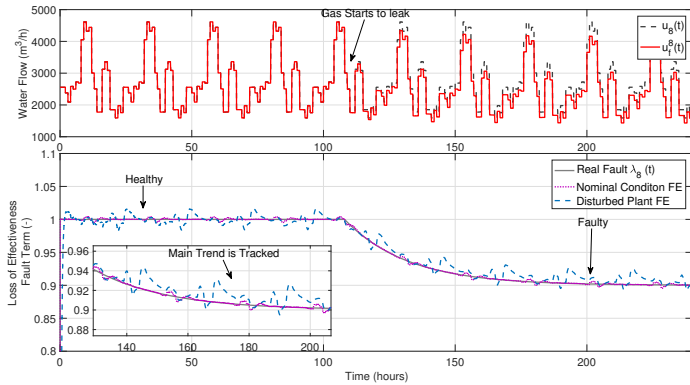
Figure 5.9: Simulation Scenario: *CHP* Gas Leak Fault ($j = 8$).

To synthesize the performance degradation of the proposed bank-of-*LPV*-observers *FE* technique in uncertain (disturbed) plants, Table 5.3 presents the root-mean-square errors of the estimation

(*RMS* of e_λ^j) for the nominal case and the uncertain case. Thereby, the performance degradation is quantified in percentage ($\frac{\text{uncertain}}{\text{nominal}} - 1$), which yields less than 20% of degradation for all tested scenarios, which is in accordance with the *RP* value presented in Table 5.2 and rather satisfactory, given that an exceedingly large plant-model mismatch was considered. In a practical application, the actual uncertainties would be much smaller, which would lead to even less performance degradation (and much more graceful results)!

Table 5.3: Performance Degradation: *RMSE*.

j	Nominal Conditions	Disturbed Plant	Degradation
11	0.0651	0.0680	4.45 %
5	0.00195	0.0222	13.43 %
8	0.0036	0.0701	18.47 %

5.6   CONCLUSIONS

This Chapter further studied the issue of Fault Estimation for a hybrid generation power system, based on a sugarcane power plant. The strategy studied was a bank of *LPV* observers, synthesized considering minimization of the mixed H_2 / H_∞ norm. Possible model uncertainties on the monitored plant were discussed and robustness conditions for adequate fault estimation are derived for such method. As showed by realistic simulation results, this *LPV* scheme achieves good results and is able to collect information on possible faults, even in some stretched operational conditions, being able to effectively reduce the influence of noise and disturbances upon the estimation. The performance degradation is noted to be relatively small.

Note that the studied robust fault estimation methodology can be easily adapted to many other energy plants, being derived from simple modelling techniques (Energy Hubs). Such *FE* scheme can serve for direct fault tolerant control goals, in order to preserve the system stability, reliability and major performance goals (guarantee supply demand and others).

Effectively, this Chapter completed the second complementary objective of this dissertation. What remains is to tackle GO 3, the *FTC* methods, which is done in the following Part of the Master Dissertation.

Part III

Central Development: Advances in Fault-Tolerant Control

6 *LPV*-FILTERED PREDICTIVE CONTROL DESIGN FOR FAULT-TOLERANT ENERGY MANAGEMENT OF HYBRID POWER SYSTEMS

6.1   ABOUT CHAPTER

Part II of this document was concerned with Observation and Monitoring, considering faults in modern microgrid. Now, the results in this Part (III) are concerned with advances in fault-tolerant control design for such energy systems.

This Chapter discusses how to design adequate control loops for the studied sugarcane-based microgrid, w.r.t. the issue of faults and their effects. The proposed approach is based on an *MPC* loop that is reconfigured by a feedback *LPV* filter, which is adjusted according to the level of faults detected on the system. This tackles GO 3 and SO 3.1.

Keywords: Fault-Tolerant Control; Model Predictive Control; Microgrids.

The content of this Chapter derived the following work:

- [128] Morato, M. M., Mendes, P. R. C., Normey-Rico, J. E., Bordons, Carlos. ***LPV*-Filtered Predictive Control Design for Fault-Tolerant Energy Management**, presented in the 12th *IFAC* Symposium on Dynamic and Control of Process Systems, including Biosystems, Florianópolis, Brazil, 2019.

6.2   INTRODUCTION

The control of hybrid generation and storage, including renewable and non-renewable sources (and their respective future estimation), is a significant issue to be studied in order to allow the optimal management and operation. Some works have already presented some results in this context, as [83] and [54]. As previously discussed, *MPC*-based control schemes have been successfully applied for the energy management of microgrids with renewable sources in a diverse set of recent applications [12, 15, 13, 84, 55, 14, 9, 59] and [11].

Energy microgrids are always vulnerable to faults and failures, which may lead them to not comply with their operational constraints; this might result in economic deprivation and lack of available power to the external network. Nonetheless, up to the Author's best knowledge, very few works have tried to deal with active fault-tolerant energy management of *microgrids*. That is, with the

design of autonomously-adjusting controllers that manage the en-
ergy flows of a given microgrid, despite the presence of faults. Some
works have to be mentioned, anyhow, but their scope is much more
limited (focused on specific energy subsystems) than the problem
faced by this work: [129] presents the fault-tolerant control of a bat-
tery system; in [35], the fault-tolerant operation of wind turbines
is presented; the patent [130] exposes ideas for the fault-tolerant
operation of solar power systems.

Therefore, bearing in mind the given context, the problem
tackled herein is the following: how to design an autonomously-
adjusting fault-tolerant controller for the energy management of a
hybrid power system (that is based on a sugarcane power plant)?
To do so, this Chapter proposes to use a filtered predictive con-
troller, as seen in literature, as a Fault Tolerant scheme. The *feed-
back* filter is Linear Parameter-Varying (*LPV*), being able to adapt
itself to both faulty and faultless situations. This Chapter presents
something rather novel in literature, because the fault-tolerant en-
ergy management problem hasn't yet been properly studied. Also,
the used methodology is new, given the *LPV*-Filtered *MPC-FTC* ap-
proach. Overall good results are obtained and illustrated with the
aid of high-fidelity simulations and comparisons to simpler control
schemes.

This Chapter is organized as follows: Section 6.4 describes
the Fault-Tolerant energy management problem; the proposed solu-
tion is presented in Section 6.5, wherein the *LPV*-Filtered Predictive
Control approach is described; finally, Section 6.6 presents high-
fidelity simulation results of the proposed control strategy, with
comparisons to other standard techniques. The chapter ends with
conclusions.

6.3   FAULTY PLANT MODEL

This Chapter considers the sugarcane-based microgrid from
the Brazilian scenario. Once again, this studied power plant is sub-
ject to multiple faults and failures; some slight model modifications
are done w.r.t. what was done in Chapter 4. These faults can rep-
resent different situations in the plant, such as: the accumulation
of debris and residues on the boilers; a bearing temperature reduc-
tion on the turbines; a pressure transmitter communication failure;
oil leakages on pressure valves; power-house management failures;
bottleneck clogging on water flow and even emergency stops from

manual operators.

Once again, to model these faults, multiplicative *loss of effectiveness* factors α_i upon each controlled energy subsystem j are used. Roughly speaking, it is assumed that the supervisory hourly controller determines set-points u_j for the local subsystems that are not correctly tracked and, the actual output from each of these subsystems are given, individually, by $\alpha_j u_j$.

Then, the control-oriented hourly-discrete *state-space* representation model of the studied (faulty) plant is given below, in Equation (6.1).

$$
\begin{aligned}
x(k+1) &= Ax(k) + B_1 w(k) + B_2 \overbrace{\Lambda(k)u(k)}^{u_f(k)}, \qquad (6.1) \\
z(k) &= C_1 x(k) + D_{11} w(k) + D_{12}\Lambda(k)u(k), \\
y(k) &= C_2 x(k) + D_{21} w(k) + D_{22}\Lambda(k)u(k),
\end{aligned}
$$

where:

$$
u_{f_j}(k) = \alpha_j(k)u_j(k), \qquad (6.2)
$$

$$
u_f(k) = \underbrace{\begin{bmatrix} \alpha_1(k) & 0 & \dots & 0 \\ 0 & \alpha_2(k) & \dots & 0 \\ \vdots & \vdots & \ddots & 0 \\ 0 & 0 & \dots & \alpha_{13}(k) \end{bmatrix}}_{\Lambda(k)} \underbrace{\begin{bmatrix} u_1(k) \\ u_2(k) \\ \vdots \\ u_{13}(k) \end{bmatrix}}_{u(k)}. \qquad (6.3)
$$

Remark 24. *The diagonal matrix $\Lambda(k)$ stands for the collection of faults (on each subsystem) $\alpha_j(k)$. These $\alpha_j(k)$ are the loss of effectiveness fault terms and, thus, if $\alpha_j(k) = 1$, subsystem j is completely healthy, whereas if $\alpha_j(k) = 0$, a complete failure has occurred.*

Remark 25. *It must be mentioned that these $\alpha_j(k)$ terms are equivalent to those $\lambda_j(t)$ terms of Part II. The notation was changed to be in accordance with publications.*

6.4   FAULT-TOLERANT ENERGY MANAGEMENT PROBLEM

Now, the complete fault-tolerant energy management problem is minutely detailed:

Assumption 3. *The faults on the energy systems, represented mathematically by $\Lambda(k)$, are accurately estimated by an efficient, online Fault Detection and Diagnosis FDD scheme. This means that the fault-tolerant controller that is designed herein has access to $\Lambda(k)$ at every iteration. This FDD scheme can be based on parity-space approaches, like [18], or even on LPV methods, as the one proposed in [110].*

Assumption 4. *The external disturbances $w(k)$ are dependent on the whether conditions on the sugarcane field (solar irrandiance and wind speed). For this, it is considered that the fault-tolerant controller has access to (accurate) estimations of these disturbances, $\hat{w}(k)$. These estimations can be derived from different methods, like the Double Exponential Smoothing (DES) technique, used in [59]. Neural Network methods are used in [11]. Figures 4.3 and 4.4 (In Chapter 4) present an excerpt from these estimations, considering real meteorological data from the state of Paraná, Brazil.*

Problem 2. *Given the accurate knowledge of $\Lambda(k)$, find an hourly-discrete controller C that determines the set-points $u(k)$ to the plant's subsystems, such that the controlled outputs $z(k)$ abide by the operational constraints presented in Chapter 2, Section 2.2.1, despite the presence and magnitude of loss of effectiveness faults on each subsystem $\alpha_j(k)$ and the load disturbances $w(k)$. This is illustrated in Figure 6.1.*
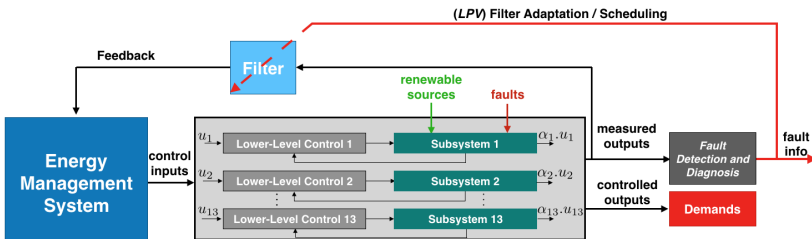
Figure 6.1: Outline of Studied Problem.

6.5   *LPV*-FILTERED PREDICTIVE CONTROL

The following Procedure presents the proposed solution to Problem 2:

Procedure 1. *A Fault-Tolerant Energy Management System to solve the studied problem can be designed considering the four steps listed next:*

1. *Firstly, find a cascaded model of the system, for which the faults are decoupled from the main dynamics. This is $G(z) = G_n(z) \times G_f(z)$, where $G(z)$ stands for the complete faulty model, $G_n(z)$ for a nominal fault-free model and $G_f(z)$ for the fault model.*

2. *Find a scheduling parameter $0 \leq \sigma(k) \leq 1$, a bounded scalar that represents the level of faults on the system, computed from $G_n(z)$.*

3. *Then, find a low-pass LPV filter F that filters the measured outputs $y(k)$. This filter must vary according to $\sigma(k)$, being scheduled (affine) by this parameter. For faultless situations, F must be an identity matrix.*

4. *Finally, design a model-based predictive controller, taking $G_n(z)$ as model and considering $\hat{w}(k)$ as the input disturbances, such that a cost function J is optimized considering the system's constraints, refer to Chapter 2, Section 2.2.1.*

The complete problem solution is schematized in Figure 6.2.
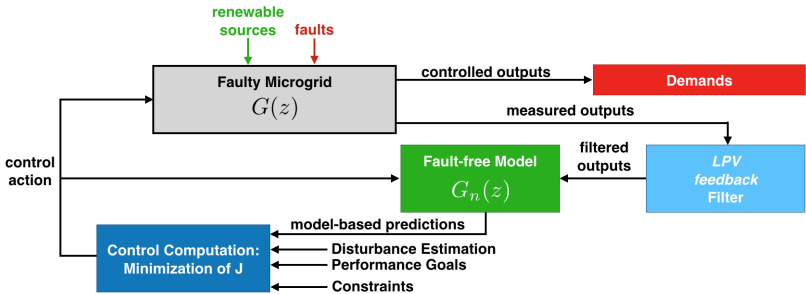
Figure 6.2: Proposed Problem Solution.

Remark 26. *Proof that this Procedure guarantees the expected stability and performance goals is immediate from linear superposition and (LPV) linear differential inclusion.*
The use of the filter to overcome faults is likewise the filter proposed

in [131] to compensate dead-time. This DTC-MPC *design has been
applied in [132] and other works. Note, still, that stability is to be
guaranteed at both extremities of closed-loop system, at $\sigma = 0$ and
$\sigma = 1$.*

6.5.1   Why a *Feedback* Filter?

Of course, a model-reconfiguration method could have been
used for the same fault-tolerant control purpose. Nonetheless, this
would not be ideal due to its difficult acceptance to industry. In in-
dustry, power systems are mostly controlled by high-level *automata*
or *PLCs*. Thus, the use of a *feedback* filter is much more suitable than
controller reconfiguration approaches, as it has smaller implemen-
tation complexity and can be done with a single additional micro-
controller.

It must be noted that this *feedback* filter has the intent to in-
dicate (indirectly) to the controller that the controlled system is
not obeying to its contract requirements. It does so by slowing the
response, such that the controller computes a more intense action
(re-arranging) which subsystems to use. The goal of abiding to con-
tract rules depends on the availability of the resources and on the
efficiency of the energy-conversion units.

This *feedback* filter is not the one from Chapter 4, that detects
and estimates faults, but an adaptive gain / low-pass that filters /
slows the feedback of controlled outputs response to the *MPC*.

6.5.2   Fault Decoupling

Considering the Faulty Hybrid Power Plant discrete-time model
($G(z)$) described by the *state-space* representation in equation (6.1),
the Fault Decoupling for the studied system is quite straightforward:
the fault model $G_f(z)$ is the fault distribution matrix $\Lambda(k)$, whereas
the nominal plant model $G_n(z)$ is given by equation (6.1), while
taking $u_f(k)$ as inputs. This is illustrated by Figure 6.3, where the
faulty plant is divided into the cascaded models $G_f(z)$ and $G_n(z)$.

6.5.3   Scheduling Parameter

Then, in terms of the scheduling parameter $\sigma(k)$, that mea-
sures the level of faults in the system, this is taken as:

$$\sigma(k) \quad = \quad \frac{\text{Tr}\{\Lambda(k)\}}{\text{size}\{\Lambda(k)\}}, \qquad (6.4)$$
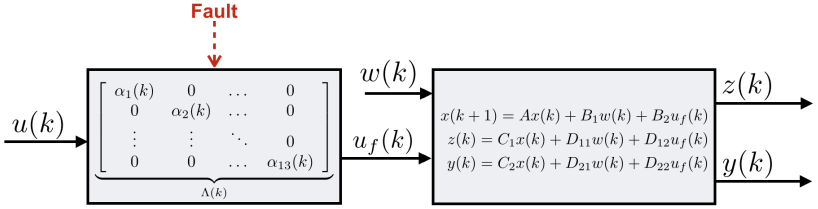
Figure 6.3: Fault Decoupling: Hybrid Energy Plant.

which is a known signal bounded within the set $[0\,,\,1]$. The operator $\text{Tr}\{\cdot\}$ is the trace of the matrix.

Notice how the scheduling signal varies as expected: for completely faultless situations, $\Lambda(k) = \text{diag}\{1_{13}\}$ and, thus, $\sigma(k) = 1$; for a complete failure on all subsystems, $\Lambda(k) = \text{diag}\{0_{13}\}$ and, thus, $\sigma(k) = 0$.

6.5.4 *LPV* Filter Synthesis

The *LPV* filter must be low-pass to decelerate the control action u in the case of faults. This ensures further robustness and more conservatism towards faults. Two conditions have to be obeyed for this synthesis, considering the chosen scheduling signal σ: that it must be an identity block when $\sigma = 1$ and that it should be a low-pass filter with time constant τ when $\sigma = 0$. These conditions are given below, with abuse of notation.

$$F(z,\sigma)|_{\sigma=1} = 1, \qquad F(z,\sigma)|_{\sigma=0} = \frac{1}{\tau\frac{z^{-1}}{T_s}+1}\ . \qquad (6.5)$$

Remark 27. *Similarly to [133], τ is a design parameter that changes the filter's bandwidth and, thus, the closed-loop robustness index.*

The straightforward *LPV* Filter that is achieved considering the stated conditions is given below, with abuse of notation. Figure 6.4 shows the filter's frequency response and how it varies, as expected, according to σ.

$$F(z,\sigma) := \left\{ \begin{array}{c} x_f(k+1) = A_f(\sigma)x_f(k) + B_f(\sigma)y(k) \\ y_f(k) = C_f(\sigma)x_f(k) + D_f(\sigma)y(k) \end{array} \right.\ , \qquad (6.6)$$

$$\begin{array}{rcl} A_f(\sigma) &=& 1 + \frac{\sigma T_s - T_s}{\tau}, \\ C_f(\sigma) &=& (1-\sigma)\ , \end{array} \left| \begin{array}{rcl} B_f(\sigma) &=& \frac{T_s - \sigma T_s}{\tau}, \\ D_f(\sigma) &=& \sigma\ . \end{array} \right. \qquad (6.7)$$
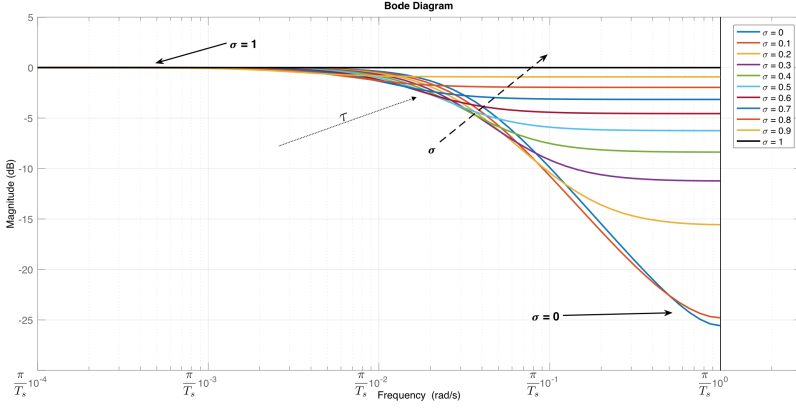
Figure 6.4: Filter: Frequency Plot.

6.5.5   Predictive Controller Synthesis

In order for the energy plant to abide to the energy produc-
tion rules, supplying the local *DNO* with $753\,MWh$ per day, the fol-
lowing cost function is established:

$$J = \sum_{i=0}^{N_c-1} D(k+i)Q_P D^T(k+i) + q_u u(k+i) \tag{6.8}$$

$$+ \sum_{i=0}^{N_p-1} \left(\hat{x}(k+i) - \hat{x}_{ref}(k+i) \right),$$

$$D(k+i) = \left[Pot_{Net}(k+i) - \frac{E_{con} - E_{sum}}{T_s} \right], \tag{6.9}$$

where E_{sum} represents the electric energy that has already been
produced; E_{con} stands for the energy sales contract value; $\hat{x}_{ref}$ is a
reference to the states; $N_p = 12\,h$ represents the prediction horizon,
while $N_c = 5\,h$ represents the control horizon. As it can be seen,
$(E_{con} - E_{sum})$ represents how much electric energy the microgrid
still has to produce until the end of the day, due to contract require-
ment, taking T_s as the sampling period of $1\,h$. J does not need to be
quadratic on u, given that the control set-points u_j are all positive.

The *MPC* Synthesis, then, resides in minimizing J, considering the fault-free model $G_n(z)$, such that the following constraints are obeyed (equivalent to those in Chapter 2, Section 2.2.1):

$$\underline{x}_j \quad \leq \quad \hat{x}_j(k+i+1) \leq \overline{x}_j \,, \qquad (6.10)$$

$$0 < \underline{u}_j \quad \leq \quad \hat{u}_j(k+i) \leq \overline{u}_i \,, \qquad (6.11)$$

$$z(k+i) \quad = \quad Demands(k) \,, \qquad (6.12)$$

for $i = 0, \ldots, N_p - 1$, where q_u, Q_P and Q_x are adequate positive definite weighting matrices.

Remark 28. *As states Assumption 4, this predictive controller uses feedforward compensation of estimated future disturbances, knowing that they influence upon $D(j+i)$, according to the microgrid energy-generation process model, see Chapter 2.*

Remark 29. *The values used for N_c, N_p, T_s and weighting variables were taken from [9], where they were proved to be adequate.*

6.5.6 Stability

In terms of stability towards faults, a quick comment has to be made: the use of the *feedback* filter to overcome uncertainties ensures further robustness to the closed-loop (*CL*) system 6.1, as it is discussed in [134]. Considering the usual M-Δ representation, the *CL* robust stability conditions (when constraints are not active) are given by:

$$\overline{sv}(\Delta(jw)) \quad < \quad \frac{1}{\overline{sv}(M(jw))}, \quad \forall w \in [0, \infty) \,. \qquad (6.13)$$

As it is verified in [135], this condition (6.13) depends, among other factors, on the used filter F[1]: a filter with a larger τ is more conservative towards faults, although it also slows the controlled output's response. This is well expected due to the trade-off between robustness margins and performance.

---

[1]*The M-Δ representation is seen in many Robust Control textbooks and references; Notation $\overline{sv}(\mathcal{M})$ stands for the maximum singular value of $\mathcal{M}$; Considering the used control scheme, $F(z, \sigma)$ would appear inside $M(jw)$, while the fault matrix $(G_f(z))$ would comprise $\Delta(jw)$.*

6.6   RESULTS AND ANALYSIS

This Section presents some simulation results in order to illustrate the effectiveness of Fault-Tolerant Energy Management System, proposed in Procedure 1. All the strategies presented herein were synthesized in *Matlab*.

6.6.1   Scenario 1: Filter Tuning

Firstly, it has to be shown how the filter parameter τ was chosen, in order for good results in terms of fault-tolerance to be achieved. For this test, multiple faults were randomly simulated on all energy subsystems, $\Lambda(k) \in [0_{13}, 1_{13}]$, considering a daily scenario with **no** renewable generation (cloudy and windless). Table 6.1 synthesizes the obtained results, showing the influence of τ (given in hours) upon the average values obtained for J (related to economic performance) and module margin and whether the system presents fault-tolerance (*FT*), the sufficient compliance to the internal demands (*DC*) and if it is too conservative (qualitatively) [2]. The overall best results were obtained with $\tau = 4\,\text{h}$, where good performances were seen, considering that the system is able to overcome the effect of faults sufficiently, while maintaining a good demand compliance and small profit loss.

Table 6.1: Performance Analysis of *FTC*: *LPV*-Filtered *MPC*.

τ	$J(\%)$	*FT*	*DC*	M_s	Conservative
1	0.03	*No*	*Yes*	1.7484	*No*
2	0.2	*Yes*	*Yes*	1.7031	*No*
3	0.4	*Yes*	*Yes*	1.5486	*OK*
4	0.6	*Yes*	*Yes*	1.4824	*Best*
5	0.77	*Yes*	*No*	1.4456	*Yes*
10	3.19	*Yes*	*No*	1.3475	*Yes*
15	5.23	*Yes*	*No*	1.3268	*Yes*

---

[2] *J: Values given in percentage, with respect to the nominal case, $J_{nom} = 1.877e^{12}$, with no Filter $F(z,\sigma)$; M_s is computed with the equivalent unconstrained* MPC*, with respect to the inverse of the minimal distance in the Nyquist diagram to the critical point $(-1, 0j)$, with $\sigma = 0$; Remark that a good value for this margin is $M_s < 2$.*

6.6.2   Scenario 2: Fault-Tolerant Energy Management

For the second scenario (main results), τ is fixed at $4\,\text{h}$ and a day with average sun and wind is considered, seen in Figures 4.3 and 4.4 (estimations given by *Neural Networks*, as done in [11]). The faults now occur only in the main energy generation subsystem (*CHP* and two turbines), and represent, for instance, effectiveness loss due to a reduction of the bearing temperature, refer to Figure 6.5. The faults that occur on the *CHP* and Turbine "A" are concomitant, to require further re-adjustments from the control scheme. Turbine "A", Turbine "B" and the *CHP* present, respectively, a loss of $25, 45$ and $25\,\%$ on their effectiveness (input-to-energy gain).
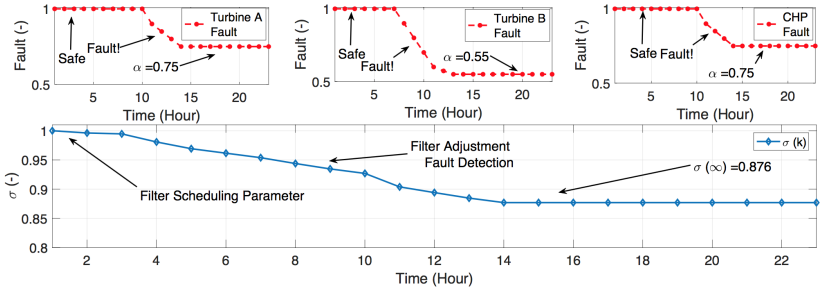
Figure 6.5: Scenario 2: Simulated Faults.

The achieved control results are given by Figures 6.6 and 6.7, which stand, respectively, for the performance of the (faulty) energy generation subsystems and global energy production throughout the day. Therein, *FTC* stands for the proposed filtered predictive controller and, for comparison goals, *SMPC* stands for the "*Standard*" *MPC* from [9], that solves the same minimization problem J but has no *feedback* filter $F(z, \sigma)$ and, thus, does not consider the effect of the faults, $G_f(z)$.

Evidently, as it can be seen in the Figures above, the *FTC* approach is able to overcome the effect of faults much faster and with ease (changing set-points as soon as fault is diagnosed), being able to produce the contract energy goal, at the end of the day, even though the energy systems fail. Note that from instant $t = 7\,\text{h}$ (first fault), the *FTC* approach manipulates the set-point in order to ensure that the end-of-the-day energy goal is achieved. On the other hand, *SMPC* takes much more time to perceive and compensate the
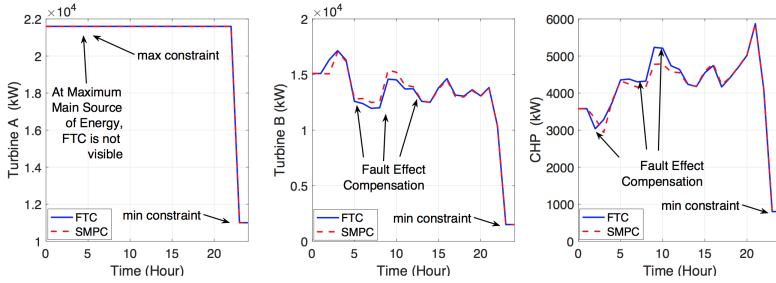
Figure 6.6: Scenario 2: Energy Generation Subsystems.
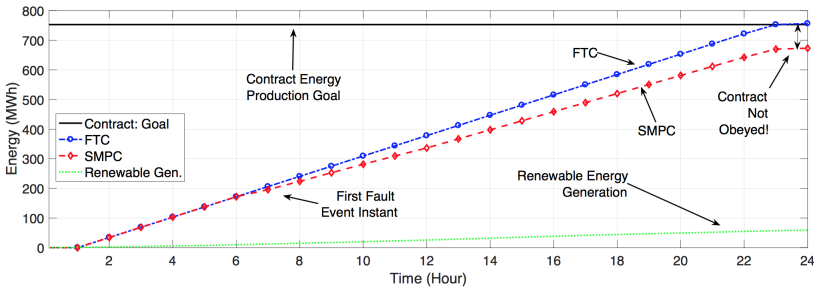
Figure 6.7: Scenario 2: Energy Production.

fault effects (faults are overlapped when $u^{FTC} = u^{SMPC}$, around 5 h after the first fault, treated by the *SMPC* as disturbance rejection). This can be complicated, as the system does not comply with the energy needs, which may imply in a fine, an economic deprivation. It has to be remarked that "Turbine A", being the main source of energy, is almost constantly fixed at its maximal operation and, as of this, both approaches choose the same set-point $u_1(k)$.

6.7   CONCLUSIONS

This Chapter presented the issue of controlling and managing a renewable microgrid based on the Sugarcane Industry, that is subject to faults in its subsystems. Considering that these faults are accurately diagnosed, an *LPV*-Filtered Predictive Controller is designed to cope with these faults, while always attending the op-

erational load demands and producing a defined amount of energy. The results enlighten the interest of the proposed *LPV*-Filter plus *MPC* paradigm to the development of Fault-Tolerant Energy Management Systems. Results show that the proposed scheme can accurately re-adjust the control law so that effects of faults are mitigated.

Part IV

Closure

7 CONCLUSION

This Master dissertation encompasses some contributions to the field of Fault Detection / Estimation and Fault-Tolerant control, with emphasis on their application to renewable microgrids. Moreover, many of the techniques herein developed derived from robust *LPV* frameworks. This work was set inside the *GPER-UFSC*, project and research group.

A summary of the work presented in this dissertation, reviewing the main contributions and exploring the possibilities of further research, is listed next.

7.1 WHAT WAS DONE, EFFECTIVELY

Given that modern technological processes are very susceptible to faults, Fault Detection / Estimation and Diagnosis are useful tools to ensure sufficient measures of reliability and safety of modern processes, which include energy systems and microgrid. Fault-Tolerant Control schemes for energy generation planning are also very important, once they would, while dealing with long-term energy generation scheduling, make the energy production immune to incipient faults of the controlled plant. These tools (*FDD* and *FTC*) would also decrease manual operator intervention on the microgrid automatic supervisor, as of to inform that faults have happened and a given system cannot be accounted for the generation on the next few hours or days.

To address the development of these tools, robust *LPV* methods were sought. Nevertheless, there is still space for further investigation; this dissertation has indeed contributed to the advancement of the *state-of-the-art* of this field, as evidenced by the published / submitted works listed below, in Section 7.3.

- As of Chapters 1, 2 and 3, a thorough theoretical background review was done, as a pillar stone for the subsequent Chapters. Therein, it was shown how *FDD* and *FTC* techniques can enhance the performance of energy management in microgrids and why they are so important. Moreover, open research threads were pointed out.

- Chapter 4 discussed the use of Linear Parameter Varying observers derived from the *LMI* computation of minimal mixed H_2/H_∞ norm. A bank of these observers was used to collect, estimate and diagnose the faults that occur on a complete mi-

crogrid with thirteen different subsystems. The achieved re-
sults were very interesting, as smooth fault estimations were
achieved. It remained to compare this approach with another
and to conclude on its robustness properties.

- Thence, Chapter 5 presented a thorough analysis of the robust-
ness qualities of the thirteen linear parameter varying H_2/H_∞
observers designed in Chapter 4. Via μ-analysis, it was possible
to find out how robust these observers indeed are. Via simula-
tion, some extreme conditions were tested, and it was verified
that the observers continued to perform reasonably well.

- To tackle the issue of *FTC*, in Chapter 6, an *MPC* fault-tolerant
scheme for the Energy Management of sugarcane microgrids
was proposed. In this method, a Linear Parameter Varying
feedback filter that adapts itself according to the level of faults
on the system acted to reconfigure the predictive control pol-
icy and enable proper behaviour of the energy generation units.

7.2   FUTURE WORKS

There are some topics that were mentioned as to be unrav-
eled, but that this work could not tackle entirely. These open threads
are:

- To test the robustness conditions of *MHE* schemes to estimate
faults in microgrids. This could help to conclude on which ap-
proach is better (*MHE* or bank-of-*LPV*-observers) to estimate
faults under extreme conditions.

- To test $H_\infty/H_2/H_-$ sensitivity constraints upon the computa-
tion of the *LPV FE* observers.

- To test an *MHE* + *MPC* scheme to act as an integrated Fault-
tolerant control scheme. Once the *MHE* solves a (backward
horizon) optimization problem, it could be integrated with an
MPC in a single optimization procedure, once they both share
the same formalism. Thereby, at every sampling instant the
FTC scheme would be estimating faults and states and com-
puting future (fault-tolerant) control actions. This has not yet
been tested for microgrids in the literature and could certainly
achieve intersting results in terms of fault-tolerance and per-
formance maintenance.

7.3 SCIENTIFIC CONTRIBUTIONS

Also, it must be pointed-out that the development presented herein enabled the publication of a good deal of scientific works (in terms of journal papers and conference proceedings). These are listed below, together with works derived from paralel development (not necessarily detailed in this document) done during the author's Master period.

In terms of accepted / submitted conference papers:

1. ***LPV-H_∞ Fault Estimation for Boilers in Sugarcane Processing Plants***, presented in the 2nd *IFAC* Workshop on Linear Parameter Varying Systems, Florianópolis, Brazil, 2018, First Author.

2. ***LPV-Filtered Predictive Control Design for Fault-Tolerant Energy Management of Hybrid Power Systems***, presented in the 12th *IFAC* Symposium on Dynamics and Control of Process Systems, including Biosystems, Florianópolis, Brazil, 2019, First Author.

3. **Moving Horizon Estimation of Faults in Renewable Microgrids**, presented in the 12th *IFAC* Symposium on Dynamics and Control of Process Systems, including Biosystems, Florianópolis, Brazil, 2019, Second Author.

4. **A Viable Sustainable Energetic Alternative for Brazil**, presented in the 7th Project Sustainability Meeting ("*VII Encontro de Sustentabilidade em Projeto*"), Florianópolis, Brazil, 2019, First Author.

5. **Dealing with Faults to Improve Resilience of Microgrids**, accepted for presentation in the 2019 IEEE PES Innovative Smart Grid Technology Latin America (ISGT LA), Gramado, Brazil, 2019, First Author.

6. **Tools for the Control of Modern Solar-Thermal Heating Plants**, submitted to the 14th Brazilian Symposium on Inteligent Automation ("*14º Simpósio Brasileiro de Automação Inteligente*"), Ouro Preto, Brazil, 2019, Second Author.

In terms of other conference papers derived from parallel works developed during the Master period:

1. *LPV-MPC* **Fault Tolerant Control of Automotive Suspension Dampers**, presented in the 2nd *IFAC* Workshop on Linear Parameter Varying Systems, Florianópolis, Brazil, 2018, First Author.

2. **Modelling the Ecological Effect of the Golden Mussel Invasion in Uruguay River**, presented in the 12th *IFAC* Symposium on Dynamics and Control of Process Systems, including Biosystems, Florianópolis, Brazil, 2019, First Author.

3. **A Linear Parameter Varying Approach for Robust Dead-Time Compensation**, presented in the 12th *IFAC* Symposium on Dynamics and Control of Process Systems, including Biosystems, Florianópolis, Brazil, 2019, First Author.

4. **Design and Analysis of Several State-Feedback Fault-Tolerant Control Strategies for Semi-Active Suspensions**, accepted for presentation to the 7th *IFAC* Symposium on System Structure and Control, Sinaia, Romania, 2019, First Author.

5. **Nonlinear Fault Estimation Methods for Automotive Semi-Active Suspension Dampers**, submitted to the 14th Brazilian Symposium on Inteligent Automation ("*14º Simpósio Brasileiro de Automação Inteligente*"), Ouro Preto, Brazil, 2019, First Author.

6. **Automation and Renewable Energies: Outreach Efforts in Brazilian Public Schools**, accepted for presentation in the ISES Solar World Congress 2019, Santiago, Chile, 2019, First Author.

7. **Novel qLPV MPC Design with Least-Squares Scheduling Prediction**, submitted to the 3rd *IFAC* Workshop on Linear Parameter-Varying Systems, Eindhoven, The Netherlands, 2019, First Author.

   In terms of accepted/submitted journal papers:

1. **Fault Analysis, Detection and Estimation for a Microgrid via H_2/H_∞ LPV Observers**, published in the *International Journal of Electrical Power and Energy Systems* (A1[1]), First Author (2018).

---

[1]*This notation refers to a Brazilian publication metric system, named Qualis CAPES. A1 stands for the highest rate, decreasing to A2, B1, B2, and so on.*

2. **Robustness Conditions of *LPV* Fault Estimation Systems for Renewable Microgrids**, published in the *International Journal of Electrical Power and Energy Systems* (A1), First Author (2019).

3. **A Two-Layer *EMS* for Cooperative Sugarcane-based Microgrids**, submitted to the *International Journal of Electrical Power and Energy Systems* (A1), First Author.

4. ***LPV -MPC* Fault-Tolerant Energy Management Strategy for Renewable Microgrids**, submitted to the *International Journal of Electrical Power and Energy Systems* (A1), First Author.

In terms of other journal papers from parallel works developed within the Master period:

1. **Design of a Fast Real-Time LPV Model Predictive Control System for Semi-Active Suspension Control of a Full Vehicle**, published in the *Journal of the Franklin Institute* (A1), First Author (2019).

2. **Fault Estimation for Automotive ER Dampers: LPV-based Observer Approach**, published in *Control Engineering Practice* (A1), First Author (2019).

3. **Predictive Control for the Regulation of the Golden Mussel *Limnoperna fortunei* (Dunker, 1857)**, accepted for publication in the *International Journal on Ecological Modelling and Systems Ecology* (B1), Second Author ;

4. **Fault-Tolerant Control-Oriented Modelling of ER Dampers in a Scaled Vehicle**, submitted to *Mechanical Systems and Signal Processing* (B1), First Author.

7.4   PERSONAL ANALYSIS

The Author's Master period at *UFSC* began in August 2018 and ended June 2019. The work herein exposed was supervised by professor *Julio Elias Normey-Rico* and co-supervised by doctor *Paulo Renato da Costa Mendes*. Professor *Carlos Bordons*, from the University of Seville (*Universidad de Sevilla*), also played a lead co-authorship role in some of the papers derived from this work. The Author also sustained a collaboration with the University of Grenoble (*Université Grenoble-Alpes*), with professors *Olivier Sename* and

Luc Dugard. The Author also collaborated with other post-graduate students, fellow master and undergraduate colleagues.

Writing from an author's point of view: the work developed during this Master period was most pleasurable for me. As in my past experiences as a scientific initiation student, professor Julio received and guided me very well. My collaborations with Carlos Bordons and Paulo Mendes also proved to be succesfull and fruitful. I hope to have developed literature-worthy publications and interesting results that can lead to further researches. My personal and academic development during this period was undoubtedly enormous.

7.5   ACKNOWLEDGEMENTS

REFERENCES

1 HOPWOOD, B.; MELLOR, M.; O'BRIEN, G. Sustainable development: mapping different approaches. *Sustainable development*, Wiley Online Library, v. 13, n. 1, p. 38–52, 2005.

2 MORATO, M. M. et al. Future hybrid local energy generation paradigm for the brazilian sugarcane industry scenario. *International Journal of Electrical Power and Energy Systems*, Elsevier, p. 139–150, 2018.

3 JOHN, R. P. et al. Micro and macroalgal biomass: a renewable source for bioethanol. *Bioresource technology*, Elsevier, v. 102, n. 1, p. 186–193, 2011.

4 PERRY, S.; KLEMEŠ, J.; BULATOV, I. Integrating waste and renewable energy to reduce the carbon footprint of locally integrated energy sectors. *Energy*, Elsevier, v. 33, n. 10, p. 1489–1497, 2008.

5 NOGUEIRA, C. E. C. et al. Exploring possibilities of energy insertion from vinasse biogas in the energy matrix of paraná state, brazil. *Renewable and Sustainable Energy Reviews*, Elsevier, v. 48, p. 300–305, 2015.

6 CARRASCO, J. M. et al. Power-electronic systems for the grid integration of renewable energy sources: A survey. *IEEE Transactions on industrial electronics*, IEEE, v. 53, n. 4, p. 1002–1016, 2006.

7 MORAGA-NICOLÁS, F. et al. Rhodolirium andicola: a new renewable source of alkaloids with acetylcholinesterase inhibitory activity, a study from nature to molecular docking. *Revista Brasileira de Farmacognosia*, SciELO Brasil, v. 28, n. 1, p. 34–43, 2018.

8 ZABED, H. et al. Bioethanol production from renewable sources: Current perspectives and technological progress. *Renewable and Sustainable Energy Reviews*, Elsevier, v. 71, p. 475–501, 2017.

9 MORATO, M. M. et al. Optimal operation of hybrid power systems including renewable sources in the sugar cane industry. *IET Renewable Power Generation*, v. 11, p. 1237–1245(8), 2017.

10 OLAMA, A.; MENDES, P. R.; CAMACHO, E. F. Lyapunov-based hybrid model predictive control for energy management of microgrids. *IET Generation, Transmission & Distribution*, IET, v. 12, n. 21, p. 5770–5780, 2018.

11   VERGARA-DIETRICH, J. D. et al. Advanced chance-constrained predictive control for the efficient energy management of renewable power systems. *Journal of Process Control*, Elsevier, v. 74, p. 120–132, 2019.

12   VALVERDE, L. et al. Modeling, simulation and experimental set-up of a renewable hydrogen-based domestic microgrid. *International Journal of Hydrogen Energy*, Elsevier, v. 38, p. 11672 – 11684, 2012.

13   PETROLLESE, M. *Optimal generation scheduling for renewable microgrids using hydrogen storage systems*. Tese (Doutorado) — Universita'degli Studi di Cagliari, 2015.

14   BÁEZ-GONZÁLEZ, P. et al. Day-ahead economic optimization of energy use in an olive mill. *Control Engineering Practice*, Pergamon, v. 54, p. 91–103, 2016.

15   GARCIA-TORRES, F.; BORDONS, C. Optimal economical schedule of hydrogen-based microgrids with hybrid storage using model predictive control. *IEEE Transactions on Industrial Electronics*, v. 62, n. 8, p. 5195–5207, 2015.

16   DAOUTIDIS, P.; ZACHAR, M.; JOGWAR, S. S. Sustainability and process control: A survey and perspective. *Journal of Process Control*, Elsevier, v. 44, p. 184–206, 2016.

17   LASSETER, R. H.; PAIGI, P. Microgrid: a conceptual solution. In: IEEE. *35th Power Electronics Specialists Conference*. [S.l.], 2004. v. 6, p. 4285–4290.

18   GERTLER, J. Fault detection and isolation using parity relations. *Control engineering practice*, Elsevier, v. 5, n. 5, p. 653–661, 1997.

19   AL-SHEIKH, H.; MOUBAYED, N. Fault detection and diagnosis of renewable energy systems: An overview. In: *International Conference on Renewable Energies for Developing Countries*. [S.l.: s.n.].

20   PRODAN, I.; ZIO, E.; STOICAN, F. Fault tolerant predictive control design for reliable microgrid energy management under uncertainties. *Energy*, Elsevier, v. 91, p. 20–34, 2015.

21   PRODAN, I.; ZIO, E. A model predictive control framework for reliable microgrid energy management. *International Journal of Electrical Power & Energy Systems*, Elsevier, v. 61, p. 399–409, 2014.

22 MARQUEZ, J.; ZAFRA-CABEZA, A.; BORDONS, C. Diagnosis and fault mitigation in a microgrid using model predictive control. In: IEEE. *International Conference on Smart Energy Systems and Technologies*. [S.l.], 2018. p. 1–6.

23 MAGNE, P.; NAHID-MOBARAKEH, B.; PIERFEDERICI, S. Dynamic consideration of DC microgrids with constant power loads and active damping system—a design method for fault-tolerant stabilizing system. *IEEE Journal of Emerging and Selected Topics in Power Electronics*, IEEE, v. 2, n. 3, p. 562–570, 2014.

24 MORSHED, M. J.; FEKIH, A. A fault-tolerant control paradigm for microgrid-connected wind energy systems. *IEEE Systems Journal*, IEEE, v. 12, n. 1, p. 360–372, 2018.

25 HOSSEINZADEH, M.; SALMASI, F. R. Fault-tolerant supervisory controller for a hybrid AC/DC micro-grid. *IEEE Transactions on Smart Grid*, IEEE, v. 9, n. 4, p. 2809–2823, 2018.

26 VENKATASUBRAMANIAN, V. et al. A review of process fault detection and diagnosis: Part i: Quantitative model-based methods. *Computers & chemical engineering*, Elsevier, v. 27, n. 3, p. 293–311, 2003.

27 ZHANG, K.; JIANG, B.; SHI, P. *Observer-based fault estimation and accomodation for dynamic systems*. [S.l.]: Springer, 2012.

28 ZHANG, K.; JIANG, B.; COCQUEMPOT, V. Fast adaptive fault estimation and accommodation for nonlinear time-varying delay systems. *Asian Journal of Control*, Wiley Online Library, v. 11, n. 6, p. 643–652, 2009.

29 GAO, Z.; DING, S. X. Actuator fault robust estimation and fault-tolerant control for a class of nonlinear descriptor systems. *Automatica*, Elsevier, v. 43, n. 5, p. 912–920, 2007.

30 MORATO, M. M. et al. Fault estimation for automotive electro-rheological dampers: LPV-based observer approach. *Control Engineering Practice*, Elsevier, v. 85, p. 11–22, 2019.

31 GATZKE, E. P.; III, F. J. D. Use of multiple models and qualitative knowledge for on-line moving horizon disturbance estimation and fault diagnosis. *Journal of Process Control*, Elsevier, v. 12, n. 2, p. 339–352, 2002.

32   AMIRAT, Y. et al. A brief status on condition monitoring and fault diagnosis in wind energy conversion systems. *Renewable and sustainable energy reviews*, Elsevier, v. 13, n. 9, p. 2629–2636, 2009.

33   CHOUDER, A.; SILVESTRE, S. Automatic supervision and fault detection of PV systems based on power losses analysis. *Energy conversion and Management*, Elsevier, v. 51, n. 10, p. 1929–1937, 2010.

34   SALAHSHOOR, K.; KORDESTANI, M.; KHOSHRO, M. S. Fault detection and diagnosis of an industrial steam turbine using fusion of SVM (support vector machine) and ANFIS (adaptive neuro-fuzzy inference system) classifiers. *Energy*, Elsevier, v. 35, n. 12, p. 5472–5482, 2010.

35   ODGAARD, P. F.; STOUSTRUP, J.; KINNAERT, M. Fault tolerant control of wind turbines–a benchmark model. *IFAC Proceedings Volumes*, Elsevier, v. 42, n. 8, p. 155–160, 2009.

36   ZAHER, A. et al. Online wind turbine fault detection through automated SCADA data analysis. *Wind Energy*, Wiley Online Library, v. 12, n. 6, p. 574–593, 2009.

37   MOHANTY, R.; BALAJI, U. S. M.; PRADHAN, A. K. An accurate noniterative fault-location technique for low-voltage DC microgrid. *IEEE Transactions on Power Delivery*, IEEE, v. 31, n. 2, p. 475–481, 2016.

38   HAO, Y. et al. An intelligent algorithm for fault location on VSC-HVDC system. *International Journal of Electrical Power & Energy Systems*, Elsevier, v. 94, p. 116–123, 2018.

39   YEAP, Y. M.; GEDDADA, N.; UKIL, A. Capacitive discharge based transient analysis with fault detection methodology in DC system. *International Journal of Electrical Power & Energy Systems*, Elsevier, v. 97, p. 127–137, 2018.

40   DHAR, S.; PATNAIK, R.; DASH, P. Fault detection and location of photovoltaic-based DC microgrid using differential protection strategy. *IEEE Transactions on Smart Grid*, IEEE, v. 9, n. 5, p. 4303–4312, 2018.

41   GILBERT, D.; MORRISON, I. A statistical method for the detection of power system faults. *International Journal of Electrical Power & Energy Systems*, Elsevier, v. 19, n. 4, p. 269–275, 1997.

42 ESLAMI, R. et al. A novel method for fault detection in future renewable electric energy delivery and management microgrids, considering uncertainties in network topology. *Electric Power Components and Systems*, Taylor & Francis, v. 45, n. 10, p. 1118–1129, 2017.

43 MORTAZAVI, S. H.; MORAVEJ, Z.; SHAHRTASH, S. M. A hybrid method for arcing faults detection in large distribution networks. *International Journal of Electrical Power & Energy Systems*, Elsevier, v. 94, p. 141–150, 2018.

44 RAO, C. V.; RAWLINGS, J. B.; LEE, J. H. Constrained linear state estimation—a moving horizon approach. *Automatica*, v. 37, n. 10, p. 1619–1628, oct 2001.

45 LIMA, B. M. et al. Moving horizon estimation of faults in renewable microgrids. In: IFAC. *12th IFAC Symposium on Dynamic and Control of Process Systems, including Biosystems, Florianópolis, Brazil*. [S.l.], 2019.

46 JOHANSSON, T. B. *Renewable energy: sources for fuels and electricity*. [S.l.]: Island press, 1993.

47 SHAFIEE, S.; TOPAL, E. A long-term view of worldwide fossil fuel prices. *Applied Energy*, Elsevier, v. 87, n. 3, p. 988–1000, 2010.

48 SHAFIEE, S.; TOPAL, E. When will fossil fuel reserves be diminished? *Energy policy*, Elsevier, v. 37, n. 1, p. 181–189, 2009.

49 JIAYI, H.; CHUANWEN, J.; RONGI, X. A review on distributed energy resources and microgrid. *Renewable and Sustainable Energy Reviews*, v. 12, n. 9, p. 2472 – 2483, 2008.

50 DELL, R.; RAND, D. Energy storage: a key technology for global energy sustainability. *Journal of Power Sources*, v. 100, n. 1, p. 2–17, 2001.

51 ALARCON-RODRIGUEZ, A.; AULT, G.; GALLOWAY, S. Multi-objective planning of distributed energy resources: A review of the state-of-the-art. *Renewable and Sustainable Energy Reviews*, Elsevier, v. 14, n. 5, p. 1353–1366, 2010.

52 PARISIO, A.; VECCHIO, C. D.; VACCARO, A. A robust optimization approach to energy hub management. *International Journal of Electrical Power & Energy Systems*, Elsevier, v. 42, n. 1, p. 98–104, 2012.

53   MO, H.; SANSAVINI, G. Real-time coordination of distributed energy resources for frequency control in microgrids with unreliable communication. *International Journal of Electrical Power & Energy Systems*, Elsevier, v. 96, p. 86–105, 2018.

54   FERRARI-TRECATE, G. et al. Modeling and control of co-generation power plants: a hybrid system approach. *IEEE Transactions on Control Systems Technology*, v. 12, n. 5, p. 694–705, 2004.

55   MENDES, P. R. C. et al. Energy management of an experimental microgrid coupled to a V2G system. *Journal of Power Sources*, Elsevier, p. 702–713, 2016.

56   PAWLOWSKI, A. et al. Application of time-series methods to disturbance estimation in predictive control problems. In: IEEE. *IEEE International Symposium on Industrial Electronics*. [S.l.], 2010. p. 409–414.

57   PAWLOWSKI, A. et al. Improving feedforward disturbance compensation capabilities in generalized predictive control. *Journal of Process Control*, Elsevier, v. 22, n. 3, p. 527–539, 2012.

58   MORATO, M. M. et al. Study of a hybrid energy generation plant in the sugar cane industry (text in portuguese). In: XXI BRAZILIAN CONGRESS OF AUTOMATIC. [S.l.], 2016.

59   MORATO, M. M. et al. Advanced control for energy management of grid-connected hybrid power systems in the sugar cane industry. *IFAC-PapersOnLine*, Elsevier, v. 50, n. 1, p. 31–36, 2017.

60   Ministério de Minas e Energia, Governo Federal. *Brazilian Energy Review: 2014 Exercise (Text in Portuguese)*. [S.l.: s.n.], 2015. 6 - 19 p.

61   TIBA, C. Solar radiation in the brazilian northeast. *Renewable Energy*, Elsevier, v. 22, n. 4, p. 565–578, 2001.

62   COSTA, M. V. Americano-da. *Modellin, Control and Optimization of Ethanol Industrial Processes: A Solar Energy Application (Text in Portuguese)*. Tese (Doutorado) — Universidade Federal de Santa Catarina, 2013.

63   GONZÁLEZ, J. R. P. *Automatic control white paper in the sugar cane industry (Text in spanish)*. [S.l.]: Programa Iberoamericano de Ciencia y Tecnología para el Desarrollo (CYTED), 2011.

64 ALVES, J. M. Paradigma técnico e co-geração de energia com bagaço de cana de açúcar em goiás. *Proceedings of the 6. Encontro de Energia no Meio Rural*, SciELO Brasil, 2006.

65 DANTAS, G. A.; LEGEY, L. F.; MAZZONE, A. Energy from sugarcane bagasse in brazil: An assessment of the productivity and cost of different technological routes. *Renewable and Sustainable Energy Reviews*, Elsevier, v. 21, p. 356–364, 2013.

66 MAUÉS, J. Maximizacao da geracao eletrica a partir do bagaco e palha em usinas de acucar e alcool. *Revista Engenharia*, v. 583, p. 88–98, 2007.

67 SANTOS, M. L. dos et al. Estudo das condições de estocagem do bagaço de cana-de-açúcar por análise térmica. *Quim. Nova*, v. 34, n. 3, p. 507–511, 2011.

68 LEAL, M. R. L. et al. Sugarcane straw availability, quality, recovery and energy use: a literature review. *Biomass and Bioenergy*, Elsevier, v. 53, p. 11–19, 2013.

69 REGO, E. E.; HERNANDEZ, F. D. M. Eletricidade por digestão anaeróbia da vinhaça de cana-de-açúcar: contornos técnicos, econômicos e ambientais de uma opção. *Proceedings of the 6. Encontro de Energia no Meio Rural*, SciELO Brasil, 2006.

70 PINTO, C. P. Tecnologia da digestão anaeróbia da vinhaça e desenvolvimento sustentável. 1999.

71 BERNAL, A. P. et al. Vinasse biogas for energy generation in brazil: An assessment of economic feasibility, energy potential and avoided CO2 emissions. *Journal of Cleaner Production*, Elsevier, 2017.

72 PELLEGRINI, M. C. *Inserção de centrais cogeradoras a bagaço de cana no parque energético do Estado de São Paulo: exemplo de aplicação de metodologia para análise dos aspectos locacionais e de integração energética*. Tese (Doutorado) — Universidade de São Paulo, 2002.

73 DEMIRBAS, A. Biofuels sources, biofuel policy, biofuel economy and global biofuel projections. *Energy conversion and management*, Elsevier, v. 49, n. 8, p. 2106–2116, 2008.

74 INNOCENTE, A. F. *Cogeneration for the Sugarcane Biomass Residuals Text in Portuguese*. Tese (Doutorado) — Universidade Estadual Paulista Júlio Mesquita Filho, 2011.

75   ENERGETIC Potential from Sugarcane Bagasse and Straw (Text in Portuguese. Tese (Doutorado).

76   TOLENTINO, G.; FLORENTINO, H. d. O.; SARTORI, M. M. P. Mathematical modeling for sugarcane residual biomass exploitation with minimum cost Text in Portuguese. *Bragantia*, Instituto Agronômico de Campinas, v. 66, p. 729–735, 2007.

77   JÚNIOR, R.; AGUDO, R. *Sugarcane Straw Exploitation Viability for Cogeneration in a Sugar and Ethanol Industry Text in Portuguese*. Tese (Doutorado), 2009.

78   GEIDL, M. et al. Energy hubs for the future. *IEEE Power and Energy Magazine*, v. 5, n. 1, p. 24, 2007.

79   GEIDL, M. *Integrated modeling and optimization of multi-carrier energy systems*. Tese (Doutorado) — ETH Zurich, 2007.

80   MORATO, M. M. et al. LPV-h_∞ fault estimation for boilers in sugarcane processing plants. *IFAC-PapersOnLine*, Elsevier, v. 51, n. 26, p. 1–6, 2018.

81   MORATO, M. M.; MENDES, P. R. C.; NORMEY-RICO, J. E. Dealing with faults to improve resilience of microgrids. In: *Proceedings of the 2019 IEEE PES Innovative Smart Grid Technologies Latin America (ISGT-LA), Gramado, Brazil*. [S.l.: s.n.], 2019.

82   MORATO, M. M. et al. Fault analysis, detection and estimation for a microgrid via h_2/h_∞ LPV observers. *International Journal of Electrical Power & Energy Systems*, Elsevier, v. 105, p. 823–845, 2019. ISSN 0142-0615.

83   GREENWELL, W.; VAHIDI, A. Predictive control of voltage and current in a fuel cell-ultracapacitor hybrid. *IEEE Transactions on Industrial Electronics*, v. 57, n. 6, p. 1954–1963, 2010.

84   MENDES, P. R. et al. A practical approach for hybrid distributed MPC. *Journal of Process Control*, Elsevier, v. 55, p. 30–41, 2017.

85   BLANKE, M. et al. Fault-tolerant control systems - a holistic view. Elsevier, 1997.

86   PERSIS, C. D.; ISIDORI, A. A geometric approach to nonlinear fault detection and isolation. *IEEE transactions on automatic control*, IEEE, v. 46, n. 6, p. 853–865, 2001.

87   HAMMOURI, H.; KINNAERT, M.; YAAGOUBI, E. E. Observer-based approach to fault detection and isolation for nonlinear systems. *IEEE transactions on automatic control*, IEEE, v. 44, n. 10, p. 1879–1884, 1999.

88   ZOLGHADRI, A.; HENRY, D.; MONSION, M. Design of nonlinear observers for fault diagnosis: a case study. *Control Engineering Practice*, Elsevier, v. 4, n. 11, p. 1535–1544, 1996.

89   ZHANG, Q.; BASSEVILLE, M.; BENVENISTE, A. *Fault detection and isolation in nonlinear dynamic systems: A combined input-output and local approach*. Tese (Doutorado) — INRIA, 1997.

90   CHEN, J.; PATTON, R. J. *Robust model-based fault diagnosis for dynamic systems*. [S.l.]: Springer Science & Business Media, 2012.

91   ISERMANN, R. Supervision, fault-detection and fault-diagnosis methods—an introduction. *Control engineering practice*, Elsevier, v. 5, n. 5, p. 639–652, 1997.

92   BRUZELIUS, F.; PETTERSSON, S.; BREITHOLTZ, C. Linear parameter-varying descriptions of nonlinear systems. In: IEEE. *American Control Conference, 2004. Proceedings of the 2004*. [S.l.], 2004. v. 2, p. 1374–1379.

93   SZÁSZI, I. et al. Linear parameter-varying detection filter design for a boeing 747-100/200 aircraft. *Journal of Guidance Control and Dynamics*, New York: The Institute, 1982-, v. 28, n. 3, p. 461–470, 2005.

94   DO, A.-L.; SENAME, O.; DUGARD, L. An LPV control approach for semi-active suspension control with actuator constraints. In: IEEE. *American Control Conference (ACC), 2010*. [S.l.], 2010. p. 4653–4658.

95   MORATO, M. M.; SENAME, O.; DUGARD, L. LPV-MPC fault tolerant control of automotive suspension dampers. *IFAC-PapersOnLine*, Elsevier, v. 51, n. 26, p. 31–36, 2018.

96   CHEN, L.; PATTON, R.; GOUPIL, P. Application of model-based LPV actuator fault estimation for an industrial benchmark. *Control Engineering Practice*, Elsevier, v. 56, p. 60–74, 2016.

97   OCA, S. de et al. Fault-tolerant control strategy for actuator faults using LPV techniques: Application to a two degree of freedom helicopter. *International Journal of Applied Mathematics and Computer Science*, v. 22, n. 1, p. 161–171, 2012.

98   ZHANG, K.; JIANG, B.; CHEN, W. An improved adaptive fault estimation design for polytopic LPV systems with application to helicopter models. In: IEEE. *Asian Control Conference, 2009. ASCC 2009. 7th*. [S.l.], 2009. p. 1108–1113.

99   ROTONDO, D. et al. Actuator multiplicative fault estimation in discrete-time LPV systems using switched observers. *Journal of the Franklin Institute*, Elsevier, v. 353, n. 13, p. 3176–3191, 2016.

100   GRENAILLE, S.; HENRY, D.; ZOLGHADRI, A. A method for designing fault diagnosis filters for LPV polytopic systems. *Journal of Control Science and Engineering*, Hindawi Publishing Corp., v. 2008, p. 1, 2008.

101   PATTON, R. J.; CHEN, L.; KLINKHIEO, S. An LPV pole-placement approach to friction compensation as an FTC problem. *Int. J. Appl. Math. Comput. Sci.*, v. 22, n. 1, p. 149–160, March 2012.

102   HERNÁNDEZ-ALCÁNTARA, D. et al. Modeling, diagnosis and estimation of actuator faults in vehicle suspensions. *Control Engineering Practice*, Elsevier, v. 49, p. 173–186, 2016.

103   MATHWORKS. *MATLAB R2017a*. 2017.

104   MORÉ, J. J. The levenberg-marquardt algorithm: implementation and theory. In: *Numerical analysis*. [S.l.]: Springer, 1978. p. 105–116.

105   NGUYEN, M. Q.; SENAME, O.; DUGARD, L. A switched LPV observer for actuator fault estimation. *IFAC-PapersOnLine*, Elsevier, v. 48, n. 26, p. 194–199, 2015.

106   RODRIGUES, M. et al. Actuator fault estimation based adaptive polytopic observer for a class of lpv descriptor systems. *International Journal of Robust and Nonlinear Control*, Wiley Online Library, v. 25, n. 5, p. 673–688, 2015.

107   KHARGONEKAR, P. P.; ROTEA, M. A. Mixed h_2/h_∞ filtering. In: IEEE. *Decision and Control, 1992., Proceedings of the 31st IEEE Conference on*. [S.l.], 1992. p. 2299–2304.

108   KHOSROWJERDI, M. J.; NIKOUKHAH, R.; SAFARI-SHAD, N. A mixed h_2/h_∞ approach to simultaneous fault detection and control. *Automatica*, Elsevier, v. 40, n. 2, p. 261–267, 2004.

109   MANGOUBI, S. R.; EDELMAYER, M. A. Model based fault detection: the optimal past, the robust present and a few thoughts on the future. *IFAC Proceedings Volumes*, Elsevier, v. 33, n. 11, p. 65–76, 2000.

110   YAMAMOTO, K. et al. Driver torque estimation in electric power steering system using an h_∞/h_2 proportional integral observer. In: IEEE. *54th IEEE Conference on Decision and Control*. [S.l.], 2015. p. 843–848.

111   KARIMI, H. R. Observer-based mixed h_2/h_∞ control design for linear systems with time-varying delays: An LMI approach. *International Journal of Control, Automation and Systems*, v. 6, n. 1, p. 1–14, 2008.

112   ZHANG, F. *The Schur complement and its applications*. [S.l.]: Springer Science & Business Media, 2006.

113   SCHERER, C. W. *The Riccati inequality and state-space H_∞-optimal control*. Tese (Doutorado) — Julius Maximilians University Würzburg, Germany, 1990.

114   LOFBERG, J. YALMIP: A toolbox for modeling and optimization in MATLAB. *IEEE International Symposium on Computer Aided Control Systems Design*, p. 284–289, 2004.

115   TOH, K.-C.; TODD, M. J.; TÜTÜNCÜ, R. H. Sdpt3—a matlab software package for semidefinite programming, version 1.3. *Optimization methods and software*, Taylor & Francis, v. 11, n. 1-4, p. 545–581, 1999.

116   POUSSOT-VASSAL, C. *Robust LPV multivariable Automotive Global Chassis Control*. Tese (Doutorado) — Institut National Polytechnique de Grenoble-INPG, 2008.

117   PARDALOS, P. M.; MIGDALAS, A.; PITSOULIS, L. *Pareto optimality, game theory and equilibria*. [S.l.]: Springer Science & Business Media, 2008.

118   MORATO, M. M. et al. Robustness conditions of LPV fault estimation systems for renewable microgrids. *International Journal of Electrical Power & Energy Systems*, Elsevier, v. 111, p. 325–350, 2019.

119   SKOGESTAD, S.; POSTLETHWAITE, I. *Multivariable feedback control: analysis and design*. [S.l.]: Wiley New York, 2007.

120   COSTA, M. V. Americano-da; NORMEY-RICO, J. E. Modeling, simulation and control of a distillation unit in an ethanol-producing plant (Text in Portuguese). In: CBA. *XXI Brazilian Congress of Automatica*. [S.l.], 2012.

121   SULAIMAN, S. A. et al. Effects of dust on the performance of PV panels. *World Academy of Science, Engineering and Technology*, Citeseer, v. 58, n. 2011, p. 588–593, 2011.

122   SPINATO, F. et al. Reliability of wind turbine subassemblies. *IET Renewable Power Generation*, IET, v. 3, n. 4, p. 387–401, 2009.

123   PRONOBIS, M. The influence of biomass co-combustion on boiler fouling and efficiency. *Fuel*, Elsevier, v. 85, n. 4, p. 474–480, 2006.

124   DIAKUNCHAK, I. S. Performance deterioration in industrial gas turbines. *Journal of Engineering for Gas Turbines and Power*, American Society of Mechanical Engineers, v. 114, n. 2, p. 161–168, 1992.

125   ROTONDO, D.; NEJJARI, F.; PUIG, V. Dilated LMI characterization for the robust finite time control of discrete-time uncertain linear systems. *Automatica*, Elsevier, v. 63, p. 16–20, 2016.

126   ROTONDO, D. *Advances in Gain-Scheduling and Fault Tolerant Control Techniques*. [S.l.]: Springer, 2018. ISSN 2190-5053.

127   ROTONDO, D.; NEJJARI, F.; PUIG, V. Robust state-feedback control of uncertain LPV systems: An LMI-based approach. *Journal of the Franklin Institute*, Elsevier, v. 351, n. 5, p. 2781–2803, 2014.

128   MORATO, M. M. et al. LPV-filtered predictive control design for fault-tolerant energy management. In: IFAC. *12th IFAC Symposium on Dynamic and Control of Process Systems, including Biosystems, Florianópolis, Brazil*. [S.l.], 2019.

129   MAHARJAN, L. et al. Fault-tolerant operation of a battery-energy-storage system based on a multilevel cascade pwm converter with star configuration. *IEEE Transactions on Power Electronics*, IEEE, v. 25, n. 9, p. 2386–2396, 2010.

130   SIRI, K. *Fault tolerant maximum power tracking solar power system*. 2002. US Patent 6,433,522.

131   NORMEY-RICO, J. E.; LIMA, D. M.; SANTOS, T. L. Robustness of nonlinear mpc for dead-time processes. *IFAC-PapersOnLine*, Elsevier, v. 48, n. 23, p. 332–341, 2015.

132   ROCA, L. et al. Robust constrained predictive feedback linearization controller in a solar desalination plant collector field. *Control Engineering Practice*, Elsevier, v. 17, n. 9, p. 1076–1088, 2009.

133   NORMEY-RICO, J. E.; CAMACHO, E. F. Unified approach for robust dead-time compensator design. *Journal of Process Control*, Elsevier, v. 19, n. 1, p. 38–47, 2009.

134   SANTOS, T. L. et al. On the explicit dead-time compensation for robust model predictive control. *Journal of Process Control*, Elsevier, v. 22, n. 1, p. 236–246, 2012.

135   SANTOS, T. L.; TORRICO, B. C.; NORMEY-RICO, J. E. Simplified filtered smith predictor for MIMO processes with multiple time delays. *ISA transactions*, Elsevier, v. 65, p. 339–349, 2016.

Part V

Appendixes

UNIVERSIDADE FEDERAL DE SANTA CATARINA
Fault Analysis, Observation and Control of Brazilian Sugarcane Microgrids:
Robust Linear Parameter Varying Methods
Marcelo Menezes Morato

Theoretical Lexicon
03/06/2019

Theoretical Lexicon: This online Chapter of the Master Dissertation provides all mathematical unwindings for the theoretical concepts held as background to this work.

1 On Dynamic Systems

A study of dynamical system is important for this work. Books [1] and [2] should certainly be recalled, for they present the key topics on dynamical (linear and nonlinear) systems, including observability, controllability, linear and nonlinear control, flatness and others. Book [3] is also a good and strong reference.

1.1 *LTI* Systems

Some key concepts on *LTI* systems, as well as for general dynamical systems are now given:

Given the generical *LTI* system put in (1), one can deduce characteristics. Note that, as usual, $x(t)$ represents a vector of system states, $u(t)$ represents a vector of system inputs and $y(t)$ represents a vector of outputs. $\dot{x}(t)$ represents $\frac{dx(t)}{dt}$. The system (1) has n states, m inputs and p outputs.

$$
\begin{aligned}
\dot{x}(t) &= Ax(t) + Bu(t)\,, \\
y(t) &= Cx(t) + Du(t)\,.
\end{aligned}
\tag{1}
$$

From this, one can define:

Definition 1 *A system is said controllable when, given inicial condition $x_0 \in \mathbb{R}^n$ and each final state $x_T \in \mathbb{R}^n$, there exists an input $u : [0,T] \to \mathbb{R}^m$ so that the solution to (1), $x : [0,T] \to \mathbb{R}^n$, for the initial condition $x(0) = x_0$ satisfies $x(T) = x_T$, for a*

generic $T > 0$. This means that that system (1) can be driven from a inicial state to an arbitrary final state in a finite time, given the adequate input. A system is said to be uncontrollable when it is not controllable.

Definition 2 *A system is said to be observable when, for every unknown inicial state $x(0) \in \mathbb{R}^n$, there exists $T > 0$ so that the knowledge of the system input $u(t) \in \mathbb{R}^n$ and the system output $y(t) \in \mathbb{R}^p$ through the time intervale $[0, T]$ is sufficient to determine, by a single way, the inicial state $x(0)$. A system is said to be unobservable when it is not observable.*

Given, now, the following matrices:

- Controllability Matrix, $\mathcal{C} = [B \, AB \, A^2 B \, \ldots \, A^{n-1} B]_{n \times nm}$;

- Observability Matrix, $\mathcal{O} = ([C \, CA \, CA^2 \, \ldots \, CA^{n-1}]_{n \times np})^T$
 .

Theorem 1 *Given the LTI system (1):*

- *The system is controllable **if and only if** $rank(\mathcal{C}) = n$ (complete line rank). In this case, one can say, simply, that the pair (A, B) is controllable, for the controllability matrix $\mathcal{C}$ depends on matrices A and B;*

- *The system is observable **if and only if** $rank(\mathcal{O}) = n$ (complete column rank). In this case, one can say, simply, that the pair (A, C) is observable, for the observability matrix $\mathcal{O}$ depends on matrices A and C;*

- *The pair (A, C) is observable **if and only if** the pair (A^T, C^T) is controllable;*

- *When (1) is SISO ($m = p = 1$), the system is controllable **if and only if** $det(\mathcal{C}) \neq 0$. And, for $p = 1$ (one output), the system is observable **if and only if** $det(\mathcal{O}) \neq 0$.*

1.2 *LTI* Control and Observation

1.3 Closed-Loop Pole Placement

It is important to depict, given the previous theorem and definitions, how to stabilize, in closed-loop (*CL*), an unstable (or stable) open-loop system. For this, consider the system put in (2), without direct transfer between entrance $u(t)$ and $y(t)$.

$$x\dot{(t)} = Ax(t) + Bu(t), \qquad (2)$$
$$y(t) = Cx(t).$$

Consider the following system input: $u(t) = r(t) - Kx(t)$, given $r(t)$ a new auxiliary entrance $(r(t) \in \mathbb{R}^m)$ and $K = (k_{ij})$ a constant gain matrix $(K \in \mathbb{R}^{m \times n})$. K is often described as a feedback matrix. In closed-loop, the system (2) results in the system (3).

$$x\dot{(t)} = (A - BK)x(t) + Br(t), \qquad (3)$$
$$y(t) = Cx(t).$$

So, the closed-loop transfer function of (3) is $G_{CL}(s) = C(sI - (A - BK))^{-1}B$, for $Y(s) = G_{CL}(s)R(s)$. From this, it can be neatly seen that the poles (eigenvalues) of $(A - BK)$ define the CL system's behaviour.

So, the closed-loop transfer function of (3) is $G_{CL}(s) = C(sI - (A - BK))^{-1}B$, for $Y(s) = G_{CL}(s)R(s)$. From this, it can be neatly seen that the poles (eigenvalues) of $(A - BK)$ define the CL system's behaviour.

Definition 3 *The **Stabilization Problem by State Feedback with Pole Placement** is so that a matrix $K \in \mathbb{R}^{m \times n}$ has to be found so that the* CL *poles of the system as arbitrarily placed on the complex plane, when $u(t) = r(t) - K.x(t)$ is said a state feedback. Particularly, if all poles of $(A - BK)$ are placed on the* LHP, *it is assured that $x^e = 0$ is a globally asymptotically stable equilibrium point of the* CL *system and that the transfer matrix $G_{CL}(s)$ is* BIBO *stable.*

Theorem 2 *The pair (A, B) is controllable **if and only if** the pair $(A - BK, B)$ is controllable, where $K \in \mathbb{R}^{m \times n}$ is a constant matrix.*

Theorem 3 *The poles (eigenvalues) of the* CL *matrix $(A - BK)$ can be arbitrarily placed on the complex plane by and adequate choice of $K \in \mathbb{R}^{m \times n}$ **if and only if** the pair (A, B) is controllable.*

1.4 The Linear Quadratic Regulator

Let it be remarked, also, the *Linear Quadratic Regulator* control approach. Let us, then, show the solution to the **Stabilization**

Problem by State Feedback by finding a matrix $K \in \mathbb{R}^{m \times n}$ so that the quadratic cost function $J(x(t), u(t))$ is minimized.

Considering $\phi(x(t_f))$ as a terminal cost for the states $x(t)$ at $t = t_f$, one can write the cost function $J(x(t), u(t))$ as:

$$
\begin{aligned}
J(x(t), u(t)) \;=\;& \phi(x(t_f)) + \int_{t_0}^{t_f} [\frac{1}{2} x^T(t) Q x(t) \\
+\;& \frac{1}{2} u^T(t) R u(t) + x^T(t) N u(t)] dt \,.
\end{aligned} \tag{4}
$$

Considering t_0 the initial time and $\phi(x(t_f)) = 0$ one have a full LQR formulation.

The solution of the minimization problem is given by:

$$
\begin{aligned}
u(t) \;&=\; -Kx(t) \,, \tag{5} \\
K \;&=\; R^{-1} B^T P \,, \tag{6}
\end{aligned}
$$

where P is the solution of the continuous time algebraic Ricatti (see [4]) equation seen below:

$$
A^T P + P A - (PB + N) R^{-1} (B^T P + N^T) + Q = 0 \,. \tag{7}
$$

.

In sum, one can weigh the matrices Q and R depending on the system CL response expected. This is control design is further investigated on [5] and [6].

1.5 Other Methods: R-S-T

It has to be remarked that all linear control methods applied to linear time-invariant systems (PIs, PIDs and all others) are algebraically equivalent to the $R - S - T$ scheme, presented in Figure 1. An application of flatness-based control of a thermal process is seen in [7].
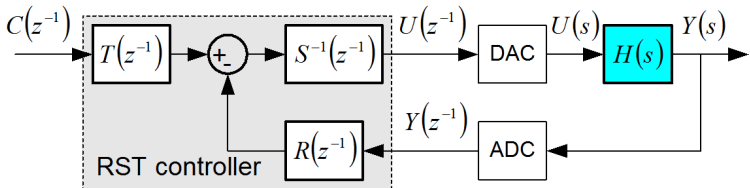
Figure 1: $R - S - T$ Control Scheme

1.6 System Observer

It is also important to put, due to this chapter's study, the concept of system observer. Let it be suposed that the (2) system states $x(t) \in \mathbb{R}^n$ cannot be measured, but are of importance. The only available measurements are those of $y(t) \in \mathbb{R}^p$.

A system observer will be herein defined as:

$$\dot{\hat{x}}(t) = A\hat{x}(t) + Bu(t) + L[y(t) - C\hat{x}(t)], \qquad (8)$$

where $\hat{x}(t)$ represents the estimated system states.

For the sake of the argument, let one consider the dynamics of the error $e(t) = x(t) - \hat{x}(t)$:

$$\dot{e}(t) = \dot{x}(t) - \dot{\hat{x}}(t) = (A - LC)e(t). \qquad (9)$$

For this, given the analysis of (9), it can be easily seen that dynamics of the estimation error $e(t) = x(t) - \hat{x}(t)$, by the proposed system observer (8), depend on the placement of the eigenvalues of the matrix $(A - LC)$. If these poles are placed on the LHP, it is assured by the proposed **asymptotical state observer** that, given any inicial condition $e(0) = x(0) - \hat{x}(0) \in \mathbb{R}^n$, it is true that:

$$\lim_{t \to \infty} e(t) = \lim_{t \to \infty} [x(t) - \hat{x}(t)] = 0. \qquad (10)$$

Theorem 4 *All eigenvalues of the matrix* $(A - LC)$ *can be arbitrarily placed on the complex plane by an adequate choice of* $L \in \mathbb{R}^{p \times n}$ **if and only if** *the pair* (A, C) *is observable.*

Note: a state observer can be used, for example, for a stabilizing state feedback input, on the estimated states, as so: $u(t) = r(t) - K.\hat{x}(t)$. Practically, the poles of $(A - LC)$ are placed on the complex plane to be **faster** than the poles of $(A - BK)$.

1.7 Kalman Filter

One other important topic to be touched, when it comes to linear systems, is the Filtering Problem: given a dynamic system, with its control inputs and disturbances, that is measured with a certain measuring device, with its intrinsic error sources, how can the observed measurements be used to optimally estimate the

system's states? This is, how can one obtain **the best estimate** of the states, considering the measurement errors?

The best estimate corresponds to a minimization problem of the state estimation error to some respect. The Kalman filter takes into account the problem of random variables and probability density distribution of the measurement noise. this is, considers that the measurement error input to the observed system is a sequence of white, zero mean, Gaussian noise with zero mean.

The procedure to design and further information about the Kalman filter is seen in the introductory article [8]. Its applications vary from actual state estimation to paramater identification and many others.

1.8   Other Methods

Many other *LTI* control and observer design methodologies have been seen throughout literature. Anyhow, reader is invited to refer to literature if curious on any other particular topic. This chapter will no longer extend upon this issue.

2   On Singular Values

Let the definition of singular values be recalled:

Definition 4 *Let there be $A \in \mathbb{R}^{m \times n}$ and two unitary matrices $U \in \mathbb{R}^{1 \times m}$ and $V \in \mathbb{R}^{1 \times n}$ such that:*

$$A = U\Sigma V^T , \tag{11}$$

$$\Sigma = \begin{bmatrix} \Sigma_1 & 0 \\ 0 & 0 \end{bmatrix} , \tag{12}$$

$$\Sigma_1 = \begin{bmatrix} \sigma_1 & 0 & \dots & 0 \\ 0 & \sigma_2 & \dots & 0 \\ \vdots & \vdots & \ddots & \vdots \\ 0 & 0 & \dots & \sigma_p \end{bmatrix} , \tag{13}$$

with $\sigma_1 \geq \sigma_2 \geq \dots \sigma_p \geq 0$ and $p = min\{m , n\}$.
A very common notation is to use:

$$\bar{\sigma} = max\{\sigma_1 \dots \sigma_p\} \tag{14}$$
$$= \sigma_{max}(A) = \sigma_1 ,$$
$$\underline{\sigma} = min\{\sigma_1 \dots \sigma_p\} \tag{15}$$
$$= \sigma_{min}(A) = \sigma_p .$$

Remark 1 *Singular values are a good way to measure the size of matrix. Singular vectors are good indicators of the strong and weak input or output directions. This is, as $Av_i = \sigma_i u_i$ and $A^T u_i = \sigma_i v_i$, then:*

$$AA^T u_i = \sigma_i^2 u_i. \tag{16}$$

3 On Vector Spaces

Some definitions have to be recalled, in terms of *Banach, Hilbert Hardy* and $\mathcal{L}_p$ spaces:

Definition 5 *1. A Banach space is a real (or complex) complete normed vector space B, with all Cauchy sequence of points in this space have a limit that is also inside B. A Banach space has norm $|| \cdot ||_p$.*

2. A Hilbert space is a (real or complex) vector space H with an inner product that is complete under the normed defined by itself, being this product $< \cdot, \cdot >$. The norm of $f \in H$ is, then, defined by equation (17). Every Hilbert space is also a Banach space since a Hilbert space is complete with respect to the norm associated with its inner product.

3. A Hardy space, symboled $\mathcal{H}_p$, is a certain space of holomorphic functions on the unit circle or upper half plane. Remark that these holomorphic functions are defined on an open subset of the complex plane $\mathbb{C}$ with values in $\mathbb{C}$ that are complex-differentiable at all and every point.

4. Finally, the $\mathcal{L}_p$ are spaces of p-power integrable functions (that posses existing integrals, generally named Lebesgue integral) and corresponding sequence spaces.

$$||f|| = \sqrt{< f, f >}. \tag{17}$$

Example 1 *Let an illustration be presented for reader, taken from [9]: $\mathbb{R}^n$ and $\mathbb{C}^n$ with the usual spatial p-norm, $|| \cdot ||_p$ for $1 \leq p < \infty$, are Banach spaces. This means that a Banach space is a vector space B over the real or complex number with a norm $|| \cdot ||_p$, such that every Cauchy sequence in B has a limite in B (with respecto to the metric $d(x, y) = ||x - y||$).*

In terms of $\mathcal{L}_2$ e $\mathcal{H}_2$ spaces:

Definition 6

$$||f||_2 \;\; = \;\; \sqrt{\frac{1}{2\pi} \int_{-\infty}^{+\infty} \boldsymbol{Tr}[f^*(jw)f(jw)]dw} < \infty \,. \quad (18)$$

The inner product for this Hilbert space is defined, for f and g $\in \mathcal{L}_2$, as:

$$< f \,, g > \;\; = \;\; \sqrt{\frac{1}{2\pi} \int_{-\infty}^{+\infty} \boldsymbol{Tr}[f^*(jw)g(jw)]dw} \,. \quad (19)$$

Definition 7 $\mathcal{H}_2$ *is a subspace of $\mathcal{L}_2$ (a Hardy space) with complex matrix functions $f(jw)$, $\forall j \in \mathbb{R}$, analytic in $Re(jw) > 0$ (functions that are locally given by a convergent power series and differentiable on each point of its definition set). In particular, the real rational subspace of $\mathcal{H}_2$, that is made of all strictly proper and real rational stable transfer matrices, is denoted by $\mathcal{RH}_2$.*

In terms of $\mathcal{L}_\infty$ and $\mathcal{H}_\infty$ spaces:

Definition 8 $\mathcal{L}_\infty$ *is the space of piece-wise continuous bounded functions. It is a Banach space of matrix-value functions on $\mathbb{C}$ and it consists of all complex of all complex bounded matrix functions $f(jw)$,$\forall w \in \mathbb{R}$, such that:*

$$sup_{w \in \mathbb{R}} \overline{\sigma}[f(jw)] \;\; < \;\; \infty \,. \quad (20)$$

Definition 9 $\mathcal{H}_\infty$ *is a closed subspace in $\mathcal{L}_\infty$ with matrix functions $f(jw)$,$\forall w \in \mathbb{R}$, analytic in $Re(jw) > 0$ (open right-half plane). The real rational subspace of $\mathcal{H}_\infty$ which consists of all proper and real rational stable matrices is denoted by $\mathcal{RH}_\infty$.*

Example 2 *In control theory, these vector spaces stand for:*

$$\frac{(s+1)(s+3)}{(s+5)^4} \;\; \in \;\; \mathcal{RH}_\infty \,, \quad (21)$$

$$\frac{(s+1)}{(s-1)(s+3)} \;\; \notin \;\; \mathcal{RH}_\infty \,, \quad (22)$$

$$\frac{(s+1)}{(s+10)} \;\; \in \;\; \mathcal{RH}_\infty \,. \quad (23)$$

4   On Norms

First of all, two definitions are important:

Definition 10 *The inferior limit of a function can be defined as the inferior bound of a function $f : \mathbb{R} \to \mathbb{R}$. This is:*

$$\inf(f(x)) = \{min(y) \,|\, y = f(x)\}. \tag{24}$$

Definition 11 *The superior limit of a function can be defined as upper bound of a function $f : \mathbb{R} \to \mathbb{R}$. This is:*

$$\sup(f(x)) = \{max(y) \,|\, y = f(x)\}. \tag{25}$$

The book [10] is essential to this study, where all the following definitions are given.

Definition 12 *Let V be a finite dimension space, then $\forall \rho \geq 1$, the application $|| \cdot ||_\rho$ is a norm, defined formally as $||v||_\rho = \left(\sum_i |v_i|^\rho \right)^{\frac{1}{\rho}}$. Let V be a vector space over $\mathbb{C}$ and let $|| \cdot ||$ be a norm define on V: then V is a normed space.*

4.1 Signal Norms

The 1-Norm of a function is defined as:

$$||x(t)||_1 = \int_0^{+\infty} |x(t)| dt. \tag{26}$$

The 2-Norm of a function is defined as:

$$||x(t)||_2 = \sqrt{\int_0^{+\infty} x^*(t)x(t) dt} \tag{27}$$

$$= \sqrt{\frac{1}{2\pi} \int_{-\infty}^{+\infty} X^*(jw)X(jw) dw}.$$

The ∞-Norm of a function is defined as:

$$||x(t)||_\infty = \sup_t |x(t)|. \tag{28}$$

4.2 System Norms

Definition 13 *The $\mathcal{H}_2$ norm of a strictly proper LTI system, from input $u(t)$ to output $y(t)$ and which belongs to $\mathcal{RH}_2$, stands for the energy ($\mathcal{L}_2$ norm) of the impulse response $g(t)$, defined*

as:

$$\|G(jw)\|_2 = \sqrt{\int_{-\infty}^{+\infty} g^*(t)g(t)dt} \tag{29}$$

$$= \sqrt{\frac{1}{2\pi}\int_{-\infty}^{+\infty} \boldsymbol{Tr}[G^*(jw)G(jw)]dw}$$

$$= sup_{u(s)\in\mathcal{H}_2}\frac{\|y(s)\|_\infty}{\|u(s)\|_2}\,. \tag{30}$$

The $\mathcal{H}_2$ norm of a system is finite if and only if the LTI transfer function $G(s)$ is strictly proper (this is if $G(s) \in \mathcal{RH}_2$.

Let one consider SISO *systems. Let $g(t)$ be the impulse response of this system. Then, the $\mathcal{H}_2$ norm of $G(s)$ is defined as:*

$$\|G\|_2 = \|g(t)\|_2\,. \tag{31}$$

Remark 2 *In terms of the physical interpretation of this $\mathcal{H}_2$ norm:*

- *For* SISO *systems, it stands for the area located under the Bode diagram;*

- *For* MIMO, *this norm is the impulso-to-energy gain of the output $y(t)$ to a white-noise (uniform spectral density) input $u(t)$;*

- *This norm can be computed either analytically or numerically.*

Definition 14 *The $\mathcal{H}_\infty$ norm of a strictly proper LTI system, from input $u(t)$ to output $y(t)$ and which belongs to $\mathcal{RH}_\infty$, stands for the induced energy-to-energy gain (induced $\mathcal{L}_2$ norm), being defined as:*

$$\|G(jw)\|_\infty = sup_{u\in\mathbb{R}}\overline{\sigma}(G(jw)) \tag{32}$$

$$= sup_{u(s)\in\mathcal{H}_2}\frac{\|y(s)\|_2}{\|u(s)\|_2}$$

$$= sup_{u(s)\in\mathcal{L}_2}\frac{\|y\|_2}{\|u\|_2}\,.$$

Let one consider MIMO *systems with n_u inputs and n_y outputs. The $\mathcal{H}_\infty$-norm of this system $G(s)$ is defined as:*

$$\|G\|_\infty = sup_{u(t)s.t.\|u(t)\|_2\neq 0}\frac{\|G(s)u(s)\|_2}{\|u(t)\|_2}\,. \tag{33}$$

This quantity represents the largest possible 2-norm gain provided by the system.

Remark 3 *In terms of the physical interpretation of this $\mathcal{H}_\infty$ norm:*

- *This norm representes the maximal gain of the system's frequency response. It is also called the worst case attenuation level, as it measures the maximal amplification that a given system can deliver over the whole frequency spectrum;*

- *For* SISO *systems, it stands for the maximal peak of the Bode diagram, that is, the largest gain if the system is fed by a harmonic input signal;*

- *For* MIMO *systems, it stands for the maximal peak of the singular-values over frequency diagram, that is, the largest gain if the system is fed by a harmonic input signal;*

- *Unlike the previous norm defined, this $\mathcal{H}_\infty$ norm cannot be computed analytically. Numerical solutions have to be used in order for the $\mathcal{H}_\infty$ norm of a given system to be obtained.*

5 On Linear Matrix Inequalities

Let a brief recall on Linear Matrix Inequalities (*LMI*s) be presented. What is presented next stands for some of the important topics on linear matrix inequalities, crucial for many of the solutions presented throughout this work. A thorough review of the application of *LMI*s in control theory can be found on [11] and [12].

5.1 Strict *LMI* Constraint

Let one define:

Definition 15 *A function $f : \mathbb{R}^m \to \mathbb{R}$ is said to be convex if and only if for all $x, y \in \mathbb{R}^m$ and $\lambda \in [0, 1]$, it is true that $f(\lambda x + (1-\lambda)y) \leq \lambda f(x) + (1-\lambda)f(y)$. Equivalently, f is convex if and only if its epigraph is convex.*

Remark 4 *The epigraph (or supergraph) of a function $f : \mathbb{R}^n \to \mathbb{R}$ is defined as the set of points lying on or above its graph. This is:*

$$epi(f) \quad = \quad \{(x,y) : x \in \mathbb{R}^n, \, y \in \mathbb{R} \,|\, f(x) \leq y\}. \quad (34)$$

From this, one can define the concept of a Linear Matrix Inequality.

Definition 16 *An* LMI *constraint on a vector* $x \in \mathbb{R}^m$ *is defined as* $F(x)$, *for* $F(x) = F_0 + \sum_{i=1}^{m} F_i x_i \succeq 0 \, (\succ 0)$, *where* $F_0 = F_0^T$ *and* $F_i = F_i^T \in \mathbb{R}^{n \times m}$.

There are two kinds of problems to be handled by the use of *LMI*s:

- The **feasibility** problem: the answer (feasible or not) to the question whether or not there exists elements $x \in X$ so that $F(x) < 0$.

- The **optimization** problem: given an objective function $J : S \to R$ where $S = \{x \mid F(x) < 0\}$, this problem is to determine $V_{opt} = inf_{x \in S} J(x)$.

Example 3 *Now, a simple illustration is presented in order to bring convex problems in terms of* LMIs. *A very well-known* LMI *constraint is the classical Lyapunov inequality of an autonomous system* $\dot{x}(t) = Ax(t)$. *The stability of this system is given by:*

$$
\begin{aligned}
x^T(t)Px(t) &> 0 \\
x^T(t)(A^T P + PA)x(t) &< 0 \, ,
\end{aligned}
\tag{35}
$$

which is equivalently translated to the following LMI*:*

$$
F(P) = \begin{bmatrix} -P & 0 \\ 0 & A^T P + PA \end{bmatrix} \prec 0 \, ,
\tag{36}
$$

where $P = P^T$ *is the decision variable. Notice how the inequality* $F(P) \prec 0$ *is linear in* P.

Remark 5 *Reader must bear in mind how* LMI*-based optimization falls in the context of convex optimization. This property is fundamental as it guarantees the global (or optimal) solution* x^* *of a given minimization problem under* LMI *constraints on* x *can be found efficiently, in polynomial time.*

Example 4 *A simple example of an* LMI *feasibility problem is the stability analysis of a system. The Linear-Quadratic control problem, on the other hand, stands for an optimization problem, whose solution is obtained by solving the following Ricatti equation (37), that can be directly equivalent to finding* $P > 0$ *so that the* LMI *(38) is true.*

$$A^T P + PA - PBR^{-1}B^T P + Q = 0 \qquad (37)$$

$$\begin{bmatrix} A^T P + PA + Q & PB \\ B^T P & R \end{bmatrix} > 0 \qquad (38)$$

5.2 Semi-Definite Programming Problem

LMI programming is a generalization of Linear Programming to cope with positive semi-definite matrices.

Remark 6 *Reader must bear in mind that semi-definite matrices stand for the set of all symmetric matrices of particular dimensions.*

Definition 17 *A Semi-Definite Programming (*SDP*) problem is define as:*

$$min \qquad c^T x \,, \qquad (39)$$
$$under \ constraint \ F(x) \ \succeq \ 0 \,,$$

being $F(x)$ an affine symmetric matrix function of $x \in \mathbb{R}^m$ and $c \in \mathbb{R}^m$ is a given real vector that defines the problem's objective.

SDP *problems are theoretically tractable and, also, they present (almost) polynomial complexity.* SDP *can be practically and efficiently solved for* LMI*s of size up to 100×100 and $m \leq 1000$, as states [13]. Reader must bear in mind that nowadays (2018), due to extensive developments in this area, this number might be even bigger.*

5.3 *LMI* in Control

Example 5 *To illustrate the use of Linear Matrix Inequalities in Control Theory, the problem of stabilizing a controllable system $\dot{x}(t) = Ax(t) + Bu(t)$, is related to the use of input $u(t) = -Kx(t)$ so that the closed-loop is stable.*

With the aid of the Lyapunov Theorem, one aims to find $P = P^T > 0$ so that:

$$A^T P + PA - KTB^T P - PBK \ < \ 0 \,, \qquad (40)$$

which translates, with the change of variables $Q = P^{-1}$ and $Y = -KP^{-1}$, to:

$$QA^T + AQ + Y^T B^T + BY \ < \ 0 \,, \qquad (41)$$

which is formulated as an LMI *without any additional conservatism.*

5.4 Quadratic Stability

A very useful concept for the stability analysis of uncertain systems can also be formulated with the use of *LMI*s. This is detailed:

Definition 18 *Let the following uncertain system be considered* $\dot{x}(t) = A(\delta)x(t)$, *with* $\delta \in \Delta$, *the set of uncertainties.*

This considered system is siad to be quadratically stable for all uncertainties δ *if there exists a single Lyapunov function* $P = P^T > 0$ *so that:*

$$A^T(\delta)P + PA(\delta) \quad < \quad 0\,, \tag{42}$$

for all $\delta \in \Delta$. *This is a sufficient condition for Robust Stability, which is obtained whenever* $A(\delta)$ *is stable for all* $\delta \in \Delta$.

5.5 Interest of *LMI*s

The use of *LMI*s allows to formulate complex optimization problems into linear structures, allowing the use of convex optimization frameworks. It usually requires the use of differente transformations, changes of variables and others in order to achieve a final linearizable problem.

Listed next are some examples of criteria that can be handled with the use of *LMI*s: $\mathcal{H}_2$ Performance; $\mathcal{H}_\infty$ Performance; Robustness Analysis; Small Gain Theorem; *LFT* representations; Robust Control Design; Robust Observer Design; Pole Placement; Stability analysis; Stabilization with input constraints; Passivity constraints; Control of Time-delay systems.

6 Useful *LMI* Lemmas

6.1 Bounded Real Lemma

Lemma 1 *The* $\mathcal{L}_2$-*norm of the output* z *of a given* LTI *system is uniformly bounded by* γ_{BRL} *times the* $\mathcal{L}_2$-*norm of the input* w, *with null initial conditions.*

As of this, a given dynamical system $G = (A, B, C, D)$ *is internally stable with a bounded* $\mathcal{H}_\infty$ *norm* $||G||_\infty < \gamma_{BRL}$ *if and only if there exists a positive definite symmetric matrix* P *such that:*

$$P > 0, \qquad (43)$$

$$\begin{bmatrix} A^T P + PA & PB & C^T \\ B^T P & -\gamma_{BRL}\mathbb{I} & D^T \\ C & D & -\gamma_{BRL}\mathbb{I} \end{bmatrix} < 0.$$

This Lemma is an LMI *if the only decision variables are* P and γ_{BRL}.

This Lemma has an alternative presentation, as states [14]:

$$\begin{bmatrix} \mathbb{I} & 0 \\ A & B \\ 0 & \mathbb{I} \\ C & D \end{bmatrix}^T \begin{bmatrix} 0 & P & 0 & 0 \\ P & 0 & 0 & 0 \\ 0 & 0 & -\gamma_{BRL}^2\mathbb{I} & 0 \\ 0 & 0 & 0 & \mathbb{I} \end{bmatrix} \begin{bmatrix} \mathbb{I} & 0 \\ A & B \\ 0 & \mathbb{I} \\ C & D \end{bmatrix} \prec 0. \quad (44)$$

6.2 Schur Lemma

Lemma 2 *Let* $Q = Q^T$ *and* $R = R^T$ *be affine matrices of compatible size. Then, the condition:*

$$\begin{bmatrix} Q & S \\ S^T & R \end{bmatrix} \succeq 0, \qquad (45)$$

is equivalent to:

$$R \succeq 0, \qquad (46)$$
$$Q - SR^{-1}S^T \succeq 0.$$

This Lemma allows to a convert a quadratic (ellipsoidal) constraints into LMI formulations.

6.3 Kalman-Yakubovich-Popov Lemma

Lemma 3 *For any triplet of matrices* $(A \in \mathbb{R}^{n \times n}, B \in \mathbb{R}^{n \times m}, M \in \mathbb{R}^{(n+m) \times (n+m)})$ *with*

$$M = \begin{bmatrix} M_{11} & M_{12} \\ M_{21} & M_{22} \end{bmatrix}, \qquad (47)$$

the following conditions are equivalent:

1. *There exists a symmetric matrix* $K = K^T \succ 0$ *such that statement (48) is true;*

2. $M_{22} < 0$ *and for all* $w \in \mathbb{R}$ *and complex vectors* $col(x, w) \neq 0$, *statement (49) is true;*

3. If equation (50) is true, then the second statement is equivalent to the condition (51), for all $w \in \mathbb{R}$ with $det(jw\mathbb{I} - A) \neq 0$.

$$\begin{bmatrix} \mathbb{I} & 0 \\ A & B \end{bmatrix}^T \begin{bmatrix} 0 & K \\ K & 0 \end{bmatrix} \begin{bmatrix} \mathbb{I} & 0 \\ A & B \end{bmatrix} + M < 0 \,, \tag{48}$$

$$\begin{bmatrix} A - jw\mathbb{I} & B \end{bmatrix} \begin{bmatrix} x \\ w \end{bmatrix} = 0 \tag{49}$$

$$\Rightarrow \begin{bmatrix} x \\ w \end{bmatrix}^T M \begin{bmatrix} x \\ w \end{bmatrix} < 0 \,,$$

$$M = -\begin{bmatrix} \mathbb{I} & 0 \\ A & B \end{bmatrix}^T \begin{bmatrix} 0 & K \\ K & 0 \end{bmatrix} \begin{bmatrix} \mathbb{I} & 0 \\ A & B \end{bmatrix} \,, \tag{50}$$

$$\begin{bmatrix} \mathbb{I} \\ C(jw\mathbb{I} - A)^{-1}B + D \end{bmatrix}^\star \times \tag{51}$$

$$\begin{bmatrix} Q & S \\ S^T & R \end{bmatrix} \begin{bmatrix} \mathbb{I} \\ C(jw\mathbb{I} - A)^{-1}B + D \end{bmatrix} > 0 \,.$$

This Lemma is used to cope with frequencial in terms of LMIs.

6.4 The Projection Lemma

Lemma 4 For given matrices $W = W^T$, M and N of appropriate size, there existes a real matrix $K = K^T$ so that:

$$W + MKNP^T + NK^TM^T \prec 0 \,, \tag{52}$$

if and only if there existes matrices U and V so that:

$$W + MU + U^TM^T \prec 0 \,, \tag{53}$$
$$W + NV + V^TN^T \prec 0 \,, \tag{54}$$

or, equivalently, if and only if:

$$M_\perp^T W M_\perp \prec 0 \,, \tag{55}$$
$$N_\perp^T W N_\perp \prec 0 \,, \tag{56}$$
$$\tag{57}$$

where $M_\perp$ and $N_\perp$ are the orthogonal complements of M and N, respectively.

This Lemma is also widely used in control theory, for it allows to eliminate variables by a change of basis, a projection in the kernel basis.

6.5 The Completion Lemma

Lemma 5 *Let there be two matrices $X = X^T$ and $Y = Y^T \in \mathbb{R}^{n \times n}$ such that $X > 0$ and $Y > 0$. Then, the following statements are equivalent:*

1. *There always exists matrices X_a and $Y_a \in \mathbb{R}^{n \times r}$ and X_b and $Y_b \in \mathbb{R}^{r \times r}$ so that the LMIs (58) and (59) are true;*

2. *The LMI (60) is true and $\operatorname{rank}\left(\begin{bmatrix} X & \mathbb{I} \\ \mathbb{I} & Y \end{bmatrix} \right) \leq n + r$;*

3. *The LMI (60) is true and $\operatorname{rank}\left(\begin{bmatrix} XY - \mathbb{I} \end{bmatrix} \right) \leq r$.*

$$\begin{bmatrix} X & X_a \\ X_a^T & X_b \end{bmatrix} \succ 0 , \tag{58}$$

$$\begin{bmatrix} X & X_a \\ X_a^T & X_b \end{bmatrix}^{-1} - \begin{bmatrix} Y & Y_a \\ Y_a^T & Y_b \end{bmatrix} = 0 , \tag{59}$$

$$\begin{bmatrix} X & \mathbb{I} \\ \mathbb{I} & Y \end{bmatrix} \succeq 0 . \tag{60}$$

This Lemma is quite useful when dealing with a matrix and its inverse entering a given LMI.

6.6 Finsler's Lemma

Lemma 6 *The following statements are equivalent:*

- $x^T A z < 0$ *for all $x \neq 0$ such that $Bx = 0$;*

- $\breve{B}^T A \breve{B} < 0$ *where $B \breve{B} = 0$;*

- $A + \gamma B^T B < 0$ *for some scalar γ;*

- $A + X B + B^T X^T < 0$ *for some matrix X;*

- $(B^{\perp})^T A B^{\perp} < 0$.

This Lemma allows one to ger rid of useless matrix variables.

7 On H_∞ Performance

H_∞ Control has been firstly introduced by [15]. The idea behind H_∞ Performance is to minimize the H_∞ norm CL transfer matrix from the external inputs w to the controlled outputs z. This is:
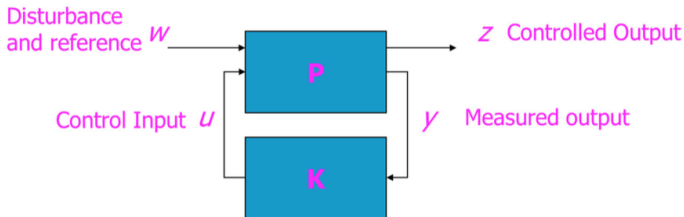
Figure 2: General H_∞ Control Configuration

minimize the energy-to-energy gain from w to z. Th general H_∞ Control configuration is presented in Figure 2.

Considering that P is the generalized plant, that contains the open-loop system G, weights and uncertainties (if any), K is the controller. The CL transfer matrix from w to z is given by the lower Linear Fractional Transformation (LFT):

$$T_{zw}(s) = F_l(P, K) \quad = \quad P_{11} + P_{12}K(I - P_{22}K)^{-1}P_{21} \, . \, (61)$$

The H_∞ control problem: Find a controller $K(s)$ which, based upon the information in y, generates a control signal u which counteracts the influence of w on z, thereby minimizing the closed-loop H_∞ norm from w to z.

The H_∞ suboptimal control problem: Given γ a pre-specified attenuation level, a H_∞ sub-optimal control design is to find a stabilizing controller that ensures:

$$||T_{zw}(s)||_\infty \quad = \quad max_w \overline{\sigma}(T_{zw}(jw)) \leq \gamma \, . \qquad (62)$$

The optimal problem aims at finding the minimal possible γ.

Remark 7 *The H_∞ control problem is a disturbance attenuation problem, formulated within the worst-case performance analysis framework. z is often defined as the tracking error signal.*

7.1 H_∞ Control: Static State-Feedback

Considering the system:

$$
\begin{aligned}
\dot{x}(t) &= Ax(t) + B_1 w(t) + B_2 u(t) \, , & (63) \\
y(t) &= Cx(t) + D_{11}(t) + D_{12}u(t) \, ,
\end{aligned}
$$

The objective is to find the state-feedback law $u(t) = -Kx(t)$ such that $||T_{zw}(s)||_\infty \leq \gamma$. The method consists in applying the

Bounded Real Lemma (Lemma 1) to the closed-loop system. This is achieved if and only if there exists a positive definite symmetric matrix P such that the Lemma is solvable.

7.2 H_∞ Control: Dynamical Output Feedback

The dynamic output feedback case consists in finding a controller $K(s)$ in the *LTI* form:

$$
\begin{aligned}
\dot{x}_K(t) &= A_K x_K(t) + B_K y(t), \\
u(t) &= C_K x_K(t) + D_K y(t),
\end{aligned}
\tag{64}
$$

such that the closed-loop system $N(s) = F_l(P,K)$ has its H_∞ norm minimized. Considering $x_{CL}(t) = [x^t(t)\ \ x_K^T(t)]^T$, one has:

$$
\begin{aligned}
\dot{x}(t) &= A_{CL} x_{CL}(t) + B_{CL} w(t), \\
u(t) &= C_{CL} x_{CL}(t) + D_{CL} w(t),
\end{aligned}
\tag{65}
$$

with

$$
A_{CL} = \begin{bmatrix} (A + B_2 D_K C_2) & (B_2 C_K), \\ (B_K C_2) & A_K \end{bmatrix},
\tag{66}
$$

$$
B_{CL} = \begin{bmatrix} (B_1 + B_2 D_K D_{21}) \\ (B_K D_{21}) \end{bmatrix},
\tag{67}
$$

$$
C_{CL} = \begin{bmatrix} (C_1 + D_{12} D_K C_2) & (D_{12} C_K) \end{bmatrix},
\tag{68}
$$

$$
D_{CL} = \begin{bmatrix} B_1 + B_2 D_K D_{21} \end{bmatrix}.
\tag{69}
$$

The aim of this case, to find matrices A_K, B_K, C_K and D_K so that $\|N(s)\|_\infty \leq \gamma$, can be found using two distinct methods: a Ricatti-based approach and a *LMI*-based solution.

8 On H_2 Performance

Similar to the H_∞ control problem, the H_2 Performance has to be described. The H_∞ norm gives the system gain when input and output are measured using the $\mathcal{L}_2$ norm. Rather than bounding the output energy, it may be desirable to keep the peak amplitude of the controlled output below a certain level. This is, for exemple, to avoid actuator saturations. Now, when one refers to the H_2 control problem, it means to find a controller K for system M such that, given γ,

$$||F_l(M, K)||_2 \leq \gamma \,. \qquad (70)$$

This H_2 problem can be expressed as:

$$\text{Trace}(Z) \quad < \quad \gamma \,, \qquad (71)$$

$$\begin{bmatrix} A_{CL}^T P + P A_{CL} & P B_{CL} \\ B_{CL}^T P & -\mathbb{I} \end{bmatrix} \quad < \quad 0 \,, \qquad (72)$$

$$\begin{bmatrix} P & C_{CL}^T \\ C_{CL} & Z \end{bmatrix} \quad > \quad 0 \,. \qquad (73)$$

9   On Robustness

First of all, two key points should be enlightened in terms of Robustness:

1. A given control system of controller K is said Robust if it is insensitive to differences between the actual system G_n and the model of the system G which was used to synthesize its controller;

2. How can one, then, take into account these differences between the system and its model? A solution is to use a set of system models. But, unfortunately, this can be a very large problem and its solution might not be exact.

Considering that these differences between the real system and its model are referred to as model uncertainties, the study of robustness can be done in three steps:

1. Determining the uncertainty set with an accurate mathematical representation;

2. Determining whether the closed-loop has Robust Stability;

3. Determining whether the closed-loop has Robust Performance.

Different forms of uncertainties can be derived according to the knowledge of the physics of the controlled systems and the ability to represent the system's physics in a convenient way. There are several origins of uncertainty to a controlled system: approximate knowledge and parametrical variations; measurement imperfections; undefined model order at higher frequencies;

the choice of reduced-order models to enable simpler control synthesis; type of controller implementation (continuous to discrete discrepancies, *etc*). Synthetically, two types of uncertainties can appear: parametric uncertainties or unmodeled dynamics.

9.1 Uncertainty Modelling

Considering an uncertain system P with controller C, their analysis of robustness can be coupled into a single feature. Towards an upper Linear Fractional Transformation (LFT), see [10], this system can be modelled with the use of a $P - K - \Delta$ structure, where the closed-loop LPV system, with scheduling parameter fixed at $\alpha = \alpha^i$ is given by:

$$N(\alpha^i) \quad = \quad \mathcal{F}_l(P(\alpha^i), C(\alpha^i)). \tag{74}$$
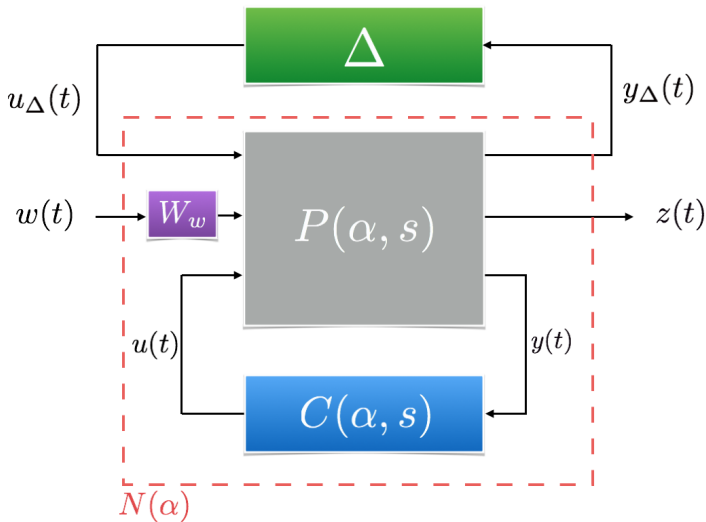
Figure 3: $P - K - \Delta$ Representation

In this global $P - K - \Delta$ General Control Configuration, seen in Figure 3, wherein W_w stands for some weighting function upon the disturbances $w(t)$, the transfer matrix is given by:

$$T_{zw} \quad = \quad F_u(N, \Delta) = N_{22} + N_{21}\Delta.(I - N_{11}\Delta)^{-1}N_{12}. \tag{75}$$

Remark 8 *In this representation, N is known and $\Delta(s)$ collects all the uncertainties, taking them into account for the stability*

analysis of the uncertain closed-loop system. As of this, $\Delta(s)$ has the following structure:

$$\Delta(s) \quad = \quad col\{ \ \delta_j \ \}. \tag{76}$$

Then, the following assumptions is made: the uncertainties are normalized, such that:

- $||\Delta(s)||_\infty \leq 1$;

- $|\delta_j| < 1$.

Notice that, from this point, the robustness criteria are:

- Robust Stability (RS): If $F_u(N, \Delta)$ is stable for all Δ, $||\Delta||_\infty < 1$ and N is internally stable;

- Robust Performance (RP) : If $||F_u(N, \Delta)||_\infty < 1$ for all Δ, $||\Delta||_\infty < 1$ and N is internally stable.

Remark 9 *To relax the analysis conditions for* RS *and* RP *of* LPV *systems, one can analyse the scheduling parameter at different vertices of its domain polytope. This is adequate, for if there is guarantees of nominal stability and performance for all possible values of α, due to the H_∞ problem solution, it is also true for the complete domain. For other tools and a complete scrutinization of Robustness Analysis for* LPV *Systems, see [16].*

Then, for RS, the analysis resides on determining wether the system remains stable for all plants inside uncertainty set. According to the definition of the upper LFT, instability may only come from the term $(I - N_{11}\Delta)$. This is equivalent to the study of the Small Gain Theorem, [17], applied to N_{11}.

Lemma 7 *Suppose $N_{11} \in RH_\infty$. Then the closed-loop system, as presented in Figure 3, for $\alpha = \alpha^i$, is well-posed and internally stable for all $\Delta \in RH_\infty$ so that:*

$$||\Delta(s)||_\infty \quad \leq \quad \delta_{RS} \tag{77}$$

if and only if

$$||N_{11}(s)||_\infty \quad < \quad \frac{1}{\delta_{RS}}. \tag{78}$$

Proof 1 *Refer to [10].*

Towards RP, the analysis becomes more complex: it is necessary to apply the Small Gain Theorem to the H_∞ norm of the full upper LFT. Let consider, then, a structured representation of $\Delta(s)$, as seen in the following equation:

$$\Delta = \begin{bmatrix} \Delta_f & 0 \\ 0 & \Delta_r \end{bmatrix}, \tag{79}$$

where Δ_f represent fictive full block complex uncertainty and Δ_r represents the real block diagonal matrix uncertainties.

Lemma 8 *Suppose $N = \mathcal{F}_l(P, K) \in RH_\infty$. Then the closed-loop system, as presented in Figure 3, for $\alpha = \alpha^i$, is well-posed and internally stable for all $\Delta \in RH_\infty$ if and only if:*

$$\mu_\Delta(N) < 1 \forall w, \tag{80}$$

where the operator $\mu_\Delta(\cdot)$ stand for the structured singular value. Remark that the structured singular value cannot be determined explicitly. For this, numerical methods exist in order to compute upper and lower bounds of $\mu_\Delta(\cdot)$, as close as possible to μ_Δ.

Proof 2 *Refer to [18].*

9.2 Robustness Analysis

Robust Stability analysis refers, then, with a given controller K, to determine wether the system remains stable for all plants inside the uncertainty set. This resides, thus, on the use of the Small Gain Theorem (Theorem 7) to determine stability towards a given uncertainty set.

9.3 Robust Control Design

In order to design a Robust Controller - this means, a controller for which its e synthesis actually takes the uncertainties into account - some of the most used methods are:

1. For **unstructured** uncertainties: To consider an uncertainty weight (unstructured form), and include the Small Gain Condition through a new controlled output of a H_∞ controller. In terms of other approaches, one can use a robustness *feedback* filter to overlap the uncertainties, as it is discussed in [19] and [20];

2. For **structured** uncertainties: To design of robust controllers in the presence of such uncertainties, methods reside in the μ-synthesis. It is handled through an interactive procedure, referred to as the DK iteration. This procedure is much more complex than a simple H_∞ control design and frequently leads to a final controller of much increased order.

3. For the use of other mathematical representations of parametric uncertainties as, for example, a polytopic model. In this situation, the set of uncertain parameters is assumed to be a polytope and, thus, the stability issue is solved by finding a single Lyapunov function for the whole uncertainty set. In the affine case, the stability can be analyzed only at the vertices of the polytope, which is a finite dimensional problem that can be treated with a Linear Parameter Varying approach.

10 On Linear Parameter Varying Systems

Some basic concepts of Linear Parameter Varying (LPV) Systems have to be presented to reader, for this kind of systems are used frequently in this work.

These concepts can be revisited in the following references [21], [22] and [9].

Definition 19 *A LPV system can be defined as in Equation (81), where, as usual, $x(t)$ represents a vector of system states, $u(t)$ represents a vector of system inputs, $w(t)$ represents a vector of disturbances, $y(t)$ represents a vector of measured outputs and $z(t)$ represents a vector of controlled outputs. $\dot{x}(t)$ represents $\frac{dx(t)}{dt}$.*
*System (81) has n states, m inputs, d disturbances, p measured outputs and p_z controlled outputs. $\rho = (\rho_1(t)$,, ... , $\rho_N(t)) \in \Omega$ is a vector of time-varying parameters, assumed to be **known** for all t, where Ω is a convex set. $\rho(\cdot)$ varies in the set of continuously differentiable parameter curves $\rho : [0, +\infty) \to \mathbb{R}^N$. The **scheduling** parameters ρ are assumed to be **bounded**: $\rho \in \mathcal{U}_\rho \subset \mathbb{R}^N$ and $\mathcal{U}_\rho$ is compact, defined by the minimal $\underline{\rho_i}$ and maximal $\overline{\rho_i}$ values of $\rho_i(t)$: $\rho_i(t) \in [\underline{\rho_i}, \overline{\rho_i}], \forall i$. The matrices $A(\cdot)$ to $D_{22}(\cdot)$ are continuous on $\mathcal{U}_\rho$.*

$$\begin{cases} \begin{bmatrix} \dot{x}(t) \\ \hline z(t) \\ y(t) \end{bmatrix} = \begin{bmatrix} A(\rho) & B_1(\rho) & B_2(\rho) \\ \hline C_1(\rho) & D_{11}(\rho) & D_{12}(\rho) \\ C_2(\rho) & D_{21}(\rho) & D_{22}(\rho) \end{bmatrix} \begin{bmatrix} x(t) \\ \hline w(t) \\ u(t) \end{bmatrix} \end{cases} (81)$$

The *LPV* system representation can be understood as something in between the classical duo of nonlinear and *LTI* systems. Theoretical analysis of the *LPV* system properties (stability, observability, controllability) often falls into the framework of linear time-varying systems or of nonlinear systems, which usually presents more difficulty compared to the classical *LTI* framework.

The scheduling parameters can be exogenous if they are external variables (non stationary systems), or endogenous if they are a function of the state variables (quasi-*LPV* system).

Sometimes, it is needed that the derivative of the scheduling parameter to be bounded, this is:

$$\dot{\rho} \in \mathcal{V}_\rho \subset \mathbb{R}^N, \qquad (82)$$

and $\mathcal{V}_\rho$ compact. This corresponds to the case of slowly-varying parameters.

Other representation should be considered if ρ is piece-wise constant or varies in a finite set of elements, as in switched systems.

Remark 10 *The theoretical analysis of* LPV *system properties, such as stability, controllability, observability and others, often falls into the framework of linear time-varying systems or even of nonlinear systems.*

Some key references are listed below, that should not be ignored by reader if interested in *LPV* systems:

- In terms of modelling and identification: [23], [24], [25] and [26];

- In terms of Control: [27], [28] and others;

- In terms of Stability and stabilization: [21] and [29];

- In terms of Geometric Analysis: [30].

11 *LPV* Classes and Models

LPV Systems can be categorized into differente classes and models. The most important classes are described below:

Class 1: *LPV* Systems with affine parameter dependence. For these systems, the system matrices are such as:

$$A(\rho) \quad = \quad A_0 + A_1\rho_1 + A_2\rho_2 + \cdots + A_n\rho_n \,. \qquad (83)$$

Class 2: *LPV* Systems with polynomial parameter dependence. For these systems, the system matrices are such as:

$$A(\rho) \quad = \quad A_0 + A_1\rho + A_2\rho^2 + \cdots + A_n\rho^n \,. \qquad (84)$$

Class 3: *LPV* Systems with rational parameter dependence. For these systems, the system matrices are such as:

$$A(\rho) \quad = \quad [A_0 + A_{n1}\rho_{n1} + \cdots + A_{nn}\rho_{nn}] \times \qquad (85)$$
$$[\mathbb{I} + A_{d1}\rho_{d1} + \cdots + A_{dn}\rho_{dn}]^{-1} \,.$$

Class 4: *Polytopic LPV* Systems. For these systems, their representation is given inside a polytope of $\mathcal{S} = 2^N$ vertices. This is:

$$\sum(\rho) = \sum_{k=1}^{\mathcal{S}} \beta_k(\rho) \left[\begin{array}{c|c} A_k & B_k \\ \hline C_k & D_k \end{array} \right] , \qquad (86)$$

$$\text{with} \sum_{k=1}^{\mathcal{S}} \beta_k(\rho) = 1 \,,$$

$$\beta_k(\rho) > 0 \,,$$

where each $\left[\begin{array}{c|c} A_k & B_k \\ \hline C_k & D_k \end{array} \right]$ is an individual *LTI* system *frozen* at the vertex k of the given polytope. This can be done once the scheduling parameter is a linear convex combination of the polytope's vertices w_k, this is:

$$\rho \quad = \quad \sum_{k=1}^{\mathcal{S}} \beta_k w_k \,, \qquad (87)$$

$$\beta_k \geq 0 \,,$$

$$\sum_{k=1}^{\mathcal{S}} \beta_k = 1 \,.$$

Class 5: *LPV* Systems that can be represented with the use of the Linear Fractional Representation (*LFR*), also referred to as the upper Linear Fractional Transformation (*LFT*). *LFR* modelling is a direct extension of *LFT* forms (originally used for uncertainty modelling in the context of μ-analysis) to descrive system that posses time-varying parameters. This class can be used to model nonlinear system and, also, linear systems scheduled by their operating conditions.

11.1 Nonlinear and Linear Differential Inclusion

The property that allows a system to be described by a Linear Parameter Varying Model is the **Linear Differential Inclusion** (*LDI*), as details [11]. As said in this reference: "*Then, of course, every trajectory of the nonlinear system (88) is also a trajectory of the* LDI *defined by (89). If we can prove that every trajectory of the LDI defined by (88) has some property (e.g., converges to zero), then a fortiori we have proved that every trajectory of the nonlinear system (89) has this property*". Considering the systems described next, where the *LDI* property is summarized.

Definition 20 *Consider the nonlinear system:*

$$
\begin{aligned}
\dot{x}(t) &= f(x(t), w(t)), & (88) \\
z(t) &= g(x(t), w(t)).
\end{aligned}
$$

Suppose that, for each x, w and t, there exists a matrix $G(x, w, t) \in \Omega$ such that:

$$
\begin{bmatrix} f(x(t), w(t)) \\ g(x(t), w(t)) \end{bmatrix} = G(x, w, t) \begin{bmatrix} x(t) \\ w(t) \end{bmatrix}, \qquad (89)
$$

where $\Omega \in \mathbb{R}^{(n_x + n_z) \times (n_x + n_w)}$ This means that the nonlinear system (88) has the Linear Differential Inclusion property and can, thus, be put into a LPV representation.

11.2 *LPV* Control and Observation

Now, let some background be presented towards the Control and Observation of *LPV* systems.

11.2.1 State-Feedback Control Design: Pole Placement

Problem 1 *Consider the following* LPV *System:*

$$
\begin{aligned}
\dot{x}(t) &= A(\rho)x(t) + B(\rho)u(t), & (90) \\
y(t) &= C(\rho)x(t) + D(\rho)u(t).
\end{aligned}
$$

The objective towards the State-Feedback Pole Placement Control Design is to find a control law:

$$
u(t) = -F(\rho)x(t) + G(\rho)r(t), \qquad (91)
$$

where $r(t)$ is a reference signal, such that the closed-loop system is stable and the output signal $y(t)$ accurately tracks $r(t)$.

With this problem stated, there is a list of issues that can be tackled: Robust State-Feedback: Design the nominal state-feedback control (F, G) for ρ at $\rho_{nominal}$; Robust State-Feedback: Check the quadratic stability and performances of the CL system; LPV State-Feedback with Fixed Perfomances: Choose the desired (fixed) poles for the CL system; LPV State-Feedback with Fixed Perfomances: Design $F(\rho)$ such that the eigenvalues of the CL system are fixed; LPV State-Feedback with Fixed Perfomances: Check stability of the CL system when ρ is time-varying; LPV State-Feedback with Adaptive Perfomances: Choose the desired (varying) poles for the CL system; LPV State-Feedback with Adaptive Perfomances: Design $F(\rho)$ such that the eigenvalues of the CL system are ρ-dependent; LPV State-Feedback with Adaptive Perfomances: Check stability of the CL system when ρ is time-varying, allowing the performances to be scheduled according to the parameter changes.

11.2.2 H_∞-State-Feedback Control Design

The state-feedback law (91) can be found in order to minimize the H_∞ norm of the transfer function between output and disturbances $T_{yw}(s)$. This consists in applying the Bounded Real Lemma to the closed-loop system, refer to Lemma 1, achieved with a definite symmetric matrix P. This can be solved either with P ρ-dependent (imposing the parameter dependency) or at various fixed points, with a gridding approach.

11.2.3 H_∞-*LPV* Control Problem

Problem 2 *Of course, the H_∞-LPV Control Problem consists in finding a controller $C(\rho)$ such that the* CL *system is stable and s.t.:*

$$\gamma_\infty \;\; > \;\; 0 , \tag{92}$$

$$sup\frac{||z||_2}{||w||_2} \;\; < \;\; \gamma_\infty . \tag{93}$$

$$\tag{94}$$

11.2.4   Polytopic Approach

One of the possible solutions to Problem 2 is to solve the problem *offline* at each vertex of the Polytope defined by the CL system on ρ. Then, the controller is computes *inline* as the convex combination of local linear controllers.

Other approaches consist in *LFT*s and Gridding.

11.2.5   *LPV* Observers

The dual problem to control, the problem of observation, can also be solved for *LPV* systems. Nonetheless, some remarks have to be made:

1. What Observability property is considered?

2. What parameter-dependency should be taken for the gain matrix $L(\rho)$?

Considering Quadratic Detectability [22], a simple solution is to consider a single Lyapunov function in order to guarantee:

$$(A(\rho) - L(\rho)C(\rho))^T P + P(A(\rho) - L(\rho)C(\rho)) \quad < \quad 0 \,. \quad (95)$$

This problem can be solved using a polytopic approach only if $C(\rho)$ is a constant matrix. If this is not solvable, a solution may come using parameter-dependent Lyapunov functions, although the coupling between $L(\rho)$ and $P(\rho)$ will lead to non affine *LMI*s (polynomial or gridding approach needed).

One key issue in the implementation of observers concerns the information on the scheduling parameter $\rho(t)$. While the previous results are valid if $\rho(t)$ is known, the following observer description has to be used if $\rho(t)$ is estimated $(\hat{\rho}(t))$:

Denoting $\Delta A = A(\rho) - A(\hat{\rho})$, $\Delta B = B(\rho) - B(\hat{\rho})$, $\Delta C = C(\rho) - C(\hat{\rho})$ and $\Delta L = L(\rho) - L(\hat{\rho})$, one arrives at the following estimation error:

$$\begin{aligned} \dot{e}(t) &= (A - LC)(\hat{\rho})e(t) && (96) \\ &+ (\Delta A + L(\hat{\rho})\Delta C)x(t) + \Delta Bu(t) \,. \end{aligned}$$

Then, wither $\Delta Ax(t)$ is treated as a disturbance or a state augmentation approach has to be used.

12   On Stability

Let it be briefly remarked the concepts on system stability, as explored in details in [31]. They can also be found in [1] and [2].

12.1 Well-Posedness

Before any detail on stability of *LTI* system is presented, the following definition has to be understood by reader:

Definition 21 *A closed-loop system is said to be well-posed if all its transfer functions are strictly proper. This converts to $[\mathbb{I} + C(\infty)G(\infty)]$ being invertible, for G the open-loop plant and C the controller.*

12.2 *BIBO* Stability

An arbitrary system G is said to be *BIBO* stable for whichever limited system entry $u(t)$ ($\|u(t)\|_\infty < \infty$) there is a resulting (mapped) limited output $y(t)$ ($\|y(t)\|_\infty < \infty$). If this is not true, the system is said to be *BIBO* unstable. The system is *BIBO* stable if and only if the inequality 97 holds, where $h(t)$ is the time impulse response of the system G.

$$M_h \quad = \quad \int_{-\infty}^{+\infty} |h(\tau)| d\tau < \infty. \tag{97}$$

Remark 11 BIBO *Stability is often referred to as **external** stability.*

12.3 Lyapunov Stability

Also referred to as **internal** ($\mathcal{L}_2$ or *asymptotical*) stability. In respect to this criterion, one can define:

Definition 22   • *A system is said to be asymptotically stable when, for whichever initial condition $x_0 \neq 0$, it is true that $\lim_{t\to\infty} y(t) = 0$.*

- *A system is said to be asymptotically unstable when, for whichever initial condition $x_0 \neq 0$, $y(t)$ becomes unbounded.*

- *A system is said to be marginally stable if one desires to obtain $y(t)$, $t \in \mathbb{R}$, limited and arbitrarily close to the origin (0), it is only needed that the initial condition x_0 is sufficiently close to zero.*

12.4 *LTI* System Stability

A system G is $\mathcal{L}_2$ stable if $||u(t)||_2 < \infty$ implies $||y(t)||_2 < \infty$. The quantification of the signal amplification (gain) is evaluated as

$$\gamma = \quad sup_{0<||u||_2<\infty} \; \frac{||y||_2}{||u||_2}. \qquad (98)$$

12.5 *LPV* System Stability

The $\mathcal{L}_2$ stability of *LPV* systems is seen in [22]. Given a parametrically dependent stable *LPV* system as in equation (81), for zero initial conditions x_0, the induced $\mathcal{L}_2$ norm is defined as:

$$||\sum_\rho||_{i,2} = sup_{\rho(t)\in\Omega} \; sup_{w(t)\neq 0\in\mathcal{L}_2} \frac{||y||_2}{||u||_2}. \qquad (99)$$

Theorem 5 *A sufficient condition for the $\mathcal{L}_2$ of the system $\sum_\rho$ is the generalized Bounded Real Lemma (Lemma 1) using parameter dependent Lyapunov functions, assuming $|\dot{\rho}_i| < \nu_i \forall i$. If there existis $P(\rho) > 0 \; \forall \rho$ such that the Lemma's LMI holds for all i, then it is true that $||\sum_\rho||_{i,2} \leq \gamma$. The first entry of the LMI in Lemma 1, $A^T P + PA$, changes to $(A^T(\rho)P(\rho) + P(\rho)A(\rho) + \sum_{i=1}^N \nu_i \frac{\partial P(\rho)}{\partial \rho_i})$.*

12.6 Small Gain Theorem

Considering a $M - \Delta$ looped system, as given in Figure 4:

Theorem 6 *Suppose $M(s) \in \mathcal{RH}_\infty$ and consider a positive scalar γ_Δ. Then, the system is well-posed and internally stable for all $\Delta(s) \in \mathcal{RH}_\infty$ so that $||\Delta||_\infty \leq \frac{1}{\gamma_\Delta}$ if and only if $||M||_\infty < \gamma_\Delta$.*

12.7 Nonlinear System Stability

Two concepts will be detailed herein in terms of the stability of nonlinear systems: structural and Lyapunov stability. Nonetheless, the stability analysis of nonlinear systems can be much extensive. Reader is invited to refer to [2] for further details.
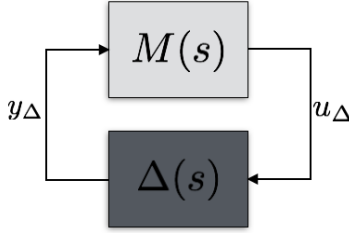
Figure 4: $M - \Delta$ Loop

12.7.1 Structural Stability

Proposition 1 *Considering $A \in \mathbb{R}^{n \times n}$ a square matrix, then, given $\epsilon > 0$, there exists $\delta > 0$ such that, if a constant matrix $\Delta A \in \mathbb{R}^{n \times n}$ does satisfy $||\Delta A||_2 < \delta$, then the distance between the eigenvalues of matrices A and $A + \Delta A$ is smaller than ϵ. This is: $||\lambda(A) - \lambda(A + \Delta A)||_2 < \epsilon$. This is named as the continuity of eigenvalues of A.*

Lemma 9 *Consider an autonomous nonlinear system $\dot{x}(t) = f(x(t), t)$ that, linearized at a given equilibrium point (x^e) is given by $\dot{x}(t) = Ax(t)$. It can be concluded that if there are some small disturbances on the nonlinear system such that there appears a ΔA upon A, the stability and type of the equilibrium point x^e are preserved. This leads to stating that a given autonomous nonlinear system is **structurally stable** when its qualitative phase behaviour is preserved under small disturbances in its vector map $f(x(t), t)$.*

12.7.2 Lyapunov Stability

Definition 23 *Let the following autonomous nonlinear system be considered, with an equilibrium point $x^e \in D$:*

$$\dot{x}(t) = f(x(t), t). \tag{100}$$

1. *x^e is said to be **stable** if, given $\epsilon > 0$, there exists $\delta = \delta(\epsilon) > 0$ such that $||x(0) - x^e||_2 < \delta \Rightarrow ||x(t) - x^e||_2 < \epsilon$ for every $t \geq 0$;*

2. *x^e is said to be **unstable** when it is not stable;*

3. *x^e is said to be **locally asymptotically stable** if it is stable and there exists $\gamma > 0$ such that $||x(0) - x^e||_2 < \gamma \Rightarrow \lim_{t \to \infty} x(t) = x^e$;*

4. x^e is said to be **globally asymptotically stable** when: a) $D = \mathbb{R}^n$; b) x^e is stable; c) $\lim_{t\to\infty} x(t) = x^e$ for every $x(0) \in \mathbb{R}^n$.

13 On Optimal and Predictive Control

Optimal Control may refer to a diverse range of control approaches, such as the Linear Quadratic Regulator, Linear Quadratic Gaussian (LQG) Control and, most, importantly Model Predictive Control (MPC). Reader is invited to refer to three main textbooks on the topic: [32], [33], [34] and [35].

13.1 Model Predictive Control

Firstly, let five pragmatic advantages of MPC be listed:

1. Control of Multivariable coupled dynamical systems;

2. Can handle constraints on state, output and control input;

3. Can express optimality concerns;

4. Can conceptually handle easily nonlinearities in the system model;

5. Has systematic design procedure.

But, synthetically, what is Model Predictive Control? It is a *feedback* implementation of optimal control using a finite, sliding prediction horizon and the *online* computation of a minimization problem. It has more than 5800 successful industrial applications in many different areas. MPC is useful, generic, widely applicable, although not quite straightforward.

As states [36], the term model predictive control does not designate a specific control strategy but a wide gamma of control methods that make explicit use of a model of the process to obtain the control signal by minimizing an objective function. The three main idead that sustain MPC are:

1. explicit use of a model to predict the process output at future time instants inside a rolling horizon;

2. calculation of a control sequence by the minimization an objective function;

3. receding approach, so that at each instant the horizon is displaced towards the future, which involves the application of the first control signal of the sequence calculated at each step.

These basic concepts are illustrated by Figure 5, where u is the control signal, N the rolling horizon and y the controlled output.
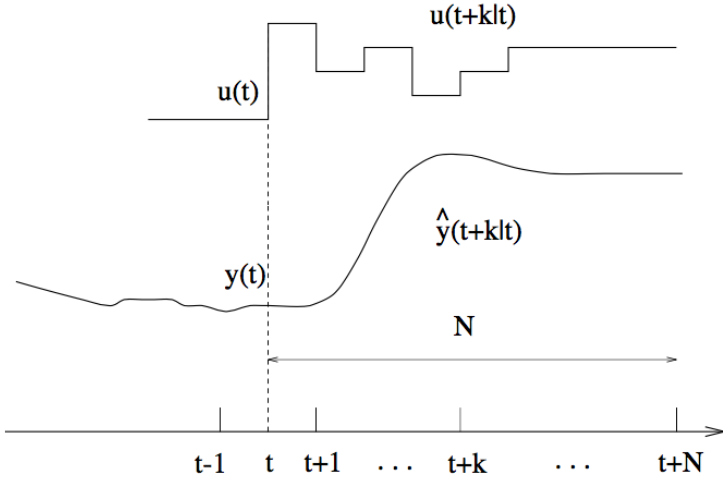
Figure 5: The Basic *MPC* ideas, as seen in [36]

The methodology behind *MPC* strategies are characterized by the following procedures, as states [36]:

1. The future outputs for a defined horizon N_p, namely the prediction horizon, are predicted at each instant t using a given process model. These predicted outputs $y(t + k|t)^1$ for $k = 1...N_p$ depend on the known values up to instant t (past inputs and outputs) and on the future control signals $u(t + k|t)$, fo $k = 0...(N_p - 1)$, which are to be sent to the system and to be calculated.

2. The set of future control signals is calculated by optimizing a determined criterion (objective function, J) in order to keep the process as close as possible to a given reference trajectory $y_r(t + k)$. This criterion usually takes the form of a quadratic function of the errors between the predicted

---

[1]The notation is used to represent the predicted value of y at instant $t + k$, computed at instant t.

output signal and the predicted reference trajectory. The control effort is included in the objective function in most cases. An explicit solution can be obtained if the criterion is quadratic, the model is linear and there are no constraints, otherwise an iterative optimization method has to be used. Remark that if there are constraints, an explicit solution can also be found, although it is no longer linear but piece-wise affine.

3. The control signal $u(t|t)$ is sent to the process, whilst the next control signals calculated are neglected, because, at the next sampling instant, $y(t+1)$ will already be known, and step 1 will be repeated with this new value and all the sequences will be brought up to date. Thus, $u(t+1|t+1)$ is calculated (which in principle will be different to $u(t+1|t)$ because of the new information available) using the receding horizon concept.

The basic structure of MPC approaches is shown in Figure 6. A model is used to predict the future plant outputs, based on past and current values and on the proposed optimal future control actions. These actions are calculated by the optimizer, that takes into account the cost function as well as the constraints.
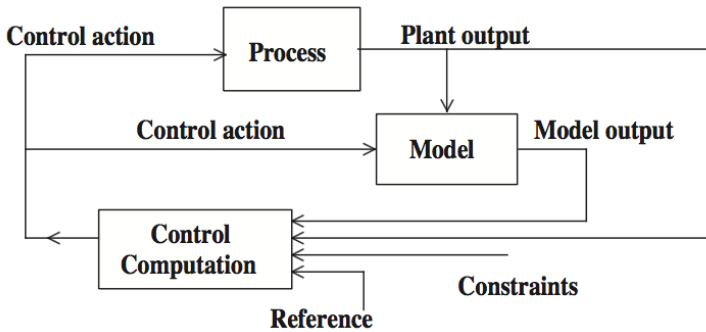

Figure 6: The Basic MPC Structure, as seen in [36]

13.1.1   The Prediction Model

The prediction model has an important role in MPC schemes as it is needed to compute the predicted output at future instants $y(t+k|t)$. This model is divides into process model and disturbance model.

Process Model Various discrete models can be used to represent a given plant's behaviour. Two types of process models are the most used: the step-response and the transfer function models.

The step-response model equation is given by:

$$y(t) = \sum_{i=1}^{+\infty} g_i \Delta u(t-i), \qquad (101)$$

where the coefficients g_i are the sampled output values for the step input and $\Delta u(t) = u(t) - u(t-1)$. This model is widely accepted in industry because it is very intuitive and clearly reflects the influence of each manipulated variable on a determined output. The process of identification is also simplified while still maintaining the ability to represent complex dynamics such as nonminimum phase and dead-time. Although the sum present in the model is infinite, it can be truncated. One of its main disadvantages is the impossibility of representing unstable processes.

The transfer function model equation is given, with abuse of notation, by:

$$A(z)y(t) = B(z)u(t-d-1), \qquad (102)$$

where d is the dead-time, and

$$A(z) = 1 + a_1 z^{-1} + a_2 z^{-2} + \cdots + a_{n_a} z^{-n_a}, \qquad (103)$$
$$B(z) = b_0 + b_1 z^{-1} + b_2 z^{-2} + \cdots + b_{n_b} z^{-n_b}. \qquad (104)$$

This representation is also valid for unstable processes and has the advantage that it only needs a few parameters, although a priori knowledge of the process is fundamental in the case of model identification, especially of the order of the A and B polynomials.

Disturbance Model Several models can be used to describe the disturbances. This is herein meaning, a model that described the differences between the measured output and the one calculated by the process model. In most practical application, step or ramp models are mostly used. When nondeterministic disturbances are considered, such as random changes occurring at random instants, the auto-regressive and integrated moving average ($ARIMA$) model is widely used. This is given by:

$$\nu(t) = \frac{C(z)e(t)}{D(z)\Delta(z)}, \qquad (105)$$

where $\Delta(z) = 1 - z^{-1}$, $e(t)$ is a white-noise of zero mean and the polynomials $C(z)$ and $D(z)$ are used to describe the stochastic characteristics of $\nu(t)$.

13.1.2 Free and Forced Responses

Most linear *MPC* applications consider the use of the concept of *free* and *forced* output responses. The idea of this concept is to express the control sequence as the sum of two signals:

$$u(t) \quad = \quad u_f(t) + u_c(t) \,, \tag{106}$$

where $u_f(t)$ corresponds to the past inputs and is kept constant and equal to the last value of the manipulated variable in future time instants. Synthetically:

$$u_f(t - k) = u(t - k), \quad \text{for } k = 1, 2, \dots , \tag{107}$$
$$u_f(t + k) = u(t - 1), \quad \text{for } k = 0, 1, 2, \dots . \tag{108}$$

The signal $u_c(t)$ is made equal to zero in the past and equal to the next control moves in the future. Synthetically:

$$u_c(t - k) = 0, \quad \text{for } k = 1, 2, \dots , \tag{109}$$
$$u_c(t + k) = u(t + k) - u(t - 1), \quad \text{for } k = 0, 1, 2, \dots . \tag{110}$$

The prediction of the output sequence is separated into two parts, the free response, which corresponds to the prediction of the output $y(t + k|t)$ when the process manipulated variable is made equal to $u_f(t)$, and the forced response, which corresponds to the prediction of the process output $y(t+k|t)$ when the control sequence is made equal to $u_c(t)$. The free response corresponds to the evolution of the process due to its present state, while the forced response is due to the future control moves, as states [35].

13.1.3 The Cost Function J

The various *MPC* algorithms suggest different cost functions for obtaining the optimal control law. The general aim is that the future predicted output $y(t+k|t)$, inside the considered prediction horizon, should follow a determined reference signal y_r and, at the same time, the control effort u necessary for doing so should be penalized. The most simple way to express such a cost function

is:

$$J = \sum_{k=d}^{N_p} \left[(y(t+k|t) - y_r(t+k))Q_y(y(t+k|t) - y_r(t+k))^T \right]$$

$$+ \sum_{k=1}^{N_c} \left[(\Delta u(t+k-1))Q_u(\Delta u(t+k-1))^T \right] \quad (111)$$

where Q_y and Q_u are weighting matrices, N_p is the prediction horizon, d is the dead-time and N_c is the control horizon. The weights define how the future control increments and error should be penalized in the cost function. They are used to indicate which variables should be prioritized and which should not. N_c indicates in what future instants the controller is allowed to change the input variable. A smaller horizon usually results in a more aggressive closed-loop behaviour.

An interesting aspect is the consideration of the future reference trajectory. Usually the future evolution of the reference is not known *a prior* and, thus, $y_r(t+k) = y_r(t)$, $\forall k > 0$ is used. In some cases, however, for instance in robotics, servos or batch processes, the future reference is known. This information can then be used in the cost function to improve the reference tracking capabilities of the controller, as states [35].

As points out [35], a big advantage of *MPC* schemes is that they can explicitly consider the constraints of the process, which are normally defined as bounds in the amplitude and in the slew rate of the control signal, and limits in the output. This is $\forall k \geq 0$, one has:

$$\underline{u} \leq u(t+k) \leq \overline{u}, \quad (112)$$
$$\underline{\Delta u} \leq \Delta u(t+k) \leq \overline{\Delta u}, \quad (113)$$
$$\underline{y} \leq y(t+k) \leq \overline{y}. \quad (114)$$

13.1.4 Finding the Control Law

$$U = \begin{bmatrix} u(k|k) & u(k+1|k) & \dots & u(k+N_c-1|k) \end{bmatrix}^T \quad (115)$$

represents the vector of control efforts inside the control horizon N_c (to be optimized).

In order to obtain this control sequence U, and apply $u[k|k]$ to the controlled system, it is necessary to minimize the function J, given in Equation (111). To do this the values of the predicted

outputs $y(t + k|t)$ are calculated as a function of the past values of the inputs and outputs, and of the future control signals, making use of the model chosen, and then the predicted values are substituted in the cost function, thus resulting in an expression whose minimization leads to the desired control sequence U. An analytical solution can be obtained for the quadratic criterion if the model is linear and there are no constraints, otherwise an iterative method of optimization should be used.

There are several MPC schemes that use the ideas just presented. These methods can be roughly categorized into two main groups. For the first group, one finds industry-derived algorithms, like the Dynamic Matrix Control (DMC), refer to [37], and the Model Algorithm Control (MAC), refer to [38]. For this group, the prediction is based on step or impulse response models of the plants and the disturbances are considered as the difference between the real and predicted outputs [39]. The other group has been derived in *academia*, based on the ideas of adaptative control [40]. In this second group, are included: the Generalized Predictive Control (GPC), refer to [41]; the Extended Prediction self-adaptive Control ($EPSAC$), refer to [42]. From these two groups, the DMC and the GPC algorithms are, maybe, the most popular and well-established methods.

No further development shall be made upon the topic of MPC algorithms. Nonetheless, some references are listed next and reader is invited to refer to them for curiosities and deeper explanations:

- An important survey of the theory and practice of Model Predictive Control is seen in [43]; Some insights on the future developments are given in [44]; A survey of industrial applications has been done in [45].

- In terms of Robust MPC, the book [46] has to be mentioned; The Robust design of GPC algorithms is proposed in [47]; A Smith-Predictor-based predictive control design is seen in [48];

- The use of the Filtered DMC has been studied deeply in [36], for the predictive control of dead-time processes; In[49], a nonlinear predictor is derived for dead-time systems with input nonlinearities;

- The state-space interpretation of Model Predictive Control is detailed in [39]; Nonlinear MPC has been studied in [34] and [50];

- *MPC* applied to Linear Parameter Varying Systems has been seen in [51], [52] and [53].

14 On Fault-Tolerant Control

A holistic and interesting approach on the concept behind Fault-Tolerant Control (*FTC*) is of uttermost importance to this work, and can be found on the article [54]. A comparative study between active and passive *FTC* approaches is seen on [55], where there se a debate of the use and application results of each of these two methods. Last but not least, on the article [56] we can find a tutorial introduction on reconfigurable *FTC*.

14.1 Passive *FTC*

Passive *FTC* approaches reside upon the notion of the controller ensuring that the closed-loop system is stable and has the desired performances for a range of system states (healthy and faulty). The idea is to overcome faults with robustness.

14.2 Active *FTC*

Let it be remark the main idea of Active *FTC*: any controlled system is *always* subject to faults and failures - these can be upon components, signal processing or even a total system crash. A classical feedback control system usually comprises actuators and sensors coupled to the real plant (system). Let us admit, then, that there are faults (measurable or not) each of these three subsystems. An active *FTC* scheme is comprised of two parts: a Fault Detection and Diagnosis (*FDD*) structure and a reconfigurable controller. The *FTC* controller, thus, has an intrinsic reconfiguration mechanism for the faults upon the system that are well detected by the *FDD* scheme. This is clear in Figure 7. Note that the that the control scheme must have access to real-tme information on whether the system is faulty and computes an efficient reconfiguration mechanism, see [57] and [55].

A notable article about an implementation of a *FDD* scheme using parity space is seen on [58]. Reconfiguration mechanisms represent a common way on how to compensate for fault effects, as explained by [59].

Figure 7: The Active *FTC* Strategy, as given in [55]

14.3 On Fault Detection / Estimation

A solid Fault Detection and Diagnosis structure is, thus, important for *FTC* as to provide timely information on the condition, location and type of malfunction that may occur on the controlled plant. It is, also, not to be forgotten that *FDD* schemes are needed for reliability of systems and for overall safety surveillance goals.

Although there exist nonlinear model-based approaches for *FDD*, as presented in [60], [61], [62] and [58], most methods suppose linear time-invariance (*LTI*) system characteristics and reside on parity space approaches, as seen in [63], [64] and [65]. Other works towards the study of faults upon uncertain dynamical systems have also been visited, as in [66].

The classical *LTI*, model-based *FDD* design usually faces problems when dealing with changes upon the observed plant's operational point. Whenever these changes occur, there should not appear (false) fault alarms or the necessity for further observer reconfiguration, which is not always true with these design methods.

More recently, some approaches have appeared to overcome these problems, based on gain-scheduling to extend the scope of the linear *FDD* methods to nonlinear systems. A natural approach is to consider the extension of *LTI* systems to Linear Parameter Varying (*LPV*) systems in order to model the monitored plant. Such models can be used to accurately describe some complex nonlinear plants, see [21].

An *LPV*-based fault estimation scheme is able to autonomously adjust and schedule observer or detection filter gains. This is suitable trade-off between full scaled nonlinear designs and *LTI* methods based on a fixed operating condition, since *LPV*-based *FDD* methods provide most of the conveniencies of *LTI* design and still guarantees good performance and stability conditions

over a wider operating set.

In recent years, literature is evermore rich on LPV control design, although the literature on LPV-based FDD is still slightly limited. Nonetheless, these novel LPV-based fault detection methods have been discussed in:

- [67], where FDD is seen coupled with the LPV description of a two-link manipulator;

- [68], where a FTC strategy for actuator faults on helicopters is seen;

- [69], where an adaptive fault estimation scheme is also applied to helicopter models;

- [70], where a method is presented for the synthesis of FDD filters based on an LMI solution for $Polytopic\ LPV$ systems;

- [71], where the authors propose the design of a low-order LPV observer to estimate the unmeasured states of the system and to estimate sensor faults for a class of uncertain LPV systems;

- [72], where an LMI-based pole-placement robust LPV estimator is presented;

- [73], where a robust fault detection scheme is proposed, considering the H_∞ disturbance attenuation.

15 Modelling and Identification for Microgrids

This last section will be dedicated on some key tool that concern the identification, observation and control of microgrids.

15.1 Energy Hubs

Let it be depicted how to model a *microgrid*'s time-wise behaviour, for future control, observation and design purposes. To do so, the *Energy Hubs* modeling methodology, as proposed in [74], is of prime importance to be depicted. All what is described related to this methodology is also presented with details in [75].

An energy hub can be used to model the interface between energy producers, consumers and the transmission line. From the system's outlook, an energy hub can be identified as a black box unit that comprises the following requirements:

1. Input and output of electric power;

2. energy conversion;

3. energy storage.

The hub serves as interface between the energy sources, producers and consumers or between different kinds of energy sources. An energy hub can, in a practical sense, model any full power system, any microgrid or even every subsystem of a microgrid, given that all subsystems are interconnected with the transmission lines and each node stands for a single hub.

The Energy Hub methodology is comprised of two stages of design: firstly, the power flow within hubs is modelled and, then, the flow between hubs is described.

The three following assumptions are made:

(i) The network is in *steady-state*. This means all transitory dynamics have already converged and that all process variables stay within bounded limits (either with constant behaviour or uniform variations);

(ii) The interconnections between the energy hubs concern, solely, the inputs and outputs of each hub;

(iii) Energy losses only occur when storing or converting energy. Losses in trasmission lines and other are disregarded;

(iv) The flow of energy within a hub is unidirectional, issuing from inputs and flowing to outputs. This is only not true in storage elements, where bidirectional flows are accepted.

An Energy Hub carefully schematized in Figure 8, where *(a)*, *(b)* and *(c)* may co-exist, but this is not a necessary condition. For example: a *PV* solar panel is comprised only of *(b)*, whereas the battery banks are only made of *(c)*.

The methodology follows by modelling separately converter and storage units of Energy Hubs. This is presented in the next two items.

Remark 12 *To describe the input/output variables of a hub, the following notation is used $\kappa_{\mathcal{I}}^{\mathcal{J}}(k)$. This is explained: Sign κ might stand either for the measured outputs of a hub (y) or for the hub's inputs (u); Subindex $\mathcal{I}$ can represent different situations and, for this, the following symbology is used:*

- *r stands for inputs variables;*

43
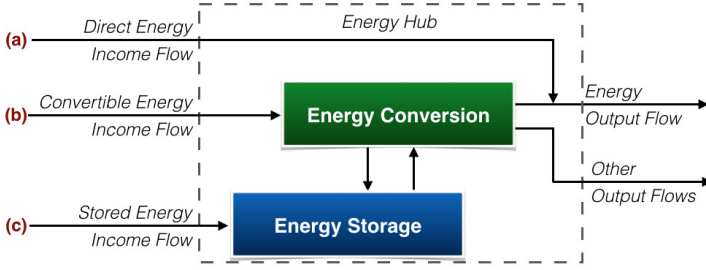
Figure 8: *Energy Hub*

- *p stands for output variables;*

- *s stands for storage interfaces;*

- *q stands for input to storage units;*

- *m stands for output to storage units.*

Superindex $\mathcal{J}$, finally, stands simply for kind of hub element the variable is related to, being either C for converter units or S for storages. This is exemplified: the variable related to the input flow of energy to a boiler (converter unit) is given by $u_r^C(k)$.

Converter Units

In terms of converter units: these are modelled as black boxes with input and output flows. They can consist of either single or multiple inputs and have either single our multiple outputs (*SISO*, *SIMO*, *MISO* or *MIMO*).

A simple converter unit is illustrated by Figure 9, below. This element convertes, at each sampling instant k, a generic input flow $u_r^C(k)$ into a generic output flow $y_p^C(k)$. The input-output conversion is defined with the use of the coupling factor $\gamma_{p,r}^C$. This factor corresponds to the *steady-state* conversion efficiency of the given converter unit. So, one has:

$$y_p^C(k) \quad = \quad \gamma_{p,r}^C u_r^C(k), \tag{116}$$

where it is implied (always) that $u_r^C(k) > 0$, which means that the flow from the input to the output of the converter unit is unidirectional.
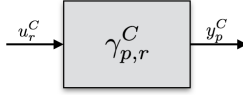
Figure 9: *Energy Hub: SISO* Converter Unit

From a physical point of view, these coupling factors can have the characteristic listed in Table 1.

In applications for which physical conservation laws have to respected, these coupling factors are bounded to the constraint that the output of the given converter unit must be smaller than or equal to its input:

$$y_p^C(k) \quad \leq \quad u_r^C(k) \Rightarrow 0 \leq \gamma_{p,r}^C \leq 1 \,. \qquad (117)$$

Table 1: Converter Unit Coupling Factors

Type of Converter Unit	Coupling factor
Conversion with Energy Loss	$0 \leq \gamma_{p,r}^C \leq 1$
Lossless Conversion	$\gamma_{p,r}^C = 1$
Conversion with Energy Gain	$\gamma_{p,r}^C \geq 1$

Having the methodology to model a single converter unit clear, it is essential to understand that a generic hub is composed of a converter cluster, with multiple converter units as the one in Figure 9, that connects all input flows $\mathbf{u}^C(k) = \left\{ u_1^C(k), \ldots, u_{n_r}^C(k) \right\}$ to all outputs flows $\mathbf{y}^C(k) = \left\{ y_1^C(k), \ldots, y_{n_p}^C(k) \right\}$, where n_r and n_p stand for the total number of hub inputs and outputs, respectively. This converter cluster has a coupling matrix Γ^C, which relates $\mathbf{u}^C(k)$ to $\mathbf{y}^C(k)$, at each sampling instant k, composed by the converter coupling factors $\gamma_{p,r}^C$. This leads to:

$$\underbrace{\begin{bmatrix} y_1^C(k) \\ \vdots \\ y_{n_p}^C(k) \end{bmatrix}}_{\mathbf{y}(k)} = \underbrace{\begin{bmatrix} \gamma_{1,1}^C & \cdots & \gamma_{1,n_r}^C \\ \vdots & \ddots & \vdots \\ \gamma_{n_p,1}^C & \cdots & \gamma_{n_p,n_r}^C \end{bmatrix}}_{\Gamma^C} \underbrace{\begin{bmatrix} u_1^C(k) \\ \vdots \\ u_{n_r}^C(k) \end{bmatrix}}_{\mathbf{u}^C(k)} . \qquad (118)$$

Given that all these coupling factors are related to the *steady-state* energy conversion, they are all constant variables and, thus, equations (116) and (118) are linear.

Storage Units

The modelling of intermediate storage units of hubs (biomass stocks, tanks, battery banks and others) considers that they are composed of an interface and an internal storage, as depicts Figure 10. The interface can be understood as a flow converter, which modulates a generic storage interface input flow $u_s^S(k)$ into another generic storage interface output flow $\breve{u}_s^S(k)$. The converted energy is, then, stored in an ideal internal stage (x_s). Mathematically, the storage interface is modelled analogously to a converter unit, where the *steady-state* input and output flows are given by:

$$\breve{u}_s^S(k) \quad = \quad e_s(k)u_s^S(k)\,. \tag{119}$$

where $e_s(k)$ represents the efficiency in terms of charging/discharging the hub's interface. This directly influences how much of the flow exchanged with the hub reaches the storage x_s. This factor depends on the direction of the exchanged (bidirectional) flow, on whether the storage unit being charged or discharged:

$$e_s(k) = \begin{cases} e_s^+ & \text{if} \quad u_s^E(k) \geq 0 & \text{(charging)}\,, \\ e_s^- & \text{else} & \text{(discharging)}\,. \end{cases} \tag{120}$$

where e_s^+ and e_s^- are, respectively, the charge and discharge efficiencies of e_s.
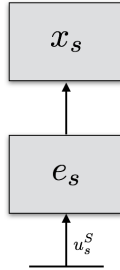
Figure 10: *Energy Hub: SISO* Storage Unit

Following the described methodology, from a discrete standpoint, with sampling period ΔT, the internal storage state of a hub, x_s evolves as in[2]:

$$x_s(k+1) \quad = \quad x_s(k) + \breve{u}_s^E(k)\Delta T\,. \tag{121}$$

---

[2]$t \in \mathbb{R}$ is the time variable and $t = k\Delta T$; for simplicity, only k is used in the discrete-time equations throughout this work.

Then, in terms of n_s multiple storage units, one has: vector $\mathbf{x}_s(k+1)$ that contains all the storage states $x_s(k+1)$ for $s = 1, \ldots, n_s$, matrix $\Lambda^S(k)$ that contains all the interface efficiencies $e_s(k)$ for $s = 1, \ldots, n_s$ and vector $\mathbf{u}_s^S(k)$ that contains all the interface flow inputs $u_s^E(k)$ for $s = 1, \ldots, n_s$. Thus:

$$
\underbrace{\begin{bmatrix} x_1(k+1) \\ \vdots \\ x_{n_s}(k+1) \end{bmatrix}}_{\mathbf{x}_s(k+1)} = \underbrace{\begin{bmatrix} x_1(k) \\ \vdots \\ x_{n_s}(k) \end{bmatrix}}_{\mathbf{x}_s(k)} \tag{122}
$$

$$
+ \underbrace{\begin{bmatrix} e_1(k) & & \\ & \ddots & \\ & & e_{n_s}(k) \end{bmatrix}}_{\Lambda^S(k)} \underbrace{\begin{bmatrix} u_1^S(k) \\ \vdots \\ u_{n_s}^S(k) \end{bmatrix}}_{\mathbf{u}_s^S(k)},
$$

where

$$
\Lambda^S(k) = \{\Lambda^{S+}, \Lambda^{S-}\} = \begin{bmatrix} \{e_1^+, e_1^-\} & & \\ & \ddots & \\ & & \{e_{n_s}^+, e_{n_s}^-\} \end{bmatrix}, \tag{123}
$$

so that each element of $\Lambda^S(k)$ is a signal function of $u_s^S(k)$. As of this, if $u_s^S(k)$ is positive, this means that the storage is charging and $e_s(k) = e_s^+$, otherwise if $u_s^S(k) \leq 0$, the storage is discharging and $e_s(k) = e_s^-$.

In terms of multiple storage units of a single hub, it has to be remarked that as storage elements may be connected to both hub inputs and outputs, as depicts Figure 11, and with internal converter units. In this cases, a mathematical transformation of the corresponding storage flows has to be performed in order to obtain an input-output description independently of where the storage device is physically connected. The following steps are well-detailed in [75].

As shows Figure 11, the flow $\breve{u}_r^C(k)$ towards the converter is given by equation (124) and the converter unit's output, on the other hand, is given by equation (125), where $\breve{y}_p^C(k)$ is the converter's output flow, $y_p^C(k)$ is the hub's output flow and $u_m^S(k)$ is the output storage's flow.

$$
\breve{u}_r^C(k) = u_r^C(k) - u_q^S(k), \tag{124}
$$

$$
\breve{y}_p^C(k) = y_p^C(k) + u_m^S(k). \tag{125}
$$
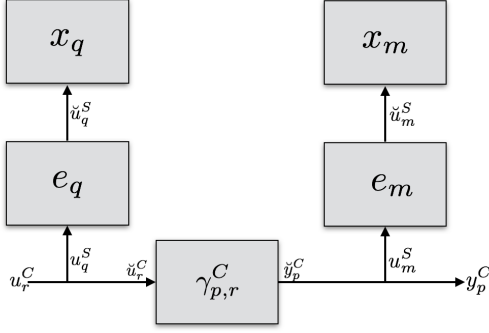
Figure 11: *Energy Hub*: Multiple Storage Units

In terms of multiple inputs and multiple outputs, this yields:

$$
\underbrace{\begin{bmatrix} y_1^C(k) \\ \vdots \\ y_{n_p}^C(k) \end{bmatrix}}_{\mathbf{y}^C(k)} = \underbrace{\begin{bmatrix} \gamma_{1,1}^C & \cdots & \gamma_{1,n_r}^C \\ \vdots & \ddots & \vdots \\ \gamma_{n_p,1}^C & \cdots & \gamma_{n_p,n_r}^C \end{bmatrix}}_{\Gamma^C} \underbrace{\begin{bmatrix} u_1^C(k) \\ \vdots \\ u_{n_r}^C(k) \end{bmatrix}}_{\mathbf{u}^C(k)} \tag{126}
$$

$$
+ \underbrace{\begin{bmatrix} \gamma_{1,1}^S & \cdots & \gamma_{1,n_s}^S \\ \vdots & \ddots & \vdots \\ \gamma_{n_p,1}^S & \cdots & \gamma_{n_p,n_s}^S \end{bmatrix}}_{\Gamma^S} \underbrace{\begin{bmatrix} u_1^S(k) \\ \vdots \\ u_{n_s}^S(k) \end{bmatrix}}_{\mathbf{u}^S(k)} .
$$

15.2 State-space Representation

This *Energy Hubs* methodology, finally, yields a complete *state-space* representation that models any kind of hub. This is:

$$
\begin{aligned}
x(k+1) &= x(k) + \Lambda^S(k)u^S(k), \\
y(k) &= \Gamma^C u^C(k) + \Gamma^S u^S(k),
\end{aligned} \tag{127}
$$

which can be condensed by defining the complete converter interface efficiency matrix $\Lambda_i(k)$, the complete coupling matrix Γ_i and the complete hub input vector $\mathbf{u}_i(k)$ as follows:

$$
\begin{aligned}
\Lambda(k) &= \begin{bmatrix} 0 & | & \Lambda^S(k) \end{bmatrix}, \tag{128} \\
\Gamma &= \begin{bmatrix} \Gamma^C & | & \Gamma^S \end{bmatrix}, \tag{129} \\
\mathbf{u}(k) &= \begin{bmatrix} u^L(k)^T & | & u^S(k)^T \end{bmatrix}^T . \tag{130}
\end{aligned}
$$

This results, finally, in:

$$
\begin{aligned}
x(k+1) &= x(k) + \Lambda(k)u(k)\,, & (131)\\
y(k) &= \Gamma u(k)\,.
\end{aligned}
$$

Using this formulation, a generic hub can be described by the set of matrices $H = \{\Lambda(k), \Gamma\}$.

Nonetheless, if one considers disturbances, representation (131) changes to the normal dynamic *LTI* system representation:

$$
\begin{aligned}
x(k+1) &= Ax(k) + B_1 q(k) + B_2 u(k)\,, & (132)\\
z(k) &= C_1 x(k) + D_{11}q(k) + D_{12}q(k)\,, & (133)\\
y(k) &= C_2 x(k) + D_{21}q(k) + D_{22}q(k)\,, & (134)
\end{aligned}
$$

where x represents the system's storage units; u represents the manipulated variables; z stands for the controlled outputs; q represents an array of external disturbances and y is the vector of measured outputs.

In Figure 12, a generalized *microgrid* is presented, considering the described *Energy Hubs* methodology.
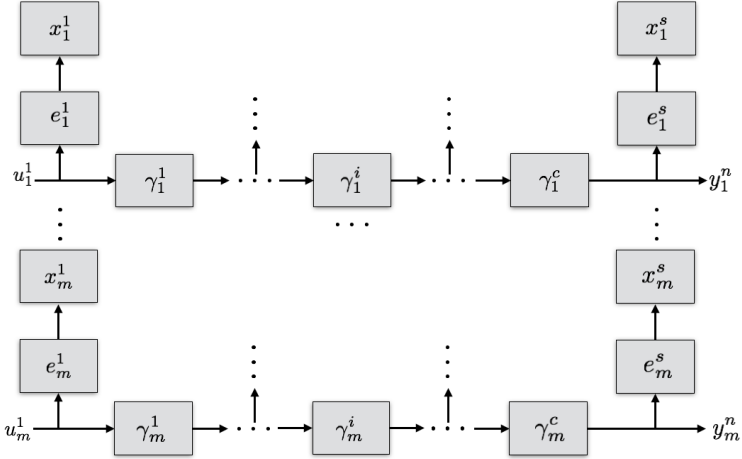

Figure 12: Generalized *Microgrid*

References

[1] CHEN, C.-T. *Linear system theory and design.* [S.l.]: Oxford University Press, Inc., 1995.

[2] KHALIL, H. K.; GRIZZLE, J. *Nonlinear systems.* [S.l.]: Prentice hall New Jersey, 1996.

[3] ISIDORI, A. *Nonlinear control systems.* [S.l.]: Springer Science & Business Media, 2013.

[4] JR, N. R. S. On newton's method for riccati equation solution. 1974.

[5] LAVRETSKY, E.; WISE, K. A. Optimal control and the linear quadratic regulator. In: _____. *Robust and Adaptive Control: With Aerospace Applications.* [S.l.]: Springer London, 2013. p. 27–50.

[6] BEMPORAD, A. et al. The explicit linear quadratic regulator for constrained systems. *Automatica*, Elsevier, v. 38, n. 1, p. 3–20, 2002.

[7] GHARSALLAOUI, H. et al. Flatness-based control and conventional rst polynomial control of a thermal process. *International Journal of Computers Communications & Control*, v. 4, n. 1, p. 41–56, 2009.

[8] BISHOP, G.; WELCH, G. et al. An introduction to the kalman filter. *Proc of SIGGRAPH, Course*, v. 8, n. 27599-23175, p. 41, 2001.

[9] SENAME, O.; GASPAR, P.; BOKOR, J. *Robust control and linear parameter varying approaches: application to vehicle dynamics.* [S.l.]: Springer, 2013.

[10] ZHOU, K.; DOYLE, J. C. *Essentials of robust control.* [S.l.]: Prentice hall Upper Saddle River, NJ, 1998.

[11] BOYD, S. P. et al. *Linear matrix inequalities in system and control theory.* [S.l.]: SIAM, 1994.

[12] DETTORI, M. *LMI techniques for control-with application to a compact disc player mechanism.* Tese (Doutorado) — TU Delft, Delft University of Technology, 2001.

[13] GHAOUI, L. E.; NICULESCU, S.-l. *Advances in linear matrix inequality methods in control.* [S.l.]: SIAM, 2000.

[14] SCHERER, C.; WEILAND, S. *Linear matrix inequalities in control*. [S.l.]: University of Stuttgart, 2000.

[15] DOYLE, J. C. Synthesis of robust controllers and filters. In: IEEE. *Decision and Control, 1983. The 22nd IEEE Conference on*. [S.l.], 1983. v. 22, p. 109–114.

[16] BRIAT, C. *Robust control and observation of LPV time-delay systems*. Tese (Doutorado) — Institut National Polytechnique de Grenoble-INPG, 2008.

[17] ZAMES, G. On the input-output stability of time-varying nonlinear feedback systems part one: Conditions derived using concepts of loop gain, conicity, and positivity. *IEEE transactions on automatic control*, IEEE, v. 11, n. 2, p. 228–238, 1966.

[18] PACKARD, A.; DOYLE, J. The complex structured singular value. *Automatica*, Elsevier, v. 29, n. 1, p. 71–109, 1993.

[19] NORMEY-RICO, J. E.; CAMACHO, E. F. Unified approach for robust dead-time compensator design. *Journal of Process Control*, Elsevier, v. 19, n. 1, p. 38–47, 2009.

[20] SANTOS, T. L.; TORRICO, B. C.; NORMEY-RICO, J. E. Simplified filtered smith predictor for MIMO processes with multiple time delays. *ISA transactions*, Elsevier, v. 65, p. 339–349, 2016.

[21] MOHAMMADPOUR, J.; SCHERER, C. W. *Control of linear parameter varying systems with applications*. [S.l.]: Springer Science & Business Media, 2012.

[22] WU, F. et al. Induced l_2-norm control for LPV systems with bounded parameter variation rates. In: *IEEE conference on Decision and Control*. [S.l.: s.n.], 1997.

[23] BRUZELIUS, F. *Linear parameter-varying systems-an approach to gain scheduling*. [S.l.]: Chalmers University of Technology, 2004.

[24] BAMIEH, B.; GIARRE, L. Identification of linear parameter varying models. *International journal of robust and nonlinear control*, Wiley Online Library, v. 12, n. 9, p. 841–853, 2002.

[25] CASELLA, F.; LOVERA, M. LPV/LFT modelling and identification: overview, synergies and a case study. In: IEEE. *International Conference on Computer-Aided Control Systems*. [S.l.], 2008. p. 852–857.

[26] TÓTH, R. et al. Discrete time LPV I/O and state space representations, differences of behavior and pitfalls of interpolation. In: IEEE. *European Control Conference*. [S.l.], 2007. p. 5418–5425.

[27] WU, F.; GRIGORIADIS, K. M. LPV systems with parameter-varying time delays: analysis and control. *Automatica*, Elsevier, v. 37, n. 2, p. 221–229, 2001.

[28] SCHERER, C. W. LPV control and full block multipliers. *Automatica*, Elsevier, v. 37, n. 3, p. 361–375, 2001.

[29] BLANCHINI, F.; MIANI, S. Stabilization of LPV systems: state feedback, state estimation, and duality. *SIAM journal on control and optimization*, SIAM, v. 42, n. 1, p. 76–97, 2003.

[30] BOKOR, J.; BALAS, G. Linear parameter varying systems: A geometric theory and applications. *IFAC Proceedings Volumes*, Elsevier, v. 38, n. 1, p. 12–22, 2005.

[31] LATHI, B. P. et al. *Linear systems and signals*. [S.l.]: Oxford University Press New York:, 2005.

[32] ZHOU, K. et al. *Robust and optimal control*. [S.l.]: Prentice hall New Jersey, 1996.

[33] CAMACHO, E. F.; BORDONS, C. *Model predictive control*. [S.l.]: Springer Science & Business Media, 2013.

[34] CAMACHO, E. F.; BORDONS, C. Nonlinear model predictive control. In: *Model Predictive control*. [S.l.]: Springer, 2007. p. 249–288.

[35] NORMEY-RICO, J.; CAMACHO, E. *Control of dead-time processes*. [S.l.]: Springer Science & Business Media, 2007.

[36] LIMA, D. M. *Predictor-based robust control of dead-time processes*. Tese (Doutorado) — Universidade Federal de Santa Catarina, 2015.

[37] CUTLER, C. R.; RAMAKER, B. L. Dynamic matrix control: A computer control algorithm. In: *Joint Automatic Control Conference*. [S.l.: s.n.], 1980. p. 72.

[38] RICHALET, J. et al. Model predictive heuristic control. *Automatica*, Pergamon Press, Inc., v. 14, n. 5, p. 413–428, 1978.

[39] LEE, J. H.; MORARI, M.; GARCIA, C. E. State-space interpretation of model predictive control. *Automatica*, Elsevier, v. 30, n. 4, p. 707–717, 1994.

[40] DATTA, A.; OCHOA, J. Adaptive internal model control: Design and stability analysis. *Automatica*, Elsevier, v. 32, n. 2, p. 261–266, 1996.

[41] CLARKE, D. W.; MOHTADI, C.; TUFFS, P. Generalized predictive control—part i. the basic algorithm. *Automatica*, Elsevier, v. 23, n. 2, p. 137–148, 1987.

[42] KEYSER, R. D.; CAUWENBERGHE, A. V. Extended prediction self-adaptive control. *IFAC Proceedings Volumes*, Elsevier, v. 18, n. 5, p. 1255–1260, 1985.

[43] GARCIA, C. E.; PRETT, D. M.; MORARI, M. Model predictive control: theory and practice—a survey. *Automatica*, Elsevier, v. 25, n. 3, p. 335–348, 1989.

[44] MORARI, M.; LEE, J. H. Model predictive control: past, present and future. *Computers & Chemical Engineering*, Elsevier, v. 23, n. 4-5, p. 667–682, 1999.

[45] QIN, S. J.; BADGWELL, T. A. A survey of industrial model predictive control technology. *Control engineering practice*, Elsevier, v. 11, n. 7, p. 733–764, 2003.

[46] BEMPORAD, A.; MORARI, M. Robust model predictive control: A survey. In: *Robustness in identification and control*. [S.l.]: Springer, 1999. p. 207–226.

[47] NORMEY-RICO, J. E.; CAMACHO, E. F. Robust design of gpc for processes with time delay. *International Journal of Robust and nonlinear control*, Wiley Online Library, v. 10, n. 13, p. 1105–1127, 2000.

[48] NORMEY-RICO, J. E.; GÓMEZ-ORTEGA, J.; CAMACHO, E. F. A smith-predictor-based generalised predictive controller for mobile robot path-tracking. *Control Engineering Practice*, Elsevier, v. 7, n. 6, p. 729–740, 1999.

[49] LIMA, D. M.; SANTOS, T. L. M.; NORMEY-RICO, J. E. Robust nonlinear predictor for dead-time systems with input nonlinearities. *Journal of Process Control*, Elsevier, v. 27, p. 1–14, 2015.

[50] ALAMIR, M. *Stabilization of nonlinear systems using receding-horizon control schemes: a parametrized approach for fast systems.* [S.l.]: Springer, 2006.

[51] WADA, N.; SAITO, K.; SAEKI, M. Model predictive control for linear parameter varying systems using parameter dependent lyapunov function. In: IEEE. *47th Midwest Symposium on Circuits and Systems.* [S.l.], 2004. v. 3, p. iii–133.

[52] LAKSHMANAN, N.; ARKUN, Y. Estimation and model predictive control of non-linear batch processes using linear parameter varying models. *International Journal of control*, Taylor & Francis, v. 72, n. 7-8, p. 659–675, 1999.

[53] BUMROONGSRI, P.; KHEAWHOM, S. An ellipsoidal offline model predictive control strategy for linear parameter varying systems with applications in chemical processes. *Systems & Control Letters*, Elsevier, v. 61, n. 3, p. 435–442, 2012.

[54] BLANKE, M. et al. Fault-tolerant control systems - a holistic view. Elsevier, 1997.

[55] JIANG, J.; YU, X. Fault-tolerant control systems: A comparative study between active and passive approaches. *Annual Reviews in control*, Elsevier, v. 36, n. 1, p. 60–72, 2012.

[56] LUNZE, J.; RICHTER, J. H. Reconfigurable fault-tolerant control: a tutorial introduction. *European journal of control*, Elsevier, v. 14, n. 5, p. 359–386, 2008.

[57] BLANKE, M.; STAROSWIECKI, M.; WU, N. E. Concepts and methods in fault-tolerant control. In: IEEE. *American Control Conference, 2001. Proceedings of the 2001.* [S.l.], 2001. v. 4, p. 2606–2620.

[58] ZHANG, Q.; BASSEVILLE, M.; BENVENISTE, A. *Fault detection and isolation in nonlinear dynamic systems: A combined input-output and local approach.* Tese (Doutorado) — INRIA, 1997.

[59] ZHANG, Y.; JIANG, J. Bibliographical review on reconfigurable fault-tolerant control systems. *Annual reviews in control*, Elsevier, v. 32, n. 2, p. 229–252, 2008.

[60] PERSIS, C. D.; ISIDORI, A. A geometric approach to nonlinear fault detection and isolation. *IEEE transactions on automatic control*, IEEE, v. 46, n. 6, p. 853–865, 2001.

[61] HAMMOURI, H.; KINNAERT, M.; YAAGOUBI, E. E. Observer-based approach to fault detection and isolation for nonlinear systems. *IEEE transactions on automatic control*, IEEE, v. 44, n. 10, p. 1879–1884, 1999.

[62] ZOLGHADRI, A.; HENRY, D.; MONSION, M. Design of nonlinear observers for fault diagnosis: a case study. *Control Engineering Practice*, Elsevier, v. 4, n. 11, p. 1535–1544, 1996.

[63] CHEN, J.; PATTON, R. J. *Robust model-based fault diagnosis for dynamic systems.* [S.l.]: Springer Science & Business Media, 2012.

[64] GERTLER, J. Fault detection and isolation using parity relations. *Control engineering practice*, Elsevier, v. 5, n. 5, p. 653–661, 1997.

[65] ISERMANN, R. Supervision, fault-detection and fault-diagnosis methods—an introduction. *Control engineering practice*, Elsevier, v. 5, n. 5, p. 639–652, 1997.

[66] HENRY, D.; ZOLGHADRI, A. Design of fault diagnosis filters: A multi-objective approach. *Journal of the Franklin Institute*, Elsevier, v. 342, n. 4, p. 421–446, 2005.

[67] PATTON, R.; KLINKHIEO, S. LPV fault estimation and FTC of a two-link manipulator. In: *2010 American Control Conference, Baltimore, MD, USA*. [S.l.: s.n.], 2010. p. 4647–4652.

[68] OCA, S. de et al. Fault-tolerant control strategy for actuator faults using LPV techniques: Application to a two degree of freedom helicopter. *International Journal of Applied Mathematics and Computer Science*, v. 22, n. 1, p. 161–171, 2012.

[69] ZHANG, K.; JIANG, B.; CHEN, W. An improved adaptive fault estimation design for polytopic LPV systems with application to helicopter models. In: IEEE. *Asian Control Conference, 2009. ASCC 2009. 7th.* [S.l.], 2009. p. 1108–1113.

[70] GRENAILLE, S.; HENRY, D.; ZOLGHADRI, A. A method for designing fault diagnosis filters for LPV polytopic systems. *Journal of Control Science and Engineering*, Hindawi Publishing Corp., v. 2008, p. 1, 2008.

[71] ABDULLAH, A.; ZRIBI, M. Sensor-fault-tolerant control for a class of linear parameter varying systems with practical

examples. *Industrial Electronics, IEEE Transactions on*, v. 60, n. 11, p. 5239–5251, 2013.

[72] PATTON, R. J.; CHEN, L.; KLINKHIEO, S. An LPV pole-placement approach to friction compensation as an FTC problem. *Int. J. Appl. Math. Comput. Sci.*, v. 22, n. 1, p. 149–160, March 2012.

[73] ARMENI, S.; CASAVOLA, A.; MOSCA, E. Robust fault detection and isolation for LPV systems under a sensitivity constraint. *International Journal of Adaptive Control and Signal Processing*, Wiley Online Library, v. 23, n. 1, p. 55–72, 2009.

[74] GEIDL, M. et al. Energy hubs for the future. *IEEE Power and Energy Magazine*, v. 5, n. 1, p. 24, 2007.

[75] MENDES, P. R. C. *Predictive Control for Energy Management of Renewable Energy Based Microgrids*. Tese (Doutorado) — Universidade Federal de Santa Catarina, 2016.